Reviewed Preprint
v1 • January 23, 2026
Not revised

Reviewed Preprint
v2 • June 1, 2026
Revised by authors

For correspondence:
funabih@rockefeller.edu

Competing interests: H.F. is affiliated with the Graduate School of Medical Sciences, the Department of Biochemistry and Biophysics, Weill Cornell Medicine and the Cell Biology Program at the Sloan Kettering Institute. The authors declare no competing interests.

Funding: See page 25

Reviewing editor: Daniel Zilberman, Institue of Science and Technology, Austria

Impacts of DNA methylation on H2A.Z deposition and nucleosome stability

Rochelle M Shih[1], Yasuhiro Arimura[1,2], Hide A Konishi[1], Hironori Funabiki[1]

[1]Laboratory of Chromosome and Cell Biology, The Rockefeller University, New York, United States • [2]Basic Sciences Division, Fred Hutchinson Cancer Center, Seattle, United States

eLife Assessment

This study provides **valuable** mechanistic insight into the mutually exclusive distributions of the histone variant H2A.Z and DNA methylation by testing two hypotheses: (i) that DNA methylation suppresses H2A.Z deposition by ATP-dependent chromatin remodelling complexes, and (ii) that DNA methylation destabilizes H2A.Z nucleosomes, thereby preventing H2A.Z retention. Through a series of well-designed and carefully executed experiments, **solid** support is presented for the first hypothesis. The evidence supporting the second hypothesis is less complete, and the extent to which either mechanism is responsible for H2A.Z exclusion from methylated DNA remains not entirely clear. This work will be of broad interest to researchers in chromatin biology and epigenetics.

https://doi.org/10.7554/eLife.109762.2.sa4

Abstract

The histone variant H2A.Z and DNA methylation are enriched at mutually exclusive genomic segments, though its mechanistic bases remain unclear. Here, we examine impacts of DNA methylation on the intrinsic stability of the H2A.Z nucleosome and chaperone-mediated H2A.Z deposition. Cryo-EM and endonuclease analyses suggest that DNA methylation subtly increases the openness and accessibility of the H2A.Z nucleosome on satellite II-derived DNA sequences. In transcriptionally silent *Xenopus* egg extracts, H2A.Z preferentially associates with unmethylated DNA though a substantial proportion of H2A.Z is recruited to methylated DNA. Preferential H2A.Z deposition to unmethylated DNA depends on the SRCAP complex, whose DNA binding is suppressed by methylation, while a SRCAP-independent and DNA methylation-insensitive mechanism for H2A.Z deposition also exists. Altogether, we propose that SRCAP drives the biased association of H2A.Z to unmethylated DNA, while additional mechanisms, potentially taking advantage of the subtle DNA methylation-induced physical effects, further assist the exclusion of H2A.Z from methylated DNA.

Introduction

Structural features of the nucleosome, a protein-DNA complex composed of ~146 bp DNA wrapped around a histone octamer, directly regulate genomic accessibility to a variety of DNA binding proteins, in part, through incorporation of histone variants with unique physical properties (Kurumizaka et al., 2021; Talbert and Henikoff, 2016). The highly evolutionarily conserved H2A variant, H2A.Z, is involved in transcriptional regulation with a well described localization at the transcription start sites (TSSs) of active genes (Bönisch and Hake, 2012; Giaimo et al., 2019; Zlatanova and Thakar, 2008). While typically associated with gene activation, H2A.Z has also been connected to a range of functions including DNA repair, chromosome segregation, heterochromatin maintenance, and transcriptional repression (Colino-Sanguino et al., 2022; Giaimo et al., 2019). Loss of H2A.Z induces lethality in many eukaryotes, such as mice, *Drosophila*, and *Tetrahymena* (Faast et al., 2001; Liu et al., 1996; Van Daal and Elgin, 1992), and dysregulation of its localization has been linked to several diseases, including

various cancers and the developmental disorder Floating-Harbor syndrome (Buschbeck and Hake, 2017; Diegmüller et al., 2025). What mechanisms mediate proper H2A.Z localization, and how that connects with its broad-reaching functions, represents an important area of study.

Genomic sequencing analysis of a wide range of eukaryotes have found H2A.Z and DNA methylation, typically occurring as 5-methylcytosine (5mC), to be strikingly anti-correlated across the genome, at both a global and local level (Berta et al., 2021; Coleman-Derr and Zilberman, 2012; Conerly et al., 2010; Murphy et al., 2018; Nie et al., 2019; Zemach et al., 2010; Zilberman et al., 2008). The high conservation of this antagonism points to the existence of a shared fundamental pathway involved in creating this dichotomy and emphasizes its functional importance. In *Arabidopsis*, H2A.Z mediates recruitment of the demethylase ROS1, thereby promoting DNA demethylation; however, this pathway uses plant-specific machinery that targets only a particular set of genomic loci (Nie et al., 2019). More general mechanisms for how the mutually exclusive H2A.Z and DNA methylation compartments exist at large remain to be resolved.

DNA methylation may mediate H2A.Z exclusion via two distinct mechanisms: 1) influencing the intrinsic physical stability of the nucleosome, and/or 2) modulating the activity of nucleosome-remodelers. H2A.Z and H2A diverge in sequence along areas important for stabilizing intra-nucleosome interactions, such as the L1 loop, docking domain, and C-terminus (Bönisch and Hake, 2012). DNA methylation can influence the geometry of DNA, particularly its roll and twist, which then likely affect nucleosome wrapping (Li et al., 2022b). A large body of work has been conducted on the physical impacts of either H2A.Z or DNA methylation on the nucleosome, but conflicting conclusions have been reported; incorporation of H2A.Z or DNA methylation independently has been shown to cause stabilizing (Chen et al., 2013; Choy et al., 2010; Collings et al., 2013; Dai et al., 2021; Ishibashi et al., 2009; Lee et al., 2015; Lee and Lee, 2012; Park et al., 2004; Thambirajah et al., 2006), destabilizing (Horikoshi et al., 2019; Jimenez-Useche et al., 2014; Jimenez-Useche and Yuan, 2012; Lee et al., 2015; Lewis et al., 2021; Li et al., 2023; Ngo et al., 2016; Rudnizky et al., 2016; Weber et al., 2010; Zhang et al., 2005), or no detectable effects (Fujii et al., 2016; Langecker et al., 2015; Osakabe et al., 2015). Nevertheless, it is possible that the combination of H2A.Z and DNA methylation's effects may physically bias against retention of H2A.Z nucleosomes on methylated DNA and contribute to their overall antagonism.

H2A.Z remodeling is primarily carried out by the Ino80 family of nucleosome remodelers. Both the SRCAP complex (SRCAP-C) and TIP60 complex (TIP60-C) mediate exchange of canonical H2A to H2A.Z within a nucleosome (Ruhl et al., 2006), while the INO80 complex (INO80-C) has been reported to evict H2A.Z (Scacchetti and Becker, 2021; Watanabe and Peterson, 2010). TIP60-C can also associate with the H2A.Z chaperone, ANP32e, to evict H2A.Z from nucleosomes (Mao et al., 2014; Obri et al., 2014). Members of this remodeler family are prime candidates for enforcing the separation of H2A.Z and DNA methylation; however, it is unknown whether any of these complexes exhibit DNA methylation sensitivity.

To determine molecular mechanisms contributing to the mutual exclusion of H2A.Z and DNA methylation within the genome, here we investigated the effects of DNA methylation on both the physical stability of H2A.Z nucleosomes and remodeler-mediated deposition of H2A.Z onto synthetic DNA constructs by employing cryo-EM structural analysis and the physiological *Xenopus* egg extract system, respectively.

Results

Cryo-EM analysis of H2A.Z nucleosomes in the presence or absence of DNA methylation

To assess the physical impacts of DNA methylation on H2A.Z nucleosomes, we solved cryo-EM structures of human H2A.Z nucleosomes reconstituted with either methylated (Me) or unmethylated (UM) Sat2R-P DNA (Fig 1, Suppl Fig 1, Suppl Table 1). The Sat2R-P sequence is

a 152 bp artificial palindromic sequence containing 9 evenly distributed CpG sites and was engineered from a published canonical nucleosome crystal structure containing a methylated derivative of the human satellite II sequence (termed Sat2R) (Osakabe et al., 2015) (Fig 1A). This sequence was chosen for three reasons: 1) human satellite II (HSat2) represents a highly abundant methylated sequence which undergoes disease-associated differential methylation (Ehrlich, 2003; Jackson et al., 2004; Tilman et al., 2012; Unoki, 2021; Wong et al., 2001), 2) it was reported that little H2A.Z associates with HSat2 repeats (Capurso et al., 2012), which are frequently hypomethylated in cancers (Ehrlich, 2009; Hall et al., 2017), and 3) its symmetric palindromic sequence was needed to increase final structure resolutions due to the two-fold pseudo symmetry about the nucleosome dyad axis. Prepared nucleosomes were run on a native PAGE gel to assess for quality, where both samples appeared as a singular band with minor comparable populations of unincorporated DNA (Suppl Fig 1A).

Cryo-EM structures of UM and Me Sat2R-P H2A.Z nucleosomes were solved at a final resolution of 3.05 Å and 2.78 Å, respectively (Fig 1B and C, Suppl Fig 1). We found that the nucleosome dyad was shifted roughly two base pairs from the center of the Sat2R-P palindrome, introducing a sequence asymmetry despite our intended use of the palindromic sequence. The shifted nucleotide positions were determined using the higher resolution densities surrounding the nucleosome dyad, which allowed for pyrimidine and purine distinction (Suppl Fig 2A-D). Two atomic models (termed v1 and v2) with mirrored DNA sequences were generated for each structure to account for the resultant sequence asymmetry, with the final EM densities likely reflecting an average of these two models (Suppl Fig 2E).

As a whole, both the methylated and unmethylated structures resembled previously published H2A.Z nucleosome structures and exhibited a linker DNA asymmetry where one side of the nucleosome (distal face 2, DF2) contained a highly flexible linker DNA region compared to the other (distal face 1, DF1) (Fig 1B and C) (Horikoshi et al., 2013; Lewis et al., 2021; Suto et al., 2000). As a palindromic DNA sequence was used, it is likely that the asymmetrical faces in the cryo-EM structures arose due to an averaging of closed and open H2A.Z nucleosome particles into the same structure rather than representing an asymmetry found in individual particles.

In a direct comparison of DF2 linker DNA lengths, we found that the Me Sat2R-P map had much weaker linker DNA density than UM Sat2R-P, resulting in a ~7 bp shorter resolved DNA model for the methylated structure (Fig 1D). This loss of linker density indicates destabilized histone-DNA interactions and increased DNA structural variability in the presence of DNA methylation. Along similar lines, Root Mean Squared Distance (RMSD) analysis identified the H2A.Z-H2B dimer of DF2, as well as the overall DNA backbone, as regions of considerable difference between the methylated and unmethylated structures, whereas DF1, the closed side of the nucleosome with a highly resolved linker DNA, was largely similar between the two (Fig 1E).

DNA methylation creates open H2AZ nucleosome structures

To further characterize areas of change, maps of unmethylated and methylated H2A.Z structures were filtered and resampled to the same resolution (~3 Å) for fair comparison (Fig 2A). Three major differences between the maps were identified. First, cryo-EM densities of the H3 N-terminus and H2A.Z C-terminus on DF2 were much weaker in the methylated structure as compared to unmethylated, preventing model construction in these areas (Fig 2B). Second, an extra density on the H2A.Z-H2B acidic patch was seen on the methylated map but was not present on the unmethylated map (Fig 2C). Third, between the two major orientations the H4 N-terminal tail can adopt (Arimura et al., 2021), the unmethylated map showed a strong preference for the inward orientation whereas the methylated structure exhibited similar populations of inward and outward orientations (Fig 2D).

The H3 N-terminus interacts with the H2A/H2A.Z C-terminus and DNA to hold the linker DNA close to the body of the nucleosome (Li et al., 2023; Li and Kono, 2016). Loss of the H3 N-terminal density from the methylated structure suggests destabilized DNA-histone interactions that are consistent with the shorter resolved linker DNA on DF2 of the methylated model compared to unmethylated (Fig 1D). The H4 N-terminal tail, on the other hand, mediates inter-nucleosomal

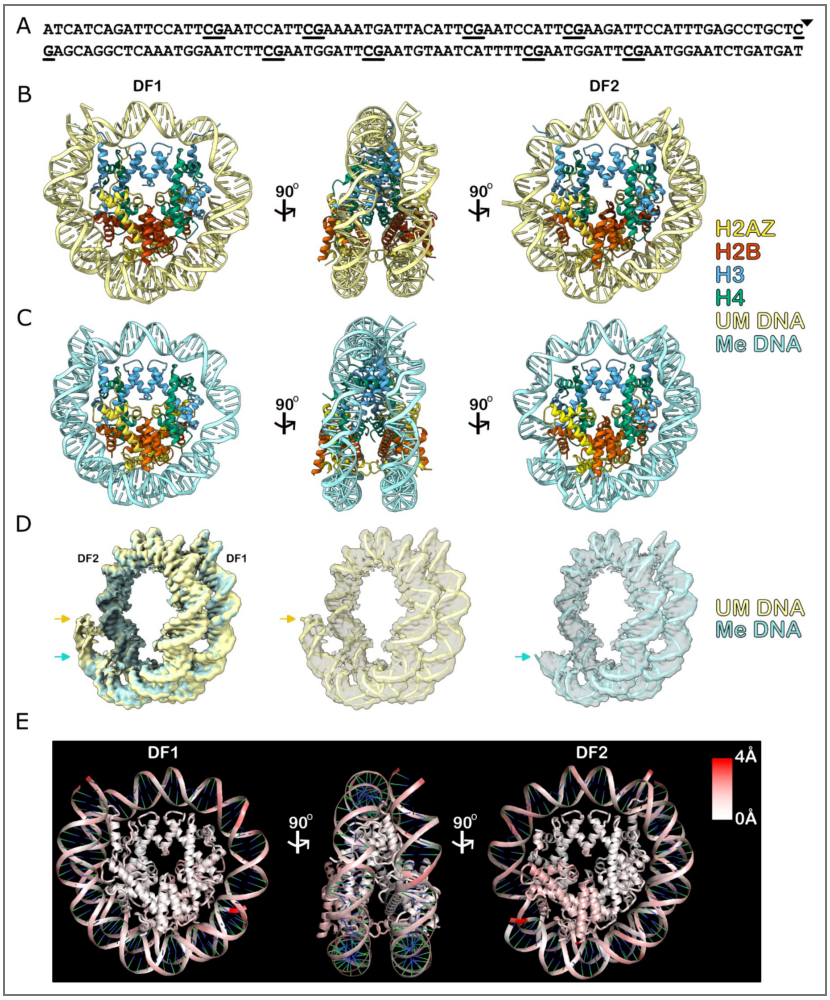

Figure 1. Cryo-EM structures of methylated and unmethylated Sat2R-P human H2A.Z nucleosomes.

(A) Diagram of the palindromic 152 bp Sat2R-P sequence. CpGs are underlined. Triangle denotes midpoint. **(B and C)** Atomic models of unmethylated (**B**) and methylated (**C**) Sat2R-P H2A.Z structures (the v1 model for both). Two face views (DF1 and DF2) and a side view (middle) are shown. **(D)** Left, overlay of unmethylated (UM) and methylated (Me) Sat2R-P DNA EM densities. Middle and right, overlays of DNA densities on top of the corresponding v1 DNA atomic models for either the unmethylated (middle) or methylated (right) structures. Arrows point to the visualizable end of the DF2 linker DNA for each structure. **(E)** RMSD analysis comparing differences between unmethylated and methylated v1 Sat2R-P H2A.Z atomic models.

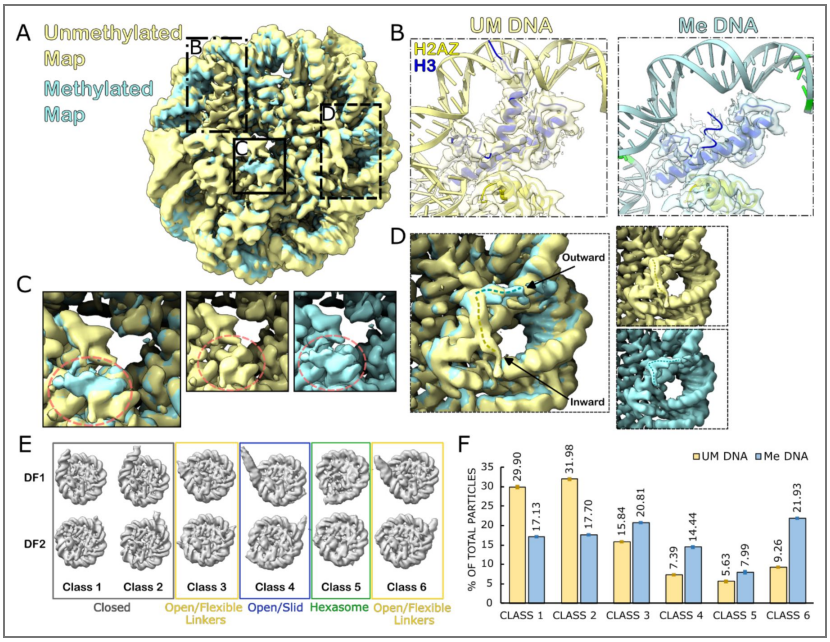

Figure 2. DNA methylation reduces H3-DNA contacts, alters H4 N-terminal tail orientations, and forms open nucleosome structures.

(A) Density maps of unmethylated (UM) and methylated (Me) Sat2R-P H2A.Z nucleosomes filtered and resampled to ~3Å. The face shown, and all following zoom-ins, is of DF2. Maps are overlaid onto each other. Boxed regions highlight major areas of difference shown in **B-D**. **(B)** Zoom-in of the H3 N-terminus on DF2 of both structures. Density maps are shown as a transparent overlay on top of the corresponding v1 atomic models. **(C)** Zoom-in of the DF2 acidic patch on both structures. Area corresponding to the extra density found in the Me structure labeled in red. **(D)** Zoom-in of the H4 N-terminal tail. Dotted lines show each structure's preferred orientation **(E)** 3D Models used in the *in silico* mixing 3D classification analysis. Classes are as follows: (1 and 2) closed nucleosome structures with varying linker lengths; (3 and 6) open nucleosomes with highly flexible linkers; (4) open nucleosomes that have shifted position from center; (5) hexasomes. Both distal faces (DF1 and DF2) are shown of each model. **(F)** Results of classification analysis. Y-axis is the proportion of particles sorted into each class as a percent of the total input particles from each sample (UM or Me). Error bars represent SEM, n = 3 technical replicates.

interactions through contacts with a neighboring acidic patch (Chen et al., 2017; Luger et al., 1997). The extra density on the Me Sat2R-P acidic patch may then have come from the H4 tail of another nucleosome, in line with the changes also observed in H4 tail orientation. These observations may be consistent with reports that DNA methylation increases condensation of nucleosomes, as well as bare DNA, *in vitro* and *in vivo* (Buitrago et al., 2021; Jimenez-Useche et al., 2014; Yang et al., 2020), though require future experimental validation.

To more quantitatively assess methylation-dependent structural changes, we conducted an *in silico* mixing 3D classification analysis (Arimura et al., 2021; Hite and MacKinnon, 2017), by combining micrographs collected from both methylated and unmethylated nucleosome samples and then sorted particles picked from the combined micrographs into six 3D classes of nucleosomes, each with varying degrees of open or closed linker DNA (Fig 2E and F, Suppl Fig 3). Most of the unmethylated particles (>60%) were sorted into the closed linker classes (Class 1 and 2) whereas the majority of methylated particles (~60%) belonged to classes with open linkers (Classes 3, 4, 6) (Fig 2F). The fraction of hexasomes (Class 5) is minor in both conditions with a slight increase in methylated particles (Class 5). Among these open linker classes that are preferentially found in methylated particles, Class 4 also represents nucleosomes where the palindromic center of the DNA has slid and is considerably offset from the dyad axis of the histone octamer. This may explain the weaker DF2 linker density seen in the high resolution Me Sat2R-P structure (Fig 1D). Additionally, the DNA backbone of the methylated nucleosome structure had a lower local resolution compared to unmethylated, despite the methylated map having a higher global resolution (Suppl Fig 4). This is consistent with the increased population of open linker and slid nucleosome particles in the methylated structure. Altogether, our cryo-EM structural analysis suggests that DNA methylation creates open H2A.Z nucleosome structures with destabilized DNA wrapping.

Cryo-EM structures of 601L H2A.Z nucleosomes show no difference between methylation status

In addition to the Sat2R-P nucleosomes, we also solved cryo-EM structures of human H2A.Z nucleosomes reconstituted on methylated and unmethylated 601L DNA, a 205 bp palindromic version of the lefthand portion of the classic Widom 601 sequence (Suppl Fig 5 and 6, Suppl Table 1) (Lowary and Widom, 1998). Final maps of the unmethylated and methylated structures were obtained at 3.09 Å and 3.25 Å, respectively (Suppl Fig 5B-E). RMSD analysis of the solved structures showed that both maps were essentially identical to each other, with the few differences present localized to highly flexible regions of the nucleosome (Suppl Fig 5F). The lack of clear structural differences when using 601L DNA is likely due to its artificially strong nucleosome positioning ability, which may have prevented detection of subtle changes caused by DNA methylation.

DNA methylation increases accessibility of H2A.Z but not H2A nucleosomes

In order to validate the observed opening of the H2A.Z nucleosome structure by DNA methylation, and to determine if this methylation effect is also present on nucleosomes containing canonical H2A, we measured nucleosome DNA accessibility via restriction enzyme digest (Fig 3, Suppl Fig 7 and 8). We tested both human H2A and H2A.Z nucleosomes reconstituted with methylated and unmethylated versions of 152 bp non-palindromic Sat2R DNA that was modified to include a singular HinfI site 18 bp in from the 5'-end containing a Cy5-fluorophore (Fig 3A). Based on our Sat2R-P H2A.Z nucleosome cryo-EM structures as well as published Sat2R H2A nucleosome crystal structures(Osakabe et al., 2015), this HinfI site is predicted to be located at SHL5.5, where the L2 loop of H2A/H2A.Z contacts the DNA minor groove (Fig 3B). Since this SHL5.5 was only resolved in DF1 but not DF2 of the methylated Sat2R-P H2A.Z structure, whereas it was resolved in both DF1 and DF2 in UM Sat2R-P H2A.Z nucleosomes, we assumed that this segment would show methylation-induced accessibility changes to the HinfI endonuclease.

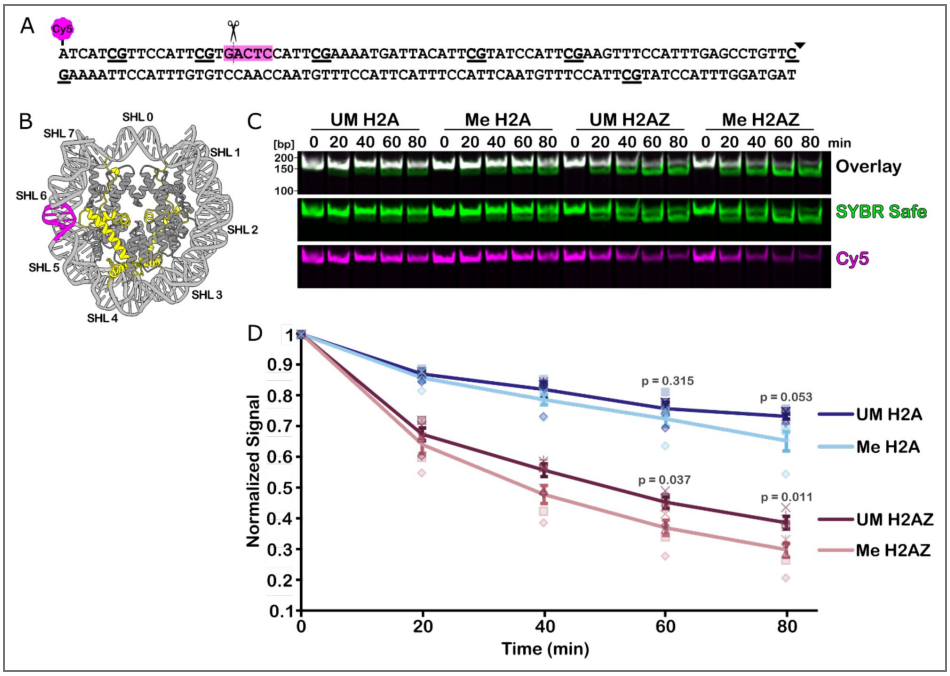

Figure 3. **DNA methylation increases H2A.Z nucleosome accessibility.**

(A) Diagram of the **15**2 bp 1HinfI_Sat2R DNA sequence used. CpG sites underlined and sequence midpoint indicated by the triangle. HinfI recognition site highlighted in magenta. A Cy5 fluorophore is attached to the 5′ end nearest the HinfI site. **(B)** Schematic of 1HinfI_Sat2R H2A.Z nucleosome with HinfI recognition site demarcated in magenta and H2A.Z in yellow. **(C)** Native gel showing HinfI digestion time course of UM and Me human H2A and H2A.Z nucleosomes. SYBR Safe was used to stain total DNA. Digestion efficiency was assessed via loss of Cy5 signal and a downward shift in the total DNA band. **(D)** Quantification of (**C**). Cy5 signals were normalized to total SYBR Safe signal for each sample. Error bars represent SEM. Each shape represents data from one independent experiment, n = 5 experiments. Statistics comparing unmethylated and methylated samples at indicated timepoints were completed with a two-tailed t-test assuming unequal variance with *p*-values listed above each comparison.

Homogeneity of the reconstituted nucleosomes was assessed via native PAGE and mass photometry analysis prior to restriction digest analysis (Suppl Fig 7A-C). Digest of bare control DNA confirmed that HinfI behaved similarly on both methylated and unmethylated Sat2R substrates over the time scale used in the experiment (Suppl Fig 7D). We found that H2A.Z nucleosomes were more accessible to enzymatic digest than H2A nucleosomes, independent of DNA methylation status (Fig 3B and C, Suppl Fig 8). This result was consistent with previous reports using similar assays on Widom 601 nucleosomes, showing that the DNA termini of H2A.Z mono-nucleosomes are more accessible than that of H2A (Jung et al., 2024; Lewis et al., 2021). When comparing methylation-dependent differences for each type of nucleosome, methylated and unmethylated H2A nucleosomes were largely digested at similar rates. Methylated H2A.Z nucleosomes, on the other hand, exhibited a small but more pronounced increase in accessibility as compared to its unmethylated counterpart (Fig 3B and C, Suppl Fig 8). These results corroborate our structural findings and suggest that the effects of DNA methylation may be negligible on an intrinsically stable nucleosome (i.e. containing H2A or with hyper-stable nucleosome positioning sequences) but can enhance nucleosome opening on an already open and accessible H2A.Z nucleosome.

H2A.Z and DNA methylation localization in *Xenopus laevis* sperm pronuclei and a fibroblast cell line

Results from our structural and biochemical experiments indicate that DNA methylation subtly increases the accessibility of H2A.Z nucleosomes. While functional implications likely exist, this slight effect on the intrinsic physical stability of the H2A.Z nucleosome is unlikely to be the sole driver of the mutually exclusive H2A.Z and DNA methylation compartmentalization in cells. To identify the major biochemical mechanism underlying this dichotomy, we turned to the *Xenopus laevis* egg extract system, a unique cell-free system that allows for characterization of chromatin proteins under physiological conditions (Almouzni and Wolffe, 1993; Hoogenboom et al., 2017; Jenness et al., 2018; Lohka and Maller, 1985; Onikubo and Shechter, 2016; Postow et al., 2008; Wassing et al., 2024; Xue et al., 2013; Zierhut et al., 2014).

To ensure that *Xenopus* egg extract is a valid tool for studying the H2A.Z-DNA methylation antagonism, we conducted CUT&Tag – Bisulfite Sequencing (CnT-BS) (Li et al., 2021), a method which allows for the direct assessment of DNA methylation on CUT&Tag reads, against H2A.Z of *Xenopus* sperm nuclei incubated in interphase extract. This condition mimics fertilization and allows for full nucleosome assembly onto sperm (primarily composed of protamines and H3/H4 tetramers) to create functional pronuclei (Oikawa et al., 2020). We also collected samples against H3 to serve as a pan-nucleosome control. Since sperm pronuclei in egg extract represents a unique transcriptionally silent state (Engelke et al., 1980; Newport and Kirschner, 1982; Veenstra et al., 1999), we also performed CnT-BS on XTC-2 cells, a *Xenopus laevis* fibroblast cell line (Pudney et al., 1973), to assess changes in DNA methylation and H2A.Z overlap across different nuclei types.

Initial comparisons of CnT-BS reads across two biological replicates of our four conditions demonstrated good reproducibility between replicates, while each set of experimental conditions exhibited distinct characteristics. A greater than 99 % bisulfite conversion efficiency rate, as assessed through our unmethylated lambda DNA spike-in, was achieved, and correlation matrices of both the mapped reads and methylation calls were highly similar between biological replicates (Suppl Fig 9, Suppl Table 2 and 3). When comparing across conditions, for both the H3/H2A.Z mapped reads and DNA methylation sites, the first degree of difference seen was between XTC-2 and sperm samples, and then H3 vs H2A.Z following after, indicating that large-scale changes in the DNA methylation and genomic landscape occurred between the two different nuclear states (Suppl Fig 9).

To assess characteristics of H2A.Z and H3 genomic distributions, we subset the *Xenopus* genome into 1,000 bp bins and classified the top 20 % of bins containing the most mapped reads for each condition based on annotated functionalities (Fisher et al., 2023). We found that a greater proportion of highly mapped H2A.Z bins were located near promoter regions as compared to H3

for both sperm and XTC-2 samples (Suppl Fig 10A). Although transcription is suppressed in *Xenopus* egg extracts, H2A.Z in sperm pronuclei were well positioned at TSSs, as generally seen for actively transcribed genes in somatic cells (Suppl Fig 10B and C). This mirrors the reported deposition of H3K4me3 at the +1 TSS sites in *Xenopus* sperm nuclei prior to remodeling as well as reports in zebrafish sperm and *Drosophila* that H2A.Z is positioned at promoters prior to zygotic genome activation (ZGA) (Ibarra-Morales et al., 2021; Murphy et al., 2018; Oikawa et al., 2020).

H2A.Z is biased towards hypomethylated regions of the genome in both *Xenopus* sperm pronuclei and the XTC-2 fibroblast cell line

We next determined the methylation status of CpGs associated with either H2A.Z or H3 across replicates of XTC-2 and sperm nuclei (Fig 4A). One notable drawback of CUT&Tag is a bias towards open and accessible regions (Kaya-Okur et al., 2020; Richard et al., 2025), which may artificially amplify open chromatin signals and lead to an underestimation of DNA methylation status. To circumvent this issue, we analyzed H3 CpG methylation in areas outside of H2A.Z peaks (which tend to be highly accessible) to compare genomic methylation profiles in H2A.Z low/absent regions (H3) vs H2A.Z enriched peaks (H2A.Z).

Overall, sperm chromatin had a higher degree of methylation than XTC-2 chromatin, with 85.3 ± 0.4 % *s.d.* of CpGs in H3 reads experiencing methylation in sperm compared to 53.5 ± 0.4 % in XTC nuclei (Suppl Table 2). Methylated CpG frequencies of H2A.Z-associated reads were reduced to 43.0 ± 0.7 % in sperm chromatin and even further down to 3.0 ± 0.3 % in XTC-2 cells. Mapping of H3 associated methylation calls to annotated genes of the *Xenopus laevis* genome showed ubiquitous distribution of methylation across the length of genes, except for at the TSSs where methylation was depleted (Suppl Fig 10B and C left). Nearly all of these H3-marked hypomethylated TSSs exhibited H2A.Z enrichment in both sperm pronuclei and XTC-2 (Suppl Fig 10B and C right), indicating that hypomethylation-exclusive positioning of H2A.Z is most prominent at the TSSs (Suppl Fig 10D).

DNA methylation-sensitive H2A.Z deposition on synthetic DNA constructs in *Xenopus* egg extract

To directly test whether the presence or absence of DNA methylation can dictate preferential H2A.Z deposition independently of other pre-existing epigenetic marks or DNA sequence, we took advantage of the *Xenopus* egg extract's ability to efficiently assemble nucleosomes *de novo* onto naked DNA templates (Laskey et al., 1977) (Fig 4B). We found that, upon incubation of DNA coated magnetic beads in interphase egg extract, H2A.Z accumulated less efficiently on methylated DNA substrates compared to unmethylated (Fig 4C and D, Suppl Fig 11), whereas this methylation-sensitive deposition was not seen for H2A.X-F, the predominant H2A histone variant in *Xenopus* egg extract (Fig 4E and F, Suppl Fig 11) (Shechter et al., 2009). The methylation bias of H2A.Z held true for arrays of either the GC-rich Widom 601 (57 % GC content) or the more AT-rich human HSat2 (38% GC content) sequence. We next asked whether both H2A.Z variants, H2A.Z.1 and H2A.Z.2 (H2A.V), exhibit the same DNA methylation sensitivity. Since our antibody does not distinguish between the two H2A.Z paralogs, we translated ALFA-tagged (Götzke et al., 2019) versions of the variants in egg extract from exogenously added mRNA and found that both paralogs displayed preferential deposition onto unmethylated DNA (Suppl Fig 12).

The SRCAP complex mediates H2A.Z's preferential deposition on unmethylated DNA

Since SRCAP-C is known to play a major role in depositing H2A.Z to nucleosomes via exchange of H2A dimers on the nucleosome with H2A.Z (Ruhl et al., 2006), we examined if the observed preferential association of H2A.Z with unmethylated DNA in *Xenopus* egg extracts is mediated by SRCAP-C. Depletion of SRCAP-C from extract using a custom antibody against *Xenopus laevis* SRCAP greatly reduced the amount of H2A.Z loaded onto unmethylated DNA compared to control

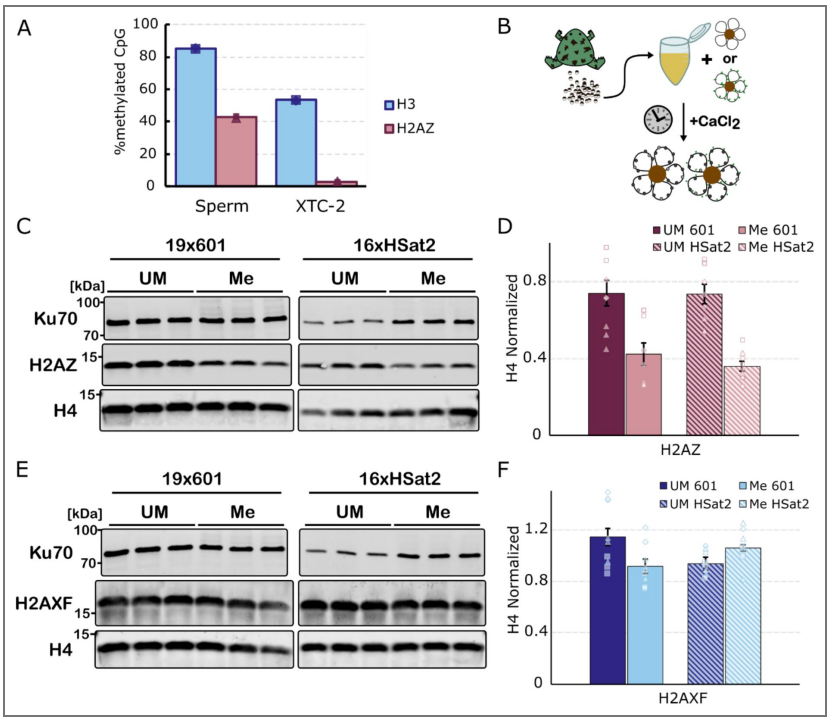

Figure 4. Presence or absence of DNA methylation influences H2A.Z deposition.

(A) Percentage of methylated CpG sites (≥ 5x coverage) associated with H2A.Z peaks or H3 reads in sperm pronuclei incubated in interphase egg extract or XTC-2 nuclei following CnT-BS library preparation. H3 data is taken from regions outside of H2A.Z enriched peaks. Data points represent biological replicates (n = 2). **(B)** Schematic of chromatinization assay. Magnetic beads coated with DNA of interest were incubated in *Xenopus* egg extract with the addition of $CaCl_2$ to induce cycling into interphase. After 60 min, DNA beads were isolated to assess for histone composition. **(C and E)** Western blot results of chromatinization assay probing for either H2A.Z (**C**) or H2A.X-F (**E**). Ku70 and H4 signals are shown as loading controls. Beads coated with unmethylated (UM) or methylated (Me) 19-mer arrays of Widom 601 (19×601) or 16-mer arrays of HSat2 (16xHSat2) were used. A representative blot of technical triplicates for each condition is presented. **(D and F)** Quantification of (**C** and **E**). H2A.Z and H2A.X-F signals were normalized to H4 intensity. Error bars represent SEM. Data points represent technical triplicates across 3 biological replicates with each shape representing data from a single independent experiment (n = 9).

depletion (ΔIgG), while H2A.Z levels on methylated DNA were not affected by SRCAP depletion (Fig 5A-C, Suppl Fig 13A-C). Consequently, in SRCAP-C-depleted (ΔSRCAP) extracts, residual H2A.Z binding to DNA became insensitive to DNA methylation status (Fig 5B and C, Suppl Fig 13C). The SRCAP depletion effect was specific to H2A.Z since the amount of H2A.X-F, the predominant H2A variant in *Xenopus* eggs (Shechter et al., 2009), on DNA was not affected by SRCAP-C depletion (Fig 5B and D, Suppl Fig 13C). Similar results were reproduced with use of a commercially available antibody raised against human SRCAP (Suppl Fig 14).

To understand the molecular basis of the SRCAP-C-dependent preferential deposition of H2A.Z to unmethylated DNA, we tested if DNA methylation inhibits SRCAP-C binding to DNA in *Xenopus* egg extracts. Indeed, SRCAP and ZNHIT1, two core subunits of SRCAP-C, were enriched on unmethylated but not on methylated DNA (Fig 5E-F, Suppl Fig 13D). In contrast, p400, the ATPase of TIP60-C, did not exhibit methylation-sensitive DNA binding (Suppl Fig 15). Since H2A.Z preferentially accumulates at TSSs, which tend to have more open/accessible chromatin, we explored the possibility that the apparent inhibition of SRCAP-C accumulation to methylated DNA was due to the potential capacity of DNA methylation to compact chromatin and change general DNA accessibility. If this were the case, we assumed that suppression of SRCAP-C binding to methylated DNA would not be detected if nucleosome assembly on DNA were to be inhibited. We tested this by depleting the HIRA complex, the major histone H3.3-H4 chaperone that is required for replication-uncoupled nucleosome assembly onto naked DNA in *Xenopus* egg extracts (Ray-Gallet et al., 2002), using antibodies against the HIRA complex subunit UBN2. Inconsistent with this hypothesis, SRCAP and ZNHIT1 still selectively bound to unmethylated DNA in UBN2-depleted extracts, where loading of H3, but not other DNA-binding proteins such as xKid and Dppa2 (Funabiki and Murray, 2000; Xue et al., 2013; Zierhut et al., 2014), was suppressed (Suppl Fig 16). These results indicate that exclusion of the H2A.Z chaperone SRCAP-C from methylated DNA is the major driver biasing H2A.Z deposition against methylated DNA.

Discussion

In this study, we described two distinct mechanisms via which DNA methylation can affect H2A.Z deposition and wrapping stability (Fig 6). We found that DNA methylation directly opposes H2A.Z deposition through inhibition of SRCAP-C DNA binding. SRCAP-C accounts for the majority of H2A.Z deposition on unmethylated DNA and is the primary mediator behind DNA methylation's exclusion of H2A.Z in the transcriptionally silent *Xenopus* egg extract. A subpopulation of H2A.Z, however, is still deposited onto methylated DNA, driven by methylation insensitive mechanism(s) whose identity remains to be established. Once formed, H2A.Z nucleosomes on methylated DNA are more open and accessible compared to their unmethylated counterparts albeit the effect by DNA methylation is relatively subtle compared to that induced by H2A.Z incorporation. The impact on intrinsic nucleosome accessibility may also be dependent on wrapping/positioning ability of the DNA sequences used. This minor decrease in DNA-histone contact stability of methylated H2A.Z nucleosomes could conceivably contribute to clearance of H2A.Z from methylated regions of the genome, though such functional mechanisms remain to be established.

Although a consensus on how DNA methylation influences nucleosome stability has yet to be achieved, our results from our cryo-EM analysis and endonuclease accessibility assay indicate that DNA methylation opens and increases accessibility of DNA segments particularly near the entry/exit region of the H2A.Z nucleosome core particle. This result is in line with reports based on FRET-based and molecular simulation studies on canonical H2A nucleosomes (Jimenez-Useche et al., 2014; Jimenez-Useche and Yuan, 2012; Li et al., 2022a; Ngo et al., 2016). Our *in silico* mixing 3D classification analysis indicates that more particles were classified as open and slid nucleosomes in the methylated H2A.Z sample than in unmethylated (Figure 2E and F), supporting the idea that DNA methylation destabilizes DNA-histone contacts. Since unmethylated G/C dinucleotides and methylated CpG are enriched at outward facing minor grooves and inward facing major grooves in the nucleosome core particles, respectively (Chodavarapu et al., 2010; Segal et al., 2006), DNA methylation may locally impact this DNA-histone contact stability. However, the ambiguity in DNA positioning of our cryo-EM structures prevents us from discussing

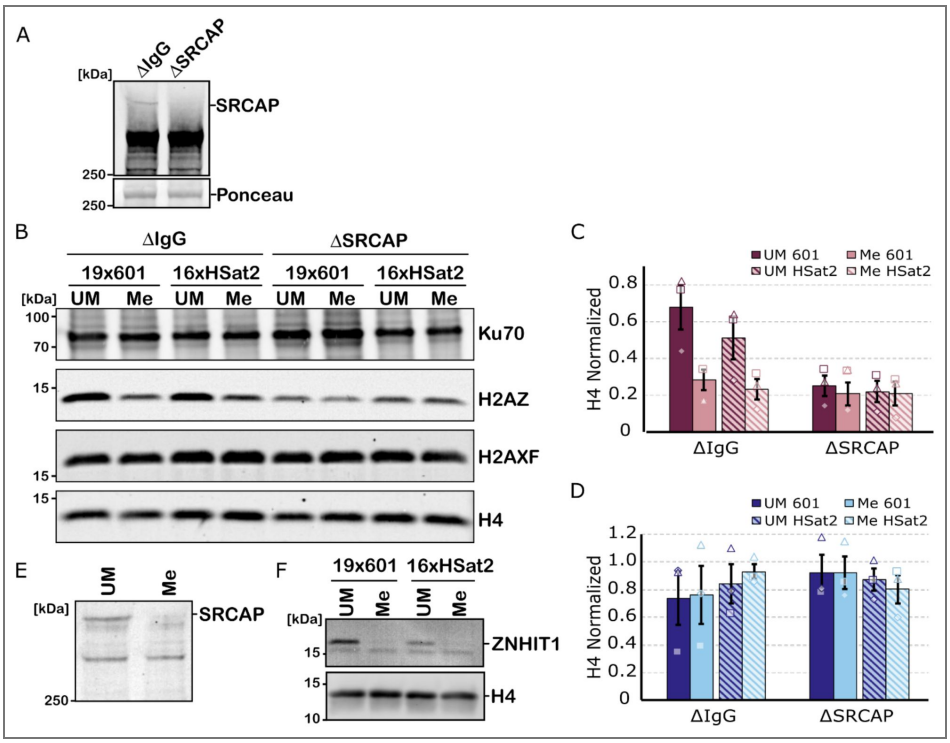

Figure 5. The SRCAP complex mediates H2A.Z's preferential association with unmethylated DNA.

(A) Western blot to detect SRCAP in control IgG-depleted *Xenopus* egg extract (ΔIgG) or SRCAP-depleted extract (ΔSRCAP). Bottom panel shows ponceau staining as a loading control. **(B)** Western blots of chromatinization assay in IgG control vs SRCAP depleted egg extract. Magnetic beads coated with 19-mer arrays of Widom 601 (19×601) or 16-mer arrays of HSat2 (16xHSat2) were incubated with interphase egg extract for 60 min, before their isolation. **(C)** Quantification of H2A.Z signal normalized to H4 from **(B)**. **(D)** Quantification of H2A.X-F signal normalized to H4 from **(B)**. Error bars in (**C**) and (**D**) represent SEM from n = 3 biological replicates and each shape represents data from one independent experiment. **(E)** Western blot staining for SRCAP on 16xHSat2 DNA beads incubated in interphase egg extract. **(F)** Western blot staining for ZNHIT1 on specified DNA beads incubated in interphase egg extract. Representative image shown from two independent experiments.

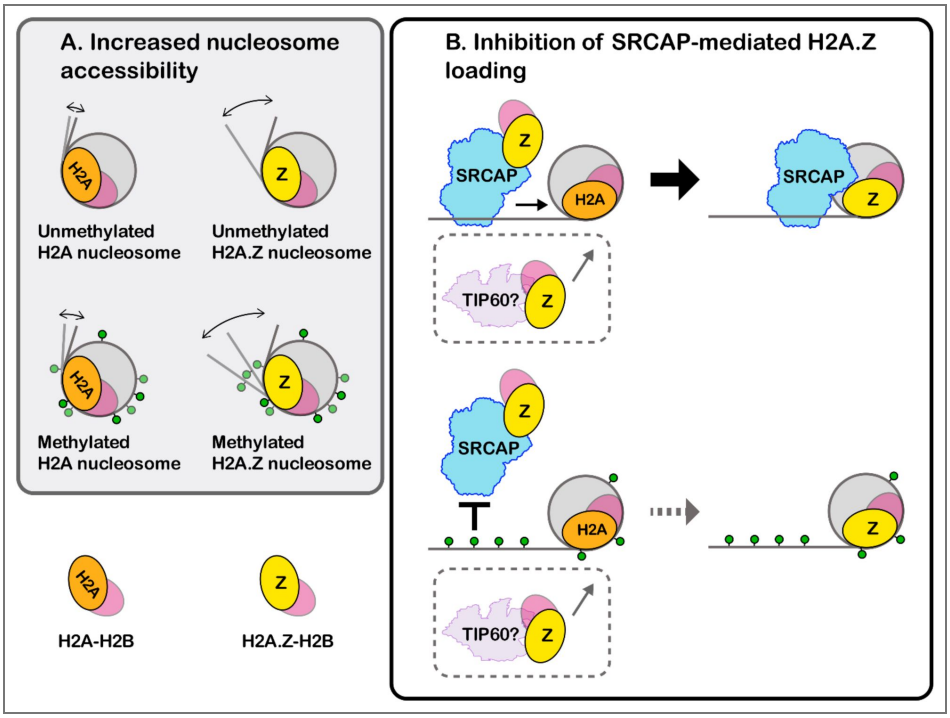

Figure 6. Schematic models for how DNA methylation influences physical nucleosome structure and SRCAP-mediated H2A.Z loading.

(A) DNA methylation has little effect on nucleosome openness/accessibility of H2A nucleosomes. H2A.Z nucleosomes are more open/accessible than H2A nucleosomes, and DNA methylation DNA slightly opens H2A.Z nucleosome further causing nucleosomal DNA ends to be more accessible. (B) SRCAP-C is capable of binding to unmethylated DNA and replacing H2A with H2A.Z on the nucleosome. SRCAP-C cannot bind to methylated DNA, and thus H2A.Z deposition is suppressed on methylated DNA. An SRCAP-independent mechanism (possibly via TIP60) deposits H2A.Z in a DNA methylation insensitive manner.

the structural coordination of specific CpG sites. Alternatively, the increase in accessibility could be due to additive effects of DNA methylation on overall DNA conformation rather than at specific methylated segments. This is in agreement with observations that methylation increases DNA stiffness, making it harder for the DNA to bend and wrap around histone octamers (Ngo et al., 2016; Pérez et al., 2012).

Consistent with previous reports using the Widom 601 sequence (Jung et al., 2024; Lewis et al., 2021), our restriction enzyme accessibility assay shows that H2A.Z nucleosomes with HSat2 are considerably more open and accessible compared to canonical H2A, regardless of methylation status. This difference is substantially larger than that induced by DNA methylation on H2A.Z, suggesting that the physical influence of DNA methylation on nucleosomes is overall subtle. This apparent subtlety, however, may be due to the internal placement of the cut site that we tested, and thus the effect of DNA methylation was preferentially observed on H2A.Z nucleosomes, which are already highly accessible. Similar findings have been reported on canonical H2A 601 nucleosomes, where the effects of DNA methylation manifest greatest on an open nucleosome subpopulation compared to their closed counterparts (Jimenez-Useche and Yuan, 2012). This is likely why we saw no methylation-dependent structural differences with the 601L sequence (Suppl Fig 5), as its innate nucleosome wrapping and positioning ability is even stronger than the classic Widom 601.

It is possible that the combined impact of DNA methylation and H2A.Z on nucleosome structure is further modulated by additional factors, including other histone variants, histone modifications, DNA sequences, and the position of DNA methylation. As H2A.Z frequently coexists with H3.3 at TSSs (Jin et al., 2009; Jin and Felsenfeld, 2007), H3.3 may conceivably contribute to H2A.Z's sensitivity to DNA methylation, though it has been reported that H3.3 does not affect intrinsic H2A.Z nucleosome accessibility *in vitro* (Horikoshi et al., 2016; Jung et al., 2024; Thakar et al., 2009). Notably, in *Xenopus* extracts, nucleosomes assembled on naked DNA are exclusively composed of the H3.3 variant (Ray-Gallet et al., 2002), but the effect of DNA methylation on H2A.Z localization almost completely disappeared with SRCAP-C depletion (Figure 5). This indicates that the combination of H3.3 and H2A.Z alone is insufficient to explain suppression of H2A.Z loading to methylated DNA. Overall, we suggest that the subtle nucleosome destabilization effect of DNA methylation is preferentially pronounced on H2A.Z nucleosomes, which already exhibit an intrinsic wrapping instability compared to canonical H2A nucleosomes (Figure 6). Whether this subtle effect has functional significance remains a subject of future studies.

In *Xenopus* egg extract, H2A.Z deposition to exogenously added methylated DNA (both Widom 601 and HSat2) was about half that of their unmethylated counterparts (Figure 5), suggesting that the influence of DNA methylation on chaperone-mediated H2A.Z loading in egg extract is less sensitive to DNA sequence than its influence on nucleosome physical accessibility. Depleting SRCAP-C from *Xenopus* egg extracts effectively reduced, but not eliminated, H2A.Z deposition to nonmethylated DNA, but had little effect on the subpopulation of H2A.Z associated with methylated DNA. Therefore, *Xenopus* egg extracts appear to possess an additional SRCAP-C independent and DNA methylation-insensitive H2A.Z deposition mechanism (Figure 6). The known H2A.Z chaperone TIP60-C, whose DNA binding was not affected by methylation (Suppl Fig 15), is a prime candidate for this latter mechanism. Of note, concentrations of SRCAP and p400 (EP400), the ATPase subunits of SRCAP-C and TIP60-C, respectively, are comparable (13 nM v.s. 6 nM) (Wühr et al., 2014).

Exactly how SRCAP-C senses DNA methylation remains a pertinent question. Recent structural studies on the yeast SWR1 complex and human SRCAP-C indicate that both the ATPase and the ZNHIT1 subunit (Swc6 in yeast) mediate binding of, and one-dimensional diffusion on, naked DNA substrates (Louder et al., 2024; Park et al., 2024), marking them as likely candidates responsible for methylation sensing. Additionally, the YEATS domain-containing subunit GAS41, found in both SRCAP-C and TIP60-C, recognizes the open chromatin marks H3K14ac and H3K27ac (Hsu et al., 2018a, 2018b), and deposition of H3K27ac, itself, is antagonized by DNA methylation at enhancers (King et al., 2016). It is possible that both direct recognition of DNA methylation and changes in the local landscape of methylated chromatin play a role in dictating

SRCAP-C localization and activity. However, SRCAP-C's preference for unmethylated DNA was maintained even under nucleosome deficient conditions (Suppl Fig 16), indicating that SRCAP-C can sense DNA methylation status independent of chromatin accessibility and histone modifications.

Supporting our observation that a SRCAP-independent mechanism(s) exists to deposit H2A.Z on methylated DNA in *Xenopus* egg extracts, a substantial fraction (~40 %) of H2A.Z-associated genomic DNA is methylated in sperm pronuclei. In the fibroblast cell line XTC-2, that methylated H2A.Z fraction is greatly reduced to 3 %. However, due to the accessibility bias inherent within CUT&Tag, our data likely underestimates the true degree of H2A.Z and DNA methylation overlap, particularly in the XTC-2 samples. For comparison, a previous study in human myometrium reported that ~20 % of CpGs overlapping with H2A.Z are methylated, indicating that a sizeable population of colocalized H2A.Z and DNA methylation exists in somatic cells, which warrants further investigation (Berta et al., 2021). Nevertheless, we believe the decreased trend in H2A.Z and DNA methylation overlap of XTC-2 cells holds true and suggests that the high degree of H2A.Z and DNA methylation coincidence in sperm pronuclei reflects its unique early development and/or transcriptionally silent state. Given the strong preference of SRCAP-C binding to unmethylated DNA in *Xenopus* egg extracts, we predict that additional pathways missing in the egg extract system are necessary to reinforce the antagonism between DNA methylation and H2A.Z enrichment.

Perhaps the greatest difference between XTC-2 cells and *Xenopus* eggs is the presence of transcription, which is one of the main evictors of H2A.Z and necessary for global H2A.Z turnover as well as pruning of randomly deposited H2A.Z within gene bodies, where methylated cytosine enriches (Hardy et al., 2009; Lashgari et al., 2017; Ranjan et al., 2020; Tramantano et al., 2016). Traversing of RNA polymerase (Pol) II across nucleosomes, aided by the FACT complex, results in transient histone dimer displacement (Belotserkovskaya et al., 2003; Bevington and Boyes, 2013; Bintu et al., 2011; Kireeva et al., 2002), leading to the possibility that the more accessible H2A.Z nucleosome structures formed on methylated DNA may have increased susceptibility to Pol II disruption. Furthermore, FACT and Spt6 do not reincorporate H2A.Z into the reassembled nucleosome post Pol II encounter, which would reinforce selective loss of H2A.Z (Heo et al., 2008; Jeronimo et al., 2015). Outside of transcription, the egg extract system also lacks both the DNMT3 enzymes responsible for *de novo* methylation and the TET system responsible for DNA methylation removal in animals (Wühr et al., 2014). In *Arabidopsis*, H2A.Z promotes ROS1-associated DNA demethylation (Nie et al., 2019) and must be excluded to ensure faithful heterochromatin formation (Zhou et al., 2023). Thus, H2A.Z-driven mechanisms to limit DNA methylation remain relevant pathways to increase the H2A.Z/DNA methylation separation within the genome which may be missing in eggs/early embryonic states.

Beyond its interaction with DNA methylation, we show that H2A.Z promoter localization occurs immediately upon conditions mimicking fertilization in a transcription-independent manner. Unlike the almost complete loss of histones seen in mammalian sperm (Ward and Coffey, 1991; Wykes and Krawetz, 2003), *Xenopus* sperm is packaged as a mixture of protamines and H3/H4 tetramers with very low levels of H2A/H2B dimers, which are then remodeled into full nucleosomes upon exposure to the egg cytoplasm (Katagiri and Ohsumi, 1994; Mann et al., 1982; Oikawa et al., 2020; Shechter et al., 2009b). In our egg extract system, which lacks the maternal genome, we expect the bulk of H2A.Z in sperm pronuclei to be newly deposited and find that H2A.Z is still specifically targeted to promotors either via underlying sequence motifs (Ibarra-Morales et al., 2021; Murphy et al., 2018) or tetramer modifications maintained in sperm (Oikawa et al., 2020). This is similar to *Drosophila* where H2A.Z is recruited to TSSs prior to both Pol II binding and ZGA, marking genes for zygotic activation (Ibarra-Morales et al., 2021), indicating conservation of this initial transcription-independent H2A.Z positioning across both vertebrates and invertebrates.

Our work here provides a critical step in the pathways dictating genomic organization by uncovering the previously undescribed methylation sensitivity of SRCAP-C along with the subtle destabilizing effects of DNA methylation on H2A.Z nucleosomes (Figure 6). Together, these

findings provide molecular mechanisms driving the conserved antagonism between H2A.Z and DNA methylation in the genome. However, many questions remain to be answered, such as the existence of both methylation sensitive and insensitive H2A.Z deposition pathways, the broader functional implications of the H2A.Z-DNA methylation antagonism as a whole, and mechanisms driving its maintenance in species that experience periods of global demethylation. These questions represent important areas of future study for our understanding of epigenome dynamics throughout development.

Materials and methods

Histone purification and refolding

pET3 vectors containing sequences for human histones H2A, H2A.Z, H2B, H3.2, and H4 (gifts from Shixin Liu) were expressed in Rosetta (DE3) cells (Novagene, Cat# 70954). Cells were pelleted 4000 x *g*, 20 min, 4 °C and resuspended in wash/lysis buffer [50 mM Tris-HCL pH 7.5, 100 mM NaCl, 1 mM EDTA, 5 mM β-mercaptoethanol, 0.2 mM PMSF] + 1 % Triton-X-100 then sonicated. Inclusion pellets were spun 25,000 x *g*, 20 min, 4 °C, and incubated with DMSO at room temperature (RT) for 30 min. Pellets were then resuspended in unfolding buffer [20 mM Tris-HCl pH 7.5, 7 M guanidine-HCl, 10 mM DTT], sonicated until pellets were fully broken up, and re-pelleted at 25,000 x *g*, 20 min, RT. The supernatant was then collected and dialyzed in urea dialysis buffer overnight at 4 °C [10 mM Tris-HCl pH 7.5, 7 M Urea, 1 mM EDTA, 5 mM β-mercaptoethanol, 100 mM or 200 mM NaCl for H2A/H2B and H3/H4, respectively]. Samples were then pelleted at 25,000 x *g*, 20 min, RT and the supernatant passed through Q Sepharose Fast Flow resin (Cytiva, Cat# 17051010). The flow-through was then collected and added to SP Sepharose Fast Flow resin (Cytiva, Cat# 17072910), washed with urea dialysis buffer, and eluted with elution buffer [10 mM Tris-HCl pH 7.5, 7 M Urea, 1 mM EDTA, 600 mM NaCl, 5 mM β-mercaptoethanol].

Equimolar ratios of histones for either octamer, or dimer and tetramer preparation were then mixed and dialyzed into refolding buffer [10 mM Tris-HCl pH 7.5, 1 mM EDTA, 5 mM β-mercaptoethanol, 2 M or 500 mM NaCl for octamers or dimers/tetramers, respectively]. Refolded histones were then purified via FPLC (ÄKTA pure, Cytiva, Cat# SN2626712) (Superdex 200 10/300 GL increase column, Cytiva, Cat# 28990944).

Generation of DNA arrays

Generation of HSat2 arrays for use in chromatinization assays or arrays of Sat2R-P halves to prepare palindromic sequences for cryo-EM analysis was done as previously described in (Dyer et al., 2003). Briefly, DNA sequences of interest (see Table 1) containing one BglII site, one BamHI site, and two EcoRV sites surrounding the sequence were generated and purchased from Integrated DNA Technologies (IDT™) and cloned into the pUC18 vector just downstream of the XbaI site. The plasmid was then digested with either XbaI (NEB Cat# R0145) and BglII (NEB Cat# R0144) (to obtain the vector) or BglII and BamHI (NEB Cat# R3136) (to obtain the insert), and agarose gel purified. Vector and insert DNA were then ligated with T4 DNA ligase (NEB Cat# M0202). The digest and ligation steps were repeated until the desired repeat number was achieved.

Palindromic DNA preparation for Cryo-EM

Arrays of Sat2R-P halves were generated as described above. Plasmid containing an array of 601L halves (601L-145-8X) was a gift from Curt Davey (Addgene plasmid # 158572; *http://n2t.net/addgene:158572*; *RRID:Addgene_158572*) (Chua et al., 2012). Arrays of palindromic DNA halves for Cryo-EM analysis were then digested with EcoRV (NEB Cat# R3195) and purified via PEG precipitation (0.5 M NaCl, 8 % w/v PEG8000). Supernatant were collected and further purified via phenol-chloroform extraction. Insert ends were dephosphorylated with QuickCIP (NEB Cat# M0525) and phenol-chloroform extracted. Samples were then digested with either HinfI (NEB Cat# R0155) (601L DNA) or AvaI (NEB Cat# R0152) (Sat2R-P DNA), phenol-

Sequence Name	Sequence	Vector	Plasmid Name	Insert Location	Source	Assay(s) Used In	Additional Notes
Sat2R-P	ATCATCAGATTCCATTCGAATCCATTCGAAAA TGATTACATTCGAATCCATTCGAAGATTCCAT TTGAGCCTGCTCGAGCAGGCTCAAATGGAA TCTTCGAATGGATTCGAATGTAATCATTTTCG AATGGATTCGAATGGAATCTGATGAT	pUC18	RMSp81	Between XbaI and BamHI sites	Generated and purchased from Integrated DNA Technologies (IDT™)	Cryo-EM	Modified from the Sat2R sequence in (Osakabe et al, 2015).
601L	ATCACAATCCCGGTGCCGAGGCCGCTCAAT TGGTCGTAGACAGCTCTAGCACCGCTTAAA CGCACGTACGGAATCCGTACGTGCGTTTAA GCGGTGCTAGAGCTGTCTACGACCAATTGA GCGGCCTCGGCACCGGGATTGTGAT	pUC57	601L-145-8X	EcoRV	(601L-145-8X) was a gift from Curt Davey (Addgene plasmid # 158572 ; http://n2t.net/addgene:158572 ; RRID:Addgene_158572)	Cryo-EM	
1HinfI_Sat2R	ATCATCGTTCCATTCGTGACTCCATTCGAAA ATGATTACATTCGTATCCATTCGAAGTTTCCA TTTGAGCCTGTTCGAAAATTCCATTTGTGTCC AACCAATGTTTCCATTCATTTCCATTCAATGTT TCCATTCGTATCCATTTGGATGAT	pUC18	RMSp161	Between XbaI and BamHI sites	Generated and purchased from Integrated DNA Technologies (IDT™)	Restriction Digest Assay	DNA generated via PCR amplification using following primers: /5Cy5/ATCATCGTTCC ATTCGTGAC; ATCATCCAAATGGATA CGAATGG
HSat2 arrays (1 repeat shown)	CGTTTGATTCCATTTGATGTTGATTCCATTCGA GTCCATTCGATGATAATTCCATTCGATTCTTT GCGATGATTCCATTCCTTTCCATTTGAGATGA TTCCATTCGAGACCATTCGATGATTGCATTCA ATTCATTCGATGACGATTATTCAATTCCGTTC AATGATTCCATTCGATTCCAATTGATGATGATT CCATTCGATTCCATTTGATGATGATTCCATGC GATTCCATTCGATGATGACTCCGATATCGGA TCTGATATC	pUC18	RMSp64	Between XbaI and BamHI sites	Generated and purchased from Integrated DNA Technologies (IDT™)	Chromatinization Assays	GenBank: X06199.1
601 arrays (1 repeat shown)	CTGGAGAATCCCGGTGCCGAGGCCGCTCA ATTGGTCGTAGCAAGCTCTAGCACCGCTTAA ACGCACGTACGCGCTGTCCCCCGCGTTTTA ACCGCCAAGGGGATTACTCCCTAGTCTCCA GGCACGTGTCAGATATATACATCCTGTGCAT GTATTGAACAGCGACTCGGGTTATGTGATGG ACCCTATACGCGGCCGCC	pUC18	pAS696	EcoRI/XbaI	Gift from Aaron Straight	Chromatinization Assays	
Oligos for Sequencing Library Preparation							
Sequence Name	**Sequence**				**Source**	**Assay(s) Used In**	**Additional Notes**
Tn5mC-Apt1	T/iMe-dC/GT/iMe-dC/GG/iMe-dC/AG/iMe-dC/GT/iMe-dC/AGATGTGTATAAGAGA/iMe-dC/AG				(Li et al, 2021); Generated and purchased from Integrated DNA Technologies (IDT™)	CnT-BS adapter oligo	Annealed with Tn5mC1.1-A1block to form adapter oligo
Tn5mC1.1-A1block	/5Phos/CTGTCTCTTATACA/3ddC/				(Li et al, 2021); Generated and purchased from Integrated DNA Technologies (IDT™)	CnT-BS adapter oligo	Annealed with Tn5mC-Apt1 to form adapter oligo
Tn5mC-ReplO1	/5Phos//iMe-dC/TGT/iMe-dC/T/iMe-dC/TTATA/iMe-dC/A/iMe-dC/AT/iMe-dC/T/iMe-dC//iMe-dC/GAG/iMe-dC//iMe-dC//iMe-dC/A/iMe-dC/GAGA/iMe-dC//3InvdT/				(Li et al, 2021); Generated and purchased from Integrated DNA Technologies (IDT™)	CnT-BS	Used during oligonucleotide replacement step

Table 1. **DNA sequences/oligos used in the study.**

chloroform extracted, and FPLC purified in 1xTE buffer (Superdex 200 10/300 GL increase column, Cytiva, Cat# 28990944). DNA halves were then incubated with T4 DNA ligase (NEB Cat# M0202) per manufacturer's protocol until all halves were completely ligated.

Methylation of DNA substrates

DNA substrates were enzymatically methylated using the *M.SssI* CpG methyltransferase (NEB, Cat# M0226). Approximately 160 U of methyltransferase were used for 50 µg of DNA in 1x NEB 2 buffer with 500 µM SAM. Samples were incubated at 37 °C for at least one hour. Completion of methylation was checked using the methylation sensitive restriction enzyme BstUI (NEB, Cat# R0518). DNA was purified using phenol-chloroform extraction prior to use.

Nucleosome Reconstitution

DNA and either histone octamers or dimers and tetramers were mixed at a final target concentration of 1 µM in 1x TE buffer and 2 M NaCl. Exact ratios of DNA to histones were titrated for each reconstitution batch, starting at equimolar ratios. Samples loaded in dialysis buttons were then added to high salt dialysis buffer [10 mM Tris-HCl pH 7.5 at 4 °C, 1 mM EDTA, 2 M NaCl, 0.01 % Triton X-100, 5 mM β-mercaptoethanol] at 4 °C. The high salt dialysis buffer was then exchanged into low salt dialysis buffer [10 mM Tris-HCl pH 7.5 at 4°C, 1 mM EDTA, 50 mM NaCl, 0.01 % Triton X-100, 5 mM β-mercaptoethanol] at a rate of ~0.7 ml/min over a period of 30-40 h. Nucleosome quality was assessed on a 5 % 37.5:1 acrylamide/bis 0.5 x TBE gel (120 V).

Mass Photometry Analysis of Nucleosomes

Mass photometry analysis was performed on a Refeyn Two^{MP} instrument and analyzed using DiscoverMP v2022R1 (with IScat v1.52.0 and IScat Utils v1.43.0). 24 x 50 mm with 170 ± 5 µm thickness No. 1.5H glass slides (ThorLabs, Cat# CG15KH1) and silicone gaskets (Grace Bio-labs, Cat# 103250) were washed 2x with alternating 100 % isopropanol and deionized water. Clean gaskets were then placed on the cleaned slides to serve as a sample chamber. 5 µl of 1x PBS was placed in the gasket to calibrate each sample collection then 5 µl of nucleosome samples were added for a target final concentration of ~5-10 ng/µl nucleosomes in the well. Measurements were conducted at room temperature.

Cryo-EM Sample Preparation and Data Collection

Human H2A.Z nucleosomes were reconstituted on either 601L or Sat2R-P DNA as described above with a final concentration aim of 1.6 µM in 1 ml. Reconstituted nucleosomes were dialyzed into buffer containing 10 mM HEPES-KOH pH 7.4 and 30 mM KCl then concentrated to a final concentration of ~1 mg/ml using Amicon® Ultra Centrifugal Filters (Cat# UFC5010). Samples were then mixed with 10x cryo-protectant buffer [10 mM HEPES-KOH pH 7.5, 30 mM KCl, 10 % Trehalose, 1 % Hexanediol, 1 mM $MgCl_2$] and 3 µl of each solution was applied to plasma-cleaned) Quantifoil gold R1.2/1.3 400-mesh grids (Quantifoil) either graphene coated (graphene coating was done in-house as specified in (Arimura et al., 2025) or not for the Sat2R-P and 601L samples, respectively. Grids were then vitrified using the Vitrobot Mark IV (FEI) at 100 % humidity, 2 sec blotting time, blot force 1. Data collection was conducted using the Titan Krios (ThermoFisher), equipped with a 300 kV field emission gun and a K3 direct electron detector (Gatan), at a magnification of x81,000 (0.86 Å/pixel). Total micrographs collected for each sample as follows: 4544 for unmethylated Sat2R-P nucleosomes; 6891 for methylated Sat2R-P; 7020 for unmethylated 601L; 5427 for methylated 601L. Data statistics summarized in Suppl Table 1.

Cryo-EM Data Analysis

Diagrams of analysis workflows are shown in Suppl Fig 1 and Suppl Fig 5. Micrographs were motion-corrected using MotionCor2 (Zheng et al., 2017) in Relion v4 (Scheres, 2012). Downstream analysis was conducted in CryoSPARC v4.6 (Structura Biotechnology Inc.). Motion-corrected micrographs then underwent patch CTF correction. Particles were picked using Topaz v0.2 (Bepler et al., 2019) trained on a set of 1,000-2,000 manually picked nucleosome-like

particles and then extracted to 384 pix (~330 Å) boxes with 4x binning and used for 2D classification into 200-250 classes. Particles from selected classes were then run through a series of heterogeneous refinements with 1-2 nucleosome-like models and 4 decoy models generated through *ab initio* reconstruction to sort out junk particles from those containing nucleosomes. The heterogenous refinements were iterated until greater than 90 % of particles in the round were classified as nucleosome-like. These particles were then further refined either via Refine 3D, CTF refinement, and polishing in Relion v4 (601L structures) or homogeneous and non-uniform refinements in CryoSPARC v4.6 (Sat2R-P). Particles for the methylated Sat2R-P structure underwent another heterogeneous refinement using a closed nucleosome, open, and hexasome model as starting classes to select for the highest resolved closed nucleosome structure. Final resolutions were determined using the gold standard FSC threshold (FSC = 0.143). Local resolution maps shown in Suppl Fig 3 were generated using the local resolution estimation tool with default parameters in CryoSPARC. The maps were then visualized on density maps filtered using the local filter tool with default parameters. For the *in silico* mixing 3D classification analysis (Suppl Fig 4): micrographs from both unmethylated and methylated Sat2R-P structures were merged and subjected to the data analysis pipeline described above. Six starting models representing different nucleosome structure types were then constructed using the ab initio 3D reconstruction tool. These models were then used as input volumes, and cleaned particles from the merged analysis were then sorted to each of these models using the heterorefinement tool in CryoSPARC.

Atomic Modeling and RMSD analysis

Initial atomic models were generated using previously published structures of human H2A.Z-containing histone core (PDB ID: 3WA9) (Horikoshi et al., 2013) and modified versions of either 601L DNA (PDB ID: 3UT9) (Chua et al., 2012) or Sat2R DNA (PDB ID: 5CPI) (Osakabe et al., 2015). Models were docked into the EM density maps using Phenix v1.21, then iteratively refined and assessed in Phenix v1.21 (Liebschner et al., 2019) and *Coot* 0.9.8.7 (Emsley et al., 2010). RMSD values were calculated in PyMOL v2.5.7 (Schrödinger) using the cealign function. For the Sat2R-P models, DNA positioning was determined using the EM densities at the dyad of the unmethylated map which allowed for pyrimidine and purine distinction. A two-base pair shift was determined by assessing ambiguity of densities around nucleotides which change from purine to pyrimidine, and *vice versa*, between mirrored DNA models versus those which retain identity. After determining best-fit DNA models for the unmethylated structure, the same DNA positionings were then used for the methylated structure.

DNA Preparation for Restriction Digest Assay

Non-palindromic 1HinfI_Sat2R DNA (Table 1) was prepared via PCR using Q5 polymerase (NEB Cat# M0491). Final concentrations of reaction mixture as follows: 1x Q5 reaction buffer; 200 µM dNTPs; 2 µM forward and reverse primers; 0.2 g/µl DNA template; 0.02 U/µl Q5 polymerase. Roughly 60-65 PCR cycles were run following manufacturer's protocol with a melting temperature of 60 °C. PCR products were phenol-chloroform extracted and then FPLC purified in 1xTE buffer (Superdex 200 10/300 GL increase column, Cytiva, Cat# 28990944).

Restriction Digest Assay

Nucleosomes were mixed at 30 ng per timepoint sample in 1x rCutSmart® buffer (NEB Cat# B6004S) [50 mM potassium acetate, 20 mM Tris-acetate pH 7.9 at RT, 10 mM magnesium acetate, 100 µg/ml recombinant albumin] and 0.5 U/µl HinfI restriction enzyme (NEB Cat# R0155S). Samples were incubated at 37 °C and added to stop buffer [final concentrations: 20 mM Tris-HCl pH 8.0 at RT, 20 mM EDTA, 0.1 % SDS, 0.6 mg/ml Proteinase K] at each timepoint. Stopped samples were then incubated at 55 °C for 40 min and run on a 10 % 37.5:1 acrylamide/bis 0.5x TBE gel (55 min at 150 V) and stained with SYBR™ Safe DNA stain (Thermo Fisher Scientific, Cat# S33102). Fluorescent signals were measured on a LI-COR Odyssey M system and quantified using ImageJ

via histogram analysis as previously described in (Stael et al., 2022). The ratio of Cy5: SYBR™ Safe signals was then determined for each time point and plotted. A two-tailed t-test assuming unequal variance was then performed on data from n = 5 experiments for statistical analysis.

Antibodies

Antibodies used in this study are listed in Table 2. Custom antibodies against *Xenopus laevis* H2A.Z, SRCAP, and UBN2 were generated through Cocalico Biologicals, Inc.™ using their standard protocol. Target binding of the H2A.Z antibody used for CnT-BS and SRCAP custom antibody in *Xenopus* egg extract was verified using mass spectrometry analysis (MS) (Supplementary Data 1 and 2).

Mass Spectrometry Validation

For the MS analysis, 20 µl of antibody-bound Protein A Dynabeads™ (Invitrogen, Cat# 10008D) (0.8 µg antibody per 1 µl of beads) were incubated at a 1:1 ratio with CSF egg extract (see next section) at 4 °C for 1h. Samples were collected via magnet and washed 3 times with sperm dilution buffer (SDB) [150 mM Sucrose, 10 mM HEPES-KOH pH 8.0, 1 mM $MgCl_2$, 100 mM KCl] then run on a 4-20% gradient SDS-PAGE gel as a 1 cm short-stack. The gel was then stained with Coomassie Brilliant Blue G-250 (Thermo Fisher) and the short stack was cut out. The cut gel was then destained using a solution of 30 % acetonitrile and 100 mM ammonium bicarbonate in water and dehydrated using 100 % acetonitrile. Samples were subjected to heat assisted (50 °C) trypsinization for 1 h. The resulting peptides were extracted three times with a solution of 70 % acetonitrile and 0.1 % formic acid then concentrated using a SpeedVac and resuspended in 10 µl volumes. 3 µl of purified peptides were subsequently analyzed by LC-MS/MS using a Dionex 3000 HPLC system equipped with an EasySPrayer (ES902), coupled to an Orbitrap ASCEND mass spectrometer from Thermo Scientific. Peptides were separated by reversed-phase chromatography using solvent A (0.1 % formic acid in water) and solvent B (80 % acetonitrile, 0.1 % formic acid in water) across a 45-min gradient. Data was processed using ProteomeDiscoverer 1.4 and quantified using ProteomeDiscoverer v1.4/Mascot v3.1. The spectra were then queried against a *Xenopus laevis* database (Wühr et al., 2014) and matched peptides filtered using a Percolator calculated FDR of 1 %. As proxy for protein amount, the average area of the three most abundant peptide signals was used. Relative enrichment of proteins in the sample was then calculated by dividing by known protein concentrations in *Xenopus laevis* eggs and then the enrichment over IgG control was calculated. Common contaminates were marked in red.

Xenopus laevis frogs and preparation of sperm and CSF egg extract

Female *Xenopus laevis* frogs were purchased from Xenopus 1. Male frogs were purchased from either Xenopus 1 (for use in non-sequencing experiments) or the National Xenopus Resource (*XLa.J-Strain*^{NXR}, Cat# NXR_0024; for use in sequencing experiments). Vertebrate animal protocols (20031 and 23020) approved by the Rockefeller University Institutional Animal Care and Use Committee were followed for housing and care.

CSF egg extract and demembranated sperm nuclei were prepared as specified previously (Tutter and Walter, 2006).

Sperm Pronuclei Preparation

Sperm from J-strain frogs were added to prepared CSF egg extract at a final concentration of 1,500 sperm/µl extract with a total extract volume of 200 µl for each sample. 90 ng (~1 % of total DNA) of lambda DNA (Promega Cat# D1521) was also added to assess bisulfite conversion efficiency and the extract solution was then cycled to interphase with the addition of $CaCl_2$ to a final concentration of 0.3 mM and incubated at 20 °C for 90 min. Samples were then diluted 1:4 with 1xDB3 buffer [10 mM HEPES-KOH pH 8.0, 100mM NaCl, 0.5 mM spermine, 0.5 mM spermidine, 1 mM ASEBF (GoldBio Cat#A-540-1), 1x ROCHE cOmplete™ protease inhibitor cocktail (Cat# 11697498001), 200 mM Sucrose, 0.1 % Tween-20], layered onto 1 ml of 60SDB3 [1xDB3 + 60 % sucrose] and centrifuged at 4 °C, 10,000 rpm for 45 min (Beckman Coulter SX241.5 rotor). Sample

Antigen	Host	Company	Catalog No.	Peptide Used for Generation	Dilution	Assay(s) Used In
Xl H2A.Z	Rabbit	Custom		CIHKSLIGKKGQQKTV	2 µg/ml	Western Blots
H2A.Z	Rabbit	Active Motif	Cat#39013		1:10	CnT-BS
H3	Mouse	Cosmo Bio USA	MABI0001-100-EX		1:100	CnT-BS
H4	Mouse	Active Motif	Cat# 61521		1:1000	Western Blots
Xl H2A.X-F	Rabbit	Custom, gift from David Shechter		Shechter et al. 2009	1:1000 (of serum)	Western Blots
Xl Ku70	Rabbit	Custom		Postow et al. 2008	2 µg/ml	Western Blots
Xl SRCAP	Rabbit	Custom		CPNSPSSHRVRKAKT	0.8 µg per 1 µl of beads (depletions); 12 µg/ml (WB)	Depletions; Western Blots
hsSRCAP	Rabbit	Kerafast	ESL103		0.8 µg per 1 µl of beads (depletions); 1:500 (WB)	Depletions; Western Blots
ZNHIT1	Rabbit	Proteintech	16595-1-AP		1:1000	Western Blots
P400	Rabbit	Bethyl	A300-541A		1:1000	Western Blots
ALFA tag	Alpaca (single domain antibody purified from E. coli)	NanoTag Biotechnologies	N1502-Li800-L		1:1000	Western Blots
Xl UBN2	Rabbit	Custom		CGGQNKGDAKLPRKNR	1.5 µg per 1 µl of beads (depletions); 2 µg/mL (WB)	Depletions; Western Blots
xKID	Rabbit	Custom		Funabiki and Murray 2000	1 µg/mL	Western Blots
Xl Dppa2	Rabbit	Custom		Xue et al. 2013	5 µg/mL	Western Blots
Secondaries						
IRDye® 800CW anti-Rabbit IgG	Goat	LICORbio	926-32211		1:10000	Western Blots
IRDye® 680RD anti-Mouse IgG	Goat	LICORbio	926-68070		1:10000	Western Blots
anti-Rabbit IgG	Guinea Pig	antibodies-online.com	ABIN101961		1:100	CnT-BS
anti-Mouse IgG	Rabbit	abcam	ab46540		1:100	CnT-BS

Table 2. **Antibodies used in this study.**

pellets were washed 2x with 1xDB3, centrifuging at 4,000 x *g*, 4 °C for 4 min, then resuspended in 1x CnT-WB [20 mM HEPES-KOH pH 7.8, 150 mM NaCl, 0.5 mM spermidine, 1x ROCHE cOmplete™ protease inhibitor cocktail, 0.1 % Tween-20].

XTC-2 Cell Line

XTC-2 cells (gift from Dr. David Shechter) were cultured in Leibovitz's L-15 Medium (Gibco™, Cat# 11415064) (0.7x amphibian strength, diluted with cell culture grade water (Corning®, Cat# 46-000-CV)) supplemented with 500 U/ml each of penicillin and streptomycin (Gibco™, Cat# 15140122), and 10 % FBS (R&D systems, Cat# S11150). XTC-2 cells were cultured in a 26 °C incubator without CO_2 supply. Cell line identity was verified via mitotic-spread karyotyping.

XTC-2 Nuclei Preparation

XTC-2 cells were harvested at 90-100 % confluency from a 15 cm dish. Nuclei isolation was performed at 4 °C using the Nuclei EZ Prep kit (Millipore Cat# NUC101-1KT) as per manufacturer's protocol and resuspended in 1x CnT-WB. For each sample, 18 ng (~1 % of total DNA) of unmethylated lambda DNA (Promega Cat# D1521) was added to 300,000 nuclei to assess for bisulfite conversion efficiency.

Purification of Tn5

Tn5 was purified as described in (Soroczynski et al., 2024). Briefly, VR124 pETv2-10His-pG-Tn5 (E54K, L372P) *E. coli* strain (Addgene #198468) were cultured to log growth phase and Tn5 expression induced with IPTG addition. Cells were harvested at 8,000 x *g*, 30 min at 4 °C, washed with ice-cold DPBS, re-pelleted and frozen. Frozen pellets were then resuspended at 4 °C in lysis buffer LysEQ [20 mM HEPES pH 7.8, 800 mM NaCl, 20 mM imidazole, 10 % glycerol, 1 mM EDTA, 2 mM TCEP-HCl, 1x EDTA-free cOmplete protease inhibitor] and sonicated. Lysates were pelleted at 20,000 x *g*, 35 min at 4 °C, then filtered through a 0.45 µm PES filter. Supernatant was then loaded onto a HisTrap HP 5 ml column (Cytiva, Cat# 17-5247-01) pre-equilibrated with LysEQ buffer. The loaded column was then washed with 10 column volumes each of WashB1 [20 mM HEPES pH 7.8, 800 mM NaCl, 30 mM imidazole, 10 % glycerol, 1 mM EDTA, 2 mM TCEP-HCl] and WashB2 [20 mM HEPES pH 7.8, 800 mM NaCl, 45 mM Imidazole, 10 % glycerol, 1 mM EDTA, 2 mM TCEP-HCl]. Protein was then eluted with EluB [20 mM HEPES pH 7.8, 800 mM NaCl, 400 mM imidazole, 10 % glycerol, 1 mM EDTA, 2 mM TCEP-HCl]. Tn5-containing fractions were pooled and dialyzed 4 °C overnight in SECB buffer [50 mM Tris-HCl pH 7.5, 800 mM NaCl, 10 % glycerol, 0.2 mM EDTA, 2 mM DTT] then filtered through a 0.45 µm PES filter and FPLC purified on a HiLoad 16/600 Superdex 200 pg column (Cytiva, Cat#: 28989335). Purified fractions were pooled and concentrated with a 30 MWCO Amicon Ultra Centrifugal filter (final concentration 12 µM) and mixed with UltraPure glycerol to a final concentration of 55 % glycerol. Purified Tn5 was stored at −20 °C.

CUT&Tag-Bisulfite Library Preparation

Sequencing libraries were prepared as previously described in (Li et al., 2021). Briefly, prepared nuclei samples were bound to 10 µl of activated concanavalin A beads (EpiCypher Cat# 21-1401) and incubated with specified primary and secondary antibodies (Table 2) in 50 µl Antibody Binding Buffer [CnT-WB + 2 mM EDTA + 0.1 % w/v BSA] for 1 h shaking at RT, washing 3x with CnT-WB between each incubation. Samples were then incubated with 50 µl of transposome complex (1:1 pG-Tn5:adaptor primer mix, ~0.1-0.2 µM final to each sample) in CnT-300 [CnT-WB with 300 mM NaCl] for 1 h at RT then washed with CnT-300. Transposome activity was initiated with addition of 300 µl Tagmentation Buffer [20 mM HEPES-KOH pH 7.8, 300 mM NaCl, 0.5 mM spermidine, 10 mM $MgCl_2$, 1x ROCHE cOmplete™ protease inhibitor cocktail, 0.1 % Tween-20] and incubated 37 °C, 1500 rpm on thermomixer, 1 h. Reactions were stopped with addition of stop buffer [15 mM EDTA, 0.1 % SDS, 0.2 mg/mL Proteinase K final concentrations] and incubated at 55 °C overnight, then phenol-chloroform extracted. Purified samples were resuspended in 11 µl of 10 mM Tris-HCl, pH 8.0 and oligonucleotide replacement/gap repaired carried out through addition of 2 µl of 10 µM Tn5mC-ReplO1 DNA oligo (Table 1), 2 µl 10x Ampligase Buffer (Lucigen), 2 µl dNTP

mix (2.5 mM for each dNTP). Solutions were subject to the following heating protocol: 50 °C 1 min, 45 °C 10 min, cool to 37 °C at −0.1 °C/second. Once at 37 °C, 3U of T4 DNA polymerase and 12.5U of Ampligase (Lucigen) were added and samples incubated for 30 min. Reactions were stopped with 20 mM EDTA final and purified using the MinElute PCR purification kit (Qiagen Cat# 28004). Samples were bisulfite converted using the EZ DNA Methylation-Lightning Kit (Zymo Research Cat# D5030) and libraries amplified (14 cycles) using NEBNext Q5U Master Mix (NEB Cat# M0597) and Illumina Nextra i5/i7 adapter primers.

Sequencing Data Analysis

Adapter trimming, deduplication, and genome alignment

Libraries were sent to Novogene for sequencing on the NovaSeqX Plus system (PE150). XTC-2 data was then downsampled to 30 million reads using seqtk (v1.5-r133) to have all samples at similar read depths. Adapter trimming and dedeuplication of the demultiplexed reads was then done using fastp v0.24.0 (Chen, 2023) [--adapter_sequence CTGTCTCTTATACAC --adapter_sequence_r2 CTGTCTCTTATACAC -g --poly_g_min_len 5 -p -l 20 --cut_tail -y -Y 20 -q 20 –dedup]. Processed reads were then aligned to the *Xenopus laevis* genome (Xenla 10.1) and methylated CpG proportions for all mapped reads calculated using Bismark v0.24.2 (Krueger and Andrews, 2011) [-q --local --score-min G,20,8 --ignore-quals --no-mixed --no-discordant --dovetail --maxins 700].

Count matrix generation and sequencing depth normalization

The *Xenopus laevis* genome was subset into 1000 bp bins. Reads from processed bam files were then tallied according to bins to generate a genome-wide count matrix. Mitochondrial associated reads and bins which contained no reads across all samples were removed. Size factors were then estimated using DESeq2 v1.42.1 (Love et al., 2014) to generate sequence depth normalized bigwig files. Count matrices were also vst transformed in DESeq2 then used to generate the read fragment correlation plot. For other analyses, only genomic bins containing at least 17 reads across at least 2 samples were kept and replicates for each condition were averaged.

DNA Methylation analysis

To get methylated CpG proportions for each sample (Fig 4A), H2A.Z peaks were first identified with SEACR (v1.3) (Meers et al., 2019) using a cutoff of 0.025 by AUC with a stringent threshold. Individual CpG data was then extracted using Bismark with a cutoff of 5 reads and disregarding the first 9 bp of read 2 (due to adapter fill-in). Methylation proportions for H2A.Z samples were then calculated for CpGs overlapping with H2A.Z peaks. For H3, only regions outside of identified H2A.Z peaks were used to assess the CpG methylation status of general genomic background non-coincident with H2A.Z enriched areas. To generate H3-associated methylation 500 bp tiles for use in plotting (Suppl Fig 9B-D), methylation data was extracted with a specified cutoff of 1 read and disregarding the first 9 bp of read 2 then imported into a methylRawList object with a minimum read coverage of 2 and counted over 500 bp tiles with a 500 bp step size and a minimum of 2 CpG sites using methylKit v1.28.0 (Akalin et al., 2012).

Generation of plots

Genomic annotations for the top 20 % of filtered bins containing the most reads for each condition were generated and proportions plotted using ChIPseeker v1.38.0 (Yu et al., 2015) with reference gene annotations gathered from Xenbase (Fisher et al., 2023). Heat maps and plot profiles were created using deepTools v3.5.5 (Ramírez et al., 2016). For comparison of H3 methylation sites and H2A.Z, a signal matrix was first generated using the tiled H3 methylation bigwigs against all annotated *Xenopus laevis* genes, removing genes with no methylation data available. The resulting gene list was then used to plot corresponding H2A.Z signals.

in vitro mRNA Synthesis

DNA sequences of proteins of interest were cloned into pSP64T plasmids modified to include a Kozak sequence (GCCACC) upstream of the coding sequence and linearized. pSP64T (DM#111) was a gift from Douglas Melton (Addgene Plasmid# 15030). RNA production was carried out using the

MEGAscript™ SP6 transcription kit (Invitrogen, Cat# AM1330) as per manufacturer's protocol, with the addition of 4.5 mM CleanCap® Reagent AG (TriLink, Cat# N-7113) and a reduction in GTP concentration down to 1.5 mM final.

Chromatinization in Egg Extract Assays

pAS696 containing a 19-mer array of Widom 601 DNA was a gift from Aaron Straight (Guse et al., 2011). 601 and HSat2 arrays were digested with XbaI and EcoRI or XbaI and BamHI, respectively, along with DraI and HaeII. DNA fragments containing the array sequence were then purified through a PEG precipitation titration, starting at 4.5 % of PEG (MW8000) and increasing in 0.5 % increments until 8 % (NaCl added to 0.5 M final concentration in the starting solution). Fragment containing fractions were then assessed via agarose gel and purified via phenol-chloroform extraction. Fragment ends were biotinylated with biotin-14-dATP (Jena Bioscience, Cat# NU-835-BIO14-S) using Klenow Fragment (3'→ 5' exo-) (NEB Cat# M0212) following manufacturer's protocol. Biotinylated DNA was phenol-chloroform extracted and bound to M-280 Streptavidin Dynabeads™ (Invitrogen, Cat# 11206D) at 300 ng DNA per 1 µl of beads. DNA bead binding was carried out at room temperature for a minimum of 1 h shaking in the following solution: 1x DNA Bead Binding buffer (DBB) [750 mM NaCl, 50 mM Tris-HCl pH 8.0, 0.25 mM EDTA, 0.05 % Triton-X-100]; 2.5 % (w/v) polyvinyl alcohol; 750 mM NaCl. DNA beads were then washed 2x with DBB and 3x with sperm dilution buffer (SDB) [150 mM Sucrose, 10 mM HEPES-KOH pH 8.0, 1 mM $MgCl_2$, 100 mM KCl] and added to egg extract at a ratio of 4 µl DNA beads to 30 µl of egg extract. Experiments that did not use mRNA for exogenous protein expression also included 0.1 mg/ml cycloheximide dissolved in EtOH. $CaCl_2$ was then added to the extracts at a final concentration of 0.3 mM and incubated at 20 °C for 1 h. Samples were then diluted 10-fold with SDB, and DNA beads were collected on a magnetic rack and washed 3x with SDB + 0.05 % Triton-X-100 before running on SDS-PAGE gel and assessed via western blot.

Western Blot Analysis

Samples were boiled in 1x SDS loading buffer [125 mM Tris-HCl pH 6.8, 0.01 % SDS, 25 % glycerol, 0.03 mg/ml bromo-phenol blue, 350 mM 2-mercaptoethanol] then run on either a 4-20 % SDS-PAGE gel (Bio-Rad, Cat# 4561096) or 3-8 % Tris-acetate gel (for SRCAP detection) (Invitrogen, Cat# EA0375BOX). Samples were then transferred from the gel to a nitrocellulose membrane (Cytiva, 0.1 µm pore size, Cat# 10600000) overnight at 4 °C in 1x transfer buffer [20 mM Tris, 150 mM Glycine, 20 % Methanol] (14V). Membranes were blocked for 30 min at RT with Intercept® (TBS) Protein-Free Blocking Buffer (LICORbio, Cat# 927-80001), followed by primary antibody incubation (diluted in Intercept® T20 (TBS) Antibody diluent (LICORbio, Cat# 927-65001)) for 1 h at RT. Membranes were then washed 3x, 5 min each wash, in 1xTBS+0.05 % Tween-20 then incubated with appropriate secondary antibodies for 1 h at RT and washed. Blots were then imaged on a LI-COR Odyssey M system and signals quantified using ImageJ via histogram analysis as previously described in (Stael et al., 2022). Ratios of either H2A.Z or H2A.X-F signals to H4 signals were then determined for normalization purposes in the chromatinization assays.

Antibody Depletion from Egg Extract

Either SRCAP or UBN2 antibody was bound to Protein A Dynabeads™ (Invitrogen, Cat# 10008D) at a concentration of either 0.8 µg or 1.5 µg antibody per 1 µl of beads, respectively, overnight at 4 °C in wash/coupling (W/C) buffer [10 mM HEPES-KOH pH 8.0, 150 mM NaCl]. Beads were then washed 2x with W/C buffer and 3x with SDB. An equal volume of beads and egg extract (supplemented with 0.1 mg/ml cycloheximide) were then incubated together for 1 h at 4 °C and beads removed via magnet.

Other Instruments and Software Used

ÄKTA pure SN2626712 (Cytiva) and UNICORN v7.11 (Cytiva) for FPLC purification of histone proteins.

UCSF ChimeraX v1.9 (Meng et al., 2023) for structure visualization.

LI-COR Odyssey M, LI-COR Acquisition v1.2, and ImageJ v1.54f (Schneider et al., 2012) for western blot and gel imaging, data analysis, and visualization.

QuantStudio™ 5 (Thermo Fisher, Cat# A28574) and QuantStudio™ Design & Analysis v2.7 for QC of sequencing samples.

Inkscape v1.3.2 for figure generation.

Data availability

DNA sequencing data can be accessed at GEO (accession number GSE295057). Raw image data and analysis code can be accessed at Zenodo DOI: 10.5281/zenodo.15360677. Cryo-EM maps and atomic models can be accessed with PDB IDs: 9OGS, 9OGZ (UM Sat2R-P); 9OGR, 9OH0 (Me Sat2R-P); 9OH1 (UM 601L); 9OH2 (Me 601L) and EMD IDs: EMD-70474 (UM Sat2R-P); EMD-70473 (Me Sat2R-P); EMD-70480 (UM 601L); EMD-70481 (Me 601L).

Acknowledgements

We thank Joanna Yeung, Justin Rendleman, Viviana Risca, and the rest of the Risca lab, as well as Richard Koche, for their invaluable advice and sharing of reagents for the sequencing and bioinformatics analysis. We thank members of the Funabiki lab for their continual advice, particularly Yiming Niu for Cryo-EM analysis help and Isabel Wassing for help in generating the α-H2A.Z antibody. We thank Dr. David Shechter for the XTC-2 cell line and α-H2A.X-F serums, Shixin Liu and Aaron Straight for plasmids, and Tarun Kapoor for use of the Refeyn Two^{MP}. This work was conducted using the High-Performance Computing Resource Center, the Evelyn Gruss Lipper Cryo-Electron Microscopy Resource Center, and the Proteomics Resource Center at the Rockefeller University (with the help of Henrik Molina and Soeren Heissel for proteomics analysis). Animal husbandry was supported by the staff at the Rockefeller Comparative Bioscience Center.

Additional information

Author contributions

R.M.S. and H.F. conceived and designed the study. R.M.S. and Y.A. designed and performed the Cryo-EM analysis. R.M.S. and H.A.K. designed physiological experiments. H.A.K. created the custom α-SRCAP antibody, prepared XTC-2 nuclei, and purified pG-Tn5. R.M.S. conducted all experiments and analysis. R.M.S. and H.F. prepared the manuscript with input from H.A.K. and Y.A.

Funding

This work was supported by the National Institutes of Health [R35GM132111] to H.F; the National Science Foundation Graduate Research Fellowship Program to R.M.S; Japan Society for the Promotion of Science Overseas Research Fellowships to H.A.K; and Osamu Hayaishi Memorial Scholarship for Study Abroad to Y.A..

Funding

Funder	Grant reference number	Author
HHS | National Institutes of Health (NIH)	R35GM132111	Hironori Funabiki
NSF | National Science Foundation Graduate Research Fellowship Program (GRFP)		Rochelle M Shih
MEXT | Japan Society for the Promotion of Science (JSPS)		Hide A Konishi
Osamu Hayaishi Memorial Scholarship for Study Abroad		Yasuhiro Arimura

Author ORCID iDs

Rochelle M Shih: https://orcid.org/0000-0002-3218-4479
Hide A Konishi: https://orcid.org/0000-0001-9529-9321
Hironori Funabiki: https://orcid.org/0000-0003-4831-4087

Additional files

Supplementary Figures

Supplementary Tables

Supplementary Data 1

Supplementary Data 2

References

Akalin A, Kormaksson M, Li S, Garrett-Bakelman FE, Figueroa ME, Melnick A, Mason CE (2012) MethylKit: a comprehensive R package for the analysis of genome-wide DNA methylation profiles. *Genome Biology* **13**:1-9 https://doi.org/10.1186/gb-2012-13-10-r87 | PubMed

Almouzni G, Wolffe AP (1993) Nuclear assembly, structure, and function: the use of Xenopus in vitro systems. *Experimental cell research* **205**:1-15 https://doi.org/10.1006/EXCR.1993.1051 | PubMed

Arimura Y, Konishi HA, Funabiki H (2025) MagIC-Cryo-EM: Structural determination on magnetic beads for scarce macromolecules in heterogeneous samples. *eLife* **13** https://doi.org/10.7554/ELIFE.103486.2

Arimura Y, Shih RM, Froom R, Funabiki H (2021) Structural features of nucleosomes in interphase and metaphase chromosomes. *Molecular cell* **81**:4377 https://doi.org/10.1016/J.MOLCEL.2021.08.010 | PubMed

Belotserkovskaya R, Oh S, Bondarenko VA, Orphanides G, Studitsky VM, Reinberg D (2003) FACT facilitates transcription-dependent nucleosome alteration. *Science* **301**:1090-1093 https://doi.org/10.1126/SCIENCE.1085703 | PubMed

Bepler T, Morin A, Rapp M, Brasch J, Shapiro L, Noble AJ, Berger B (2019) Positive-unlabeled convolutional neural networks for particle picking in cryo-electron micrographs. *Nature Methods* **16**:1153-1160 https://doi.org/10.1038/s41592-019-0575-8 | PubMed

Berta DG, Kuisma H, Välimäki N, Räisänen M, Jäntti M, Pasanen A, Karhu A, Kaukomaa J, Taira A, Cajuso T, *et al.* (2021) Deficient H2A.Z deposition is associated with genesis of uterine leiomyoma. *Nature* **596**:398-403 https://doi.org/10.1038/s41586-021-03747-1 | PubMed

Bevington S, Boyes J (2013) Transcription-coupled eviction of histones H2A/H2B governs V(D)J recombination. *EMBO Journal* **32**:1381-1392 https://doi.org/10.1038/emboj.2013.42 | PubMed

Bintu L, Kopaczynska M, Hodges C, Lubkowska L, Kashlev M, Bustamante C (2011) The elongation rate of RNA polymerase determines the fate of transcribed nucleosomes. *Nature structural & molecular biology* **18**:1394-1399 https://doi.org/10.1038/NSMB.2164 | PubMed

Bönisch C, Hake SB (2012) Histone H2A variants in nucleosomes and chromatin: More or less stable?. *Nucleic Acids Research* **40**:10719-10741 https://doi.org/10.1093/nar/gks865 | PubMed

Buitrago D, Labrador M, Arcon JP, Lema R, Flores O, Esteve-Codina A, Blanc J, Villegas N, Bellido D, Gut M, *et al.* (2021) Impact of DNA methylation on 3D genome structure. *Nature Communications* **12**:1-17 https://doi.org/10.1038/s41467-021-23142-8 | PubMed

Buschbeck M, Hake SB (2017) Variants of core histones and their roles in cell fate decisions, development and cancer. *Nature Reviews Molecular Cell Biology* **18**:299-314 https://doi.org/10.1038/nrm.2016.166 | PubMed

Chen P, Zhao J, Wang Y, Wang M, Long H, Liang D, Huang L, Wen Z, Li W, Li X, *et al.* (2013) H3.3 actively marks enhancers and primes gene transcription via opening higher-ordered chromatin. *Genes and Development* **27**:2109-2124 https://doi.org/10.1101/gad.222174.113 | PubMed

Chen Q, Yang R, Korolev N, Liu CF, Nordenskiöld L (2017) Regulation of Nucleosome Stacking and Chromatin Compaction by the Histone H4 N-Terminal Tail–H2A Acidic Patch Interaction. *Journal of Molecular Biology* **429**:2075-2092 https://doi.org/10.1016/J.JMB.2017.03.016 | PubMed

Chen S (2023) Ultrafast one-pass FASTQ data preprocessing, quality control, and deduplication using fastp. *iMeta* **2**:e107 https://doi.org/10.1002/IMT2.107 | PubMed

Chodavarapu RK, Feng S, Bernatavichute Y V., Chen PY, Stroud H, Yu Y, Hetzel JA, Kuo F, Kim J, Cokus SJ, *et al.* (2010) Relationship between nucleosome positioning and DNA methylation. *Nature* **466**:388-392 https://doi.org/10.1038/nature09147 | PubMed

Choy JS, Wei S, Lee JY, Tan S, Chu S, Lee TH (2010) DNA methylation increases nucleosome compaction and rigidity. *Journal of the American Chemical Society* **132**:1782-1783 https://doi.org/10.1021/ja910264z | PubMed

Chua EYD, Vasudevan D, Davey GE, Wu B, Davey CA (2012) The mechanics behind DNA sequence-dependent properties of the nucleosome. *Nucleic acids research* **40**:6338-6352 https://doi.org/10.1093/NAR/GKS261 | PubMed

Coleman-Derr D, Zilberman D (2012) Deposition of Histone Variant H2A.Z within Gene Bodies Regulates Responsive Genes. *PLoS Genetics* **8**:e1002988 https://doi.org/10.1371/journal.pgen.1002988 | PubMed

Colino-Sanguino Y, Clark SJ, Valdes-Mora F (2022) The H2A.Z-nucleosome code in mammals: emerging functions. *Trends in Genetics* **38**:273-289 https://doi.org/10.1016/J.TIG.2021.10.003 | PubMed

Collings CK, Waddell PJ, Anderson JN (2013) Effects of DNA methylation on nucleosome stability. *Nucleic Acids Research* **41**:2918-2931 https://doi.org/10.1093/NAR/GKS893 | PubMed

Conerly ML, Teves SS, Diolaiti D, Ulrich M, Eisenman RN, Henikoff S (2010) Changes in H2A.Z occupancy and DNA methylation during B-cell lymphomagenesis. *Genome Research* **20**:1383-1390 https://doi.org/10.1101/gr.106542.110 | PubMed

Dai L, Xiao X, Pan L, Shi L, Xu N, Zhang Z, Feng X, Ma L, Dou S, Wang P, *et al.* (2021) Recognition of the inherently unstable H2A nucleosome by Swc2 is a major determinant for unidirectional H2A.Z exchange. *Cell Reports* **35**:109183 https://doi.org/10.1016/J.CELREP.2021.109183 | PubMed

Diegmüller F, Leers J, Hake SB (2025) The "Ins and Outs and What-Abouts" of H2A.Z: A tribute to C. David Allis. *The Journal of biological chemistry* **301** https://doi.org/10.1016/J.JBC.2025.108154 | PubMed

Dyer PN, Edayathumangalam RS, White CL, Bao Y, Chakravarthy S, Muthurajan UM, Luger K (2003) Reconstitution of Nucleosome Core Particles from Recombinant Histones and DNA. *Methods in Enzymology* **375**:23-44 https://doi.org/10.1016/S0076-6879(03)75002-2 | PubMed

Ehrlich M (2009) DNA hypomethylation in cancer cells. *Epigenomics* **1**:239-259 https://doi.org/10.2217/EPI.09.33 | PubMed

Ehrlich M (2003) The ICF syndrome, a DNA methyltransferase 3B deficiency and immunodeficiency disease. *Clinical Immunology* **109**:17-28 https://doi.org/10.1016/S1521-6616(03)00201-8 | PubMed

Emsley P, Lohkamp B, Scott WG, Cowtan K (2010) Biological Crystallography Features and development of Coot. *Acta Crystallographica Section D Biological Crystallography* **D66**:486-501 https://doi.org/10.1107/S0907444910007493 | PubMed

Engelke DR, Ng SY, Shastry BS, Roeder RG (1980) Specific interaction of a purified transcription factor with an internal control region of 5S RNA genes. *Cell* **19**:717-728 https://doi.org/10.1016/S0092-8674(80)80048-1 | PubMed

Faast R, Thonglairoam V, Schulz TC, Beall J, Wells JRE, Taylor H, Matthaei K, Rathjen PD, Tremethick DJ, Lyons I (2001) Histone variant H2A.Z is required for early mammalian development. *Current Biology* **11**:1183-1187 https://doi.org/10.1016/S0960-9822(01)00329-3 | PubMed

Fisher M, James-Zorn C, Ponferrada V, Bell AJ, Sundararaj N, Segerdell E, Chaturvedi P, Bayyari N, Chu S, Pells T, *et al.* (2023) Xenbase: key features and resources of the Xenopus model organism knowledgebase. *Genetics* **224**:18 https://doi.org/10.1093/GENETICS/IYAD018 | PubMed

Fujii Y, Wakamori M, Umehara T, Yokoyama S (2016) Crystal structure of human nucleosome core particle containing enzymatically introduced CpG methylation. *FEBS Open Bio* **6**:498-514 https://doi.org/10.1002/2211-5463.12064 | PubMed

Funabiki H, Murray AW (2000) The Xenopus Chromokinesin Xkid Is Essential for Metaphase Chromosome Alignment and Must Be Degraded to Allow Anaphase Chromosome Movement. *Cell* **102**:411-424 https://doi.org/10.1016/S0092-8674(00)00047-7 | PubMed

Giaimo BD, Ferrante F, Herchenröther A, Hake SB, Borggrefe T (2019) The histone variant H2A.Z in gene regulation. *Epigenetics & Chromatin* **12**:1-22 https://doi.org/10.1186/S13072-019-0274-9 | PubMed

Götzke H, Kilisch M, Martínez-Carranza M, Sograte-Idrissi S, Rajavel A, Schlichthaerle T, Engels N, Jungmann R, Stenmark P, Opazo F, *et al.* (2019) The ALFA-tag is a highly versatile tool for nanobody-based bioscience applications. *Nature Communications* **10**:1-12 https://doi.org/10.1038/s41467-019-12301-7 | PubMed

Guse A, Carroll CW, Moree B, Fuller CJ, Straight AF (2011) In vitro centromere and kinetochore assembly on defined chromatin templates. *Nature* **477**:354-358 https://doi.org/10.1038/NATURE10379 | PubMed

Hall LL, Byron M, Carone DM, Whitfield TW, Pouliot GP, Fischer A, Jones P, Lawrence JB (2017) Demethylated HSATII DNA and HSATII RNA Foci Sequester PRC1 and MeCP2 into Cancer-Specific Nuclear Bodies. *Cell reports* **18**:2943-2956 https://doi.org/10.1016/J.CELREP.2017.02.072 | PubMed

Hardy S, Jacques PÉ, Gévry N, Forest A, Fortin MÈ, Laflamme L, Gaudreau L, Robert F (2009) The euchromatic and heterochromatic landscapes are shaped by antagonizing effects of transcription on H2A.Z deposition. *PLoS genetics* **5**:e1000687 https://doi.org/10.1371/JOURNAL.PGEN.1000687 | PubMed

Heo K, Kim H, Choi SH, Choi J, Kim K, Gu J, Lieber MR, Yang AS, An W (2008) FACT-mediated exchange of histone variant H2AX regulated by phosphorylation of H2AX and ADP-ribosylation of Spt16. *Molecular cell* **30**:86-97 https://doi.org/10.1016/J.MOLCEL.2008.02.029 | PubMed

Hite RK, MacKinnon R (2017) Structural Titration of Slo2.2, a Na+-Dependent K+ Channel. *Cell* **168**:390-399.e11. https://doi.org/10.1016/J.CELL.2016.12.030 | PubMed

Hoogenboom WS, Klein Douwel D, Knipscheer P (2017) Xenopus egg extract: A powerful tool to study genome maintenance mechanisms. *Developmental Biology* https://doi.org/10.1016/j.ydbio.2017.03.033 | PubMed

Horikoshi N, Arimura Y, Taguchi H, Kurumizaka H (2016) Crystal structures of heterotypic nucleosomes containing histones H2A.Z and H2A. *Open Biology* **6**:160127 https://doi.org/10.1098/rsob.160127 | PubMed

Horikoshi N, Kujirai T, Sato K, Kimura H, Kurumizaka H (2019) Structure-based design of an H2A.Z.1 mutant stabilizing a nucleosome in vitro and in vivo. *Biochemical and Biophysical Research Communications* **515**:719-724 https://doi.org/10.1016/j.bbrc.2019.06.012 | PubMed

Horikoshi N, Sato K, Shimada K, Arimura Y, Osakabe A, Tachiwana H, Hayashi-Takanaka Y, Iwasaki W, Kagawa W, Harata M, *et al.* (2013) Structural polymorphism in the L1 loop regions of human H2A.Z.1 and H2A.Z.2. *Acta Crystallographica Section D: Biological Crystallography* **69**:2431-2439 https://doi.org/10.1107/S090744491302252X | PubMed

Hsu CC, Shi J, Yuan C, Zhao D, Jiang S, Lyu J, Wang X, Li H, Wen H, Li W, *et al.* (2018a) Recognition of histone acetylation by the GAS41 YEATS domain promotes H2A.Z deposition in non-small cell lung cancer. *Genes and Development* **32**:58-69 https://doi.org/10.1101/gad.303784.117 | PubMed

Hsu CC, Zhao D, Shi J, Peng D, Guan H, Li Y, Huang Y, Wen H, Li W, Li H, *et al.* (2018b) Gas41 links histone acetylation to H2A.Z deposition and maintenance of embryonic stem cell identity. *Cell discovery* **4** https://doi.org/10.1038/S41421-018-0027-0 | PubMed

Ibarra-Morales D, Rauer M, Quarato P, Rabbani L, Zenk F, Schulte-Sasse M, Cardamone F, Gomez-Auli A, Cecere G, Iovino N (2021) Histone variant H2A.Z regulates zygotic genome activation. *Nature communications* **12** https://doi.org/10.1038/S41467-021-27125-7 | PubMed

Ishibashi T, Dryhurst D, Rose KL, Shabanowitz J, Hunt DF, Ausió J (2009) Acetylation of vertebrate H2A.Z and its effect on the structure of the nucleosome. *Biochemistry* **48**:5007-5017 https://doi.org/10.1021/bi900196c | PubMed

Jackson K, Yu MC, Arakawa K, Fiala E, Youn B, Fiegl H, Müller-Holzner E, Widschwendter M, Ehrlich M (2004) DNA hypomethylation is prevalent even in low-grade breast cancers. *Cancer biology & therapy* **3**:1225-1231 https://doi.org/10.4161/CBT.3.12.1222 | PubMed

Jenness C, Giunta S, Müller MM, Kimura H, Muir TW, Funabiki H (2018) HELLS and CDCA7 comprise a bipartite nucleosome remodeling complex defective in ICF syndrome. *Proceedings of the National Academy of Sciences of the United States of America* **115**:E876-E885 https://doi.org/10.1073/PNAS.1717509115 | PubMed

Jeronimo C, Watanabe S, Kaplan CD, Peterson CL, Robert F (2015) The Histone Chaperones FACT and Spt6 Restrict H2A.Z from Intragenic Locations. *Molecular cell* **58**:1113-1123 https://doi.org/10.1016/J.MOLCEL.2015.03.030 | PubMed

Jimenez-Useche I, Nurse NP, Tian Y, Kansara BS, Shim D, Yuan C (2014) DNA Methylation Effects on Tetra-Nucleosome Compaction and Aggregation. *Biophysical Journal* **107**:1629-1636 https://doi.org/10.1016/J.BPJ.2014.05.055 | PubMed

Jimenez-Useche I, Yuan C (2012) The Effect of DNA CpG Methylation on the Dynamic Conformation of a Nucleosome. *Biophysical Journal* **103**:2502-2512 https://doi.org/10.1016/J.BPJ.2012.11.012 | PubMed

Jin C, Felsenfeld G (2007) Nucleosome stability mediated by histone variants H3.3 and H2A.Z. *Genes and Development* **21**:1519-1529 https://doi.org/10.1101/gad.1547707 | PubMed

Jin C, Zang C, Wei G, Cui K, Peng W, Zhao K, Felsenfeld G (2009) H3.3/H2A.Z double variant-containing nucleosomes mark "nucleosome-free regions" of active promoters and other regulatory regions. *Nature Genetics* **41**:941-945 https://doi.org/10.1038/ng.409 | PubMed

Jung H, Sokolova V, Lee G, Stevens VR, Tan D (2024) Structural and Biochemical Characterization of the Nucleosome Containing Variants H3.3 and H2A.Z. *Epigenomes* **8**:21 https://doi.org/10.3390/epigenomes8020021

Katagiri C, Ohsumi K (1994) Remodeling of sperm chromatin induced in egg extracts of amphibians. *Int J Dev Biol* **38**:209-216 https://doi.org/10.1387/ijdb.7981030 | PubMed

Kaya-Okur HS, Janssens DH, Henikoff JG, Ahmad K, Henikoff S (2020) Efficient low-cost chromatin profiling with CUT&Tag. *Nature Protocols* **15**:3264-3283 https://doi.org/10.1038/s41596-020-0373-x | PubMed

King AD, Huang K, Rubbi L, Liu S, Wang CY, Wang Y, Pellegrini M, Fan G (2016) Reversible Regulation of Promoter and Enhancer Histone Landscape by DNA Methylation in Mouse Embryonic Stem Cells. *Cell reports* **17**:289-302 https://doi.org/10.1016/J.CELREP.2016.08.083 | PubMed

Kireeva ML, Walter W, Tchernajenko V, Bondarenko V, Kashlev M, Studitsky VM (2002) Nucleosome remodeling induced by RNA polymerase II: loss of the H2A/H2B dimer during transcription. *Molecular cell* **9**:541-552 https://doi.org/10.1016/S1097-2765(02)00472-0 | PubMed

Krueger F, Andrews SR (2011) Bismark: a flexible aligner and methylation caller for Bisulfite-Seq applications. *Bioinformatics* **27**:1571-1572 https://doi.org/10.1093/BIOINFORMATICS/BTR167 | PubMed

Kurumizaka H, Kujirai T, Takizawa Y (2021) Contributions of Histone Variants in Nucleosome Structure and Function. *Journal of Molecular Biology* **433**:166678 https://doi.org/10.1016/J.JMB.2020.10.012 | PubMed

Langecker M, Ivankin A, Carson S, Kinney SRM, Simmel FC, Wanunu M (2015) Nanopores suggest a negligible influence of CpG methylation on nucleosome packaging and stability. *Nano Letters* **15**:783-790 https://doi.org/10.1021/nl504522n | PubMed

Lashgari A, Millau JF, Jacques PÉ, Gaudreau L (2017) Global inhibition of transcription causes an increase in histone H2A.Z incorporation within gene bodies. *Nucleic acids research* **45**:12715-12722 https://doi.org/10.1093/NAR/GKX879 | PubMed

Laskey RA, Mills AD, Morris NR (1977) Assembly of SV40 chromatin in a cell-free system from Xenopus eggs. *Cell* **10**:237-243 https://doi.org/10.1016/0092-8674(77)90217-3 | PubMed

Lee JY, Lee J, Yue H, Lee TH (2015) Dynamics of Nucleosome Assembly and Effects of DNA Methylation. *Journal of Biological Chemistry* **290**:4291-4303 https://doi.org/10.1074/JBC.M114.619213 | PubMed

Lee JY, Lee TH (2012) Effects of DNA methylation on the structure of nucleosomes. *Journal of the American Chemical Society* **134**:173-175 https://doi.org/10.1021/ja210273w | PubMed

Lewis TS, Sokolova V, Jung H, Ng H, Tan D (2021) Structural basis of chromatin regulation by histone variant H2A.Z. *Nucleic Acids Research* https://doi.org/10.1093/nar/gkab907 | PubMed

Li R, Grimm SA, Wade PA (2021) CUT&Tag-BS for simultaneous profiling of histone modification and DNA methylation with high efficiency and low cost. *Cell Reports Methods* **1**:100118 https://doi.org/10.1016/J.CRMETH.2021.100118 | PubMed

Li S, Peng Y, Landsman D, Panchenko AR (2022a) DNA methylation cues in nucleosome geometry, stability and unwrapping. *Nucleic acids research* **50**:1864-1874 https://doi.org/10.1093/NAR/GKAC097 | PubMed

Li S, Peng Y, Panchenko AR (2022b) DNA methylation: Precise modulation of chromatin structure and dynamics. *Current Opinion in Structural Biology* **75**:102430 https://doi.org/10.1016/J.SBI.2022.102430 | PubMed

Li S, Wei T, Panchenko AR (2023) Histone variant H2A.Z modulates nucleosome dynamics to promote DNA accessibility. *Nature Communications* **14**:1-10 https://doi.org/10.1038/s41467-023-36465-5 | PubMed

Li Z, Kono H (2016) Distinct Roles of Histone H3 and H2A Tails in Nucleosome Stability. *Scientific Reports* **6**:1-12 https://doi.org/10.1038/srep31437 | PubMed

Liebschner D, Afonine P V., Baker ML, Bunkoczi G, Chen VB, Croll TI, Hintze B, Hung LW, Jain S, McCoy AJ, *et al.* (2019) Macromolecular structure determination using X-rays, neutrons and electrons: recent developments in Phenix. urn:issn:2059-7983. *Acta crystallographica. Section D, Structural biology* **75**:861-877 https://doi.org/10.1107/S2059798319011471 | PubMed

Liu X, Li B, Gorovsky MA (1996) Essential and nonessential histone H2A variants in Tetrahymena thermophila. *Molecular and Cellular Biology* **16**:4305 https://doi.org/10.1128/MCB.16.8.4305 | PubMed

Lohka MI, Maller JL (1985) Induction of nuclear envelope breakdown, chromosome condensation, and spindle formation in cell-free extracts. *Journal of Cell Biology* **101**:518-523 https://doi.org/10.1083/JCB.101.2.518 | PubMed

Louder RK, Park G, Ye Z, Cha JS, Gardner AM, Lei Q, Ranjan A, Höllmüller E, Stengel F, Pugh BF, *et al.* (2024) Molecular basis of global promoter sensing and nucleosome capture by the SWR1 chromatin remodeler. *Cell* **187** https://doi.org/10.1016/J.CELL.2024.09.007 | PubMed

Love MI, Huber W, Anders S (2014) Moderated estimation of fold change and dispersion for RNA-seq data with DESeq2. *Genome Biology* **15**:1-21 https://doi.org/10.1186/s13059-014-0550-8 | PubMed

Lowary PT, Widom J (1998) New DNA sequence rules for high affinity binding to histone octamer and sequence-directed nucleosome positioning. *Journal of Molecular Biology* **276**:19-42 https://doi.org/10.1006/jmbi.1997.1494 | PubMed

Luger K, Mäder AW, Richmond RK, Sargent DF, Richmond TJ. (1997) Crystal structure of the nucleosome core particle at 2.8 Å resolution. *Nature* **389**:251-260 https://doi.org/10.1038/38444 | PubMed

Mann M, Risley MS, Eckhardt RA, Kasinsky HE (1982) Characterization of spermatid/sperm basic chromosomal proteins in the genus Xenopus (Anura, Pipidae). *The Journal of experimental zoology* **222**:173-186 https://doi.org/10.1002/JEZ.1402220209 | PubMed

Mao Z, Pan L, Wang W, Sun J, Shan S, Dong Q, Liang X, Dai L, Ding X, Chen S, *et al.* (2014) Anp32e, a higher eukaryotic histone chaperone directs preferential recognition for H2A.Z. *Cell Research* **24**:389-399 https://doi.org/10.1038/cr.2014.30 | PubMed

Meers MP, Tenenbaum D, Henikoff S (2019) Peak calling by Sparse Enrichment Analysis for CUT&RUN chromatin profiling. *Epigenetics and Chromatin* **12**:1-11 https://doi.org/10.1186/s13072-019-0287-4 | PubMed

Meng EC, Goddard TD, Pettersen EF, Couch GS, Pearson ZJ, Morris JH, Ferrin TE (2023) UCSF ChimeraX: Tools for structure building and analysis. *Protein Science* **32**:e4792 https://doi.org/10.1002/PRO.4792 | PubMed

Murphy PJ, Wu SF, James CR, Wike CL, Cairns BR (2018) Placeholder Nucleosomes Underlie Germline-to-Embryo DNA Methylation Reprogramming. *Cell* **172**:993-1006.e13. https://doi.org/10.1016/j.cell.2018.01.022 | PubMed

Newport J, Kirschner M (1982) A Major Developmental Transition in Early Xenopus Embryos: I. Characterization and Timing of Cellular Changes at the Midblastula Stage. *Cell* **30**:675-686 https://doi.org/10.1016/0092-8674(82)90272-0 | PubMed

Ngo TTM, Yoo J, Dai Q, Zhang Q, He C, Aksimentiev A, Ha T (2016) Effects of cytosine modifications on DNA flexibility and nucleosome mechanical stability. *Nature Communications* **7**:1-9 https://doi.org/10.1038/ncomms10813 | PubMed

Nie WF, Lei M, Zhang M, Tang K, Huang H, Zhang C, Miki D, Liu P, Yang Y, Wang X, *et al.* (2019) Histone acetylation recruits the SWR1 complex to regulate active DNA demethylation in Arabidopsis. *Proceedings of the National Academy of Sciences of the United States of America* **116**:16641-16650 https://doi.org/10.1073/pnas.1906023116 | PubMed

Obri A, Ouararhni K, Papin C, Diebold ML, Padmanabhan K, Marek M, Stoll I, Roy L, Reilly PT, Mak TW, *et al.* (2014) ANP32E is a histone chaperone that removes H2A.Z from chromatin. *Nature* **505**:648-653 https://doi.org/10.1038/nature12922 | PubMed

Oikawa M, Simeone A, Hormanseder E, Teperek M, Gaggioli V, O'Doherty A, Falk E, Sporniak M, D'Santos C, Franklin VNR, *et al.* (2020) Epigenetic homogeneity in histone methylation underlies sperm programming for embryonic transcription. *Nature Communications* **11** https://doi.org/10.1038/S41467-020-17238-W | PubMed

Onikubo T, Shechter D (2016) Chaperone-mediated chromatin assembly and transcriptional regulation in Xenopus laevis. *The International journal of developmental biology* **60**:271-276 https://doi.org/10.1387/IJDB.130188DS | PubMed

Osakabe A, Adachi F, Arimura Y, Maehara K, Ohkawa Y, Kurumizaka H (2015) Influence of DNA methylation on positioning and DNA flexibility of nucleosomes with pericentric satellite DNA. *Open Biology* **5** https://doi.org/10.1098/RSOB.150128 | PubMed

Park G, Patel AB, Wu C, Louder RK. (2024) Structures of H2A.Z-associated human chromatin remodelers SRCAP and TIP60 reveal divergent mechanisms of chromatin engagement. *bioRxiv* https://doi.org/10.1101/2024.07.30.605802 | PubMed

Park YJ, Dyer PN, Tremethick DJ, Luger K (2004) A new fluorescence resonance energy transfer approach demonstrates that the histone variant H2AZ stabilizes the histone octamer within the nucleosome. *Journal of Biological Chemistry* **279**:24274-24282 https://doi.org/10.1074/jbc.M313152200 | PubMed

Pérez A, Castellazzi CL, Battistini F, Collinet K, Flores O, Deniz O, Ruiz ML, Torrents D, Eritja R, Soler-López M, *et al.* (2012) Impact of methylation on the physical properties of DNA. *Biophysical Journal* **102**:2140-2148 https://doi.org/10.1016/j.bpj.2012.03.056 | PubMed

Postow L, Ghenoiu C, Woo EM, Krutchinsky AN, Chait BT, Funabiki H (2008) Ku80 removal from DNA through double strand break-induced ubiquitylation. *The Journal of cell biology* **182**:467-479 https://doi.org/10.1083/JCB.200802146 | PubMed

Pudney M, Varma MGR, Leake CJ (1973) Establishment of a cell line (XTC-2) from the South African clawed toad,Xenopus laevis. *Experientia* **29**:466-467 https://doi.org/10.1007/BF01926785 | PubMed

Ramírez F, Ryan DP, Grüning B, Bhardwaj V, Kilpert F, Richter AS, Heyne S, Dündar F, Manke T (2016) deepTools2: a next generation web server for deep-sequencing data analysis. *Nucleic Acids Research* **44**:W160-W165 https://doi.org/10.1093/NAR/GKW257 | PubMed

Ranjan A, Nguyen VQ, Liu S, Wisniewski J, Kim JM, Tang X, Mizuguchi G, Elalaoui E, Nickels TJ, Jou V, *et al.* (2020) Live-cell single particle imaging reveals the role of RNA polymerase II in histone H2A.Z eviction. *eLife* **9**:e55667 https://doi.org/10.7554/eLife.55667 | PubMed

Ray-Gallet D, Quivy JP, Scamps C, Martini EMD, Lipinski M, Almouzni G (2002) HIRA is critical for a nucleosome assembly pathway independent of DNA synthesis. *Molecular cell* **9**:1091-1100 https://doi.org/10.1016/S1097-2765(02)00526-9 | PubMed

Richard F, Jethmalani Y, Janssens D, Luo W, Wang R, Wu Y, Zhou Z, Ma Y, Zhang W, Wang Z, *et al.* (2025) Benchmark of chromatin–protein interaction methods in haploid round spermatids. *Frontiers in Cell and Developmental Biology* **13**:1572405 https://doi.org/10.3389/FCELL.2025.1572405 | PubMed

Rudnizky S, Bavly A, Malik O, Pnueli L, Melamed P, Kaplan A (2016) H2A.Z controls the stability and mobility of nucleosomes to regulate expression of the LH genes. *Nature Communications* **7** https://doi.org/10.1038/ncomms12958 | PubMed

Ruhl DD, Jin J, Cai Y, Swanson S, Florens L, Washburn MP, Conaway RC, Conaway JW, Chrivia JC (2006) Purification of a human SRCAP complex that remodels chromatin by incorporating the histone variant H2A.Z into nucleosomes. *Biochemistry* **45**:5671-5677 https://doi.org/10.1021/bi060043d | PubMed

Scacchetti A, Becker PB (2021) Variation on a theme: Evolutionary strategies for H2A.Z exchange by SWR1-type remodelers. *Current Opinion Cell Biology* **70**:1-9 https://doi.org/10.1016/J.CEB.2020.10.014 | PubMed

Scheres SHW (2012) RELION: Implementation of a Bayesian approach to cryo-EM structure determination. *Journal of Structural Biology* **180**:519-530 https://doi.org/10.1016/J.JSB.2012.09.006 | PubMed

Schneider CA, Rasband WS, Eliceiri KW (2012) NIH Image to ImageJ: 25 years of image analysis. *Nature Methods* **9**:671-675 https://doi.org/10.1038/nmeth.2089 | PubMed

Segal E, Fondufe-Mittendorf Y, Chen L, Thåström A, Field Y, Moore IK, Wang JPZ, Widom J (2006) A genomic code for nucleosome positioning. *Nature* **442**:772-778 https://doi.org/10.1038/NATURE04979 | PubMed

Shechter D, Chitta RK, Xiao A, Shabanowitz J, Hunt DF, Allis CD (2009) A distinct H2A.X isoform is enriched in Xenopus laevis eggs and early embryos and is phosphorylated in the absence of a checkpoint. *Proceedings of the National Academy of Sciences of the United States of America* **106**:749-754 https://doi.org/10.1073/pnas.0812207106 | PubMed

Soroczynski J, Anderson LJ, Yeung JL, Rendleman JM, Oren DA, Konishi HA, Risca VI. (2024) OpenTn5: Open-Source Resource for Robust and Scalable Tn5 Transposase Purification and Characterization. *bioRxiv* https://doi.org/10.1101/2024.07.11.602973 | PubMed

Stael S, Miller LP, Fernández-Fernández ÁD, Van Breusegem F. (2022) Detection of Damage-Activated Metacaspase Activity by Western Blot in Plants. *Methods in Molecular Biology* **2447**:127-137 https://doi.org/10.1007/978-1-0716-2079-3_11 | PubMed

Suto RK, Clarkson MJ, Tremethick DJ, Luger K (2000) Crystal structure of a nucleosome core particle containing the variant histone H2A.Z. *Nature Structural Biology* **7**:1121-1124 https://doi.org/10.1038/81971 | PubMed

Talbert PB, Henikoff S (2016) Histone variants on the move: substrates for chromatin dynamics. *Nature Reviews Molecular Cell Biology* **18**:115-126 https://doi.org/10.1038/nrm.2016.148 | PubMed

Thakar A, Gupta P, Ishibashi T, Finn R, Silva-Moreno B, Uchiyama S, Fukui K, Tomschik M, Ausio J, Zlatanova J (2009) H2A.Z and H3.3 histone variants affect nucleosome structure: Biochemical and biophysical studies. *Biochemistry* **48**:10852-10857 https://doi.org/10.1021/bi901129e | PubMed

Thambirajah AA, Dryhurst D, Ishibashi T, Li A, Maffey AH, Ausió J (2006) H2A.Z stabilizes chromatin in a way that is dependent on core histone acetylation. *Journal of Biological Chemistry* **281**:20036-20044 https://doi.org/10.1074/jbc.M601975200 | PubMed

Tilman G, Arnoult N, Lenglez S, Van Beneden A, Loriot A, De Smet C, Decottignies A. (2012) Cancer-linked satellite 2 DNA hypomethylation does not regulate Sat2 non-coding RNA expression and is initiated by heat shock pathway activation. *Epigenetics* **7**:903-913 https://doi.org/10.4161/EPI.21107 | PubMed

Tramantano M, Sun L, Au C, Labuz D, Liu Z, Chou M, Shen C, Luk E (2016) Constitutive turnover of histone H2A.Z at yeast promoters requires the preinitiation complex. *eLife* **5** https://doi.org/10.7554/ELIFE.14243 | PubMed

Tutter A V., Walter JC (2006) Chromosomal DNA replication in a soluble cell-free system derived from Xenopus eggs. *Methods in molecular biology* **322**:121-137 https://doi.org/10.1007/978-1-59745-000-3_9 | PubMed

Unoki M (2021) Chromatin remodeling in replication-uncoupled maintenance DNA methylation and chromosome stability: Insights from ICF syndrome studies. *Genes to Cells* **26**:349-359 https://doi.org/10.1111/GTC.12850 | PubMed

Van Daal A, Elgin SCR. (1992) A Histone Variant, H2AvD, is Essential in Drosophila melanogaster. *Molecular Biology of the Cell* **3**:593-602 https://doi.org/10.1091/mbc.3.6.593 | PubMed

Veenstra GJC, Destrée OHJ, Wolffe AP (1999) Translation of maternal TATA-binding protein mRNA potentiates basal but not activated transcription in Xenopus embryos at the midblastula transition. *Molecular and cellular biology* **19**:7972-7982 https://doi.org/10.1128/MCB.19.12.7972 | PubMed

Ward WS, Coffey DS (1991) DNA packaging and organization in mammalian spermatozoa: comparison with somatic cells. *Biology of reproduction* **44**:569-574 https://doi.org/10.1095/BIOLREPROD44.4.569 | PubMed

Wassing IE, Nishiyama A, Shikimachi R, Jia Q, Kikuchi A, Hiruta M, Sugimura K, Hong X, Chiba Y, Peng J, *et al.* (2024) CDCA7 is an evolutionarily conserved hemimethylated DNA sensor in eukaryotes. *Science advances* **10**:eadp5753 https://doi.org/10.1126/SCIADV.ADP5753 | PubMed

Watanabe S, Peterson C (2010) The INO80 family of chromatin-remodeling enzymes: regulators of histone variant dynamics. *Cold Spring Harb Symp Quant Biol* **75**:35-42 https://doi.org/10.1101/sqb.2010.75.063 | PubMed

Weber CM, Henikoff JG, Henikoff S (2010) H2A.Z nucleosomes enriched over active genes are homotypic. *Nature Structural and Molecular Biology* **17**:1500-1507 https://doi.org/10.1038/nsmb.1926 | PubMed

Wong N, Lam WC, Lai PBS, Pang E, Lau WY, Johnson PJ (2001) Hypomethylation of Chromosome 1 Heterochromatin DNA Correlates with q-Arm Copy Gain in Human Hepatocellular Carcinoma. *The American Journal of Pathology* **159**:465 https://doi.org/10.1016/S0002-9440(10)61718-X | PubMed

Wühr M, Freeman RM, Presler M, Horb ME, Peshkin L, Gygi SP, Kirschner MW (2014) Deep proteomics of the Xenopus laevis egg using an mRNA-derived reference database. *Current biology : CB* **24**:1467-1475 https://doi.org/10.1016/J.CUB.2014.05.044 | PubMed

Wykes SM, Krawetz SA (2003) The structural organization of sperm chromatin. *The Journal of biological chemistry* **278**:29471-29477 https://doi.org/10.1074/JBC.M304545200 | PubMed

Xue JZ, Woo EM, Postow L, Chait BT, Funabiki H (2013) Chromatin-bound Xenopus Dppa2 shapes the nucleus by locally inhibiting microtubule assembly. *Developmental cell* **27**:47-59 https://doi.org/10.1016/J.DEVCEL.2013.08.002 | PubMed

Yang YJ, Dong HL, Qiang XW, Fu H, Zhou EC, Zhang C, Yin L, Chen XF, Jia FC, Dai L, *et al.* (2020) Cytosine Methylation Enhances DNA Condensation Revealed by Equilibrium Measurements Using Magnetic Tweezers. *Journal of the American Chemical Society* **142**:9203-9209 https://doi.org/10.1021/jacs.9b11957 | PubMed

Yu G, Wang LG, He QY (2015) ChIPseeker: an R/Bioconductor package for ChIP peak annotation, comparison and visualization. *Bioinformatics* **31**:2382-2383 https://doi.org/10.1093/BIOINFORMATICS/BTV145 | PubMed

Zemach A, McDaniel IE, Silva P, Zilberman D (2010) Genome-wide evolutionary analysis of eukaryotic DNA methylation. *Science* **328**:916-919 https://doi.org/10.1126/science.1186366 | PubMed

Zhang H, Roberts DN, Cairns BR (2005) Genome-wide dynamics of Htz1, a histone H2A variant that poises repressed/basal promoters for activation through histone loss. *Cell* **123**:219-231 https://doi.org/10.1016/j.cell.2005.08.036 | PubMed

Zheng SQ, Palovcak E, Armache JP, Verba KA, Cheng Y, Agard DA (2017) MotionCor2: anisotropic correction of beam-induced motion for improved cryo-electron microscopy. *Nature Methods* **14**:331-332 https://doi.org/10.1038/nmeth.4193 | PubMed

Zhou J, Lei X, Shafiq S, Zhang W, Li Q, Li K, Zhu J, Dong Z, He XJ, Sun Q (2023) DDM1-mediated R-loop resolution and H2A.Z exclusion facilitates heterochromatin formation in Arabidopsis. *Science advances* **9** https://doi.org/10.1126/SCIADV.ADG2699 | PubMed

Zierhut C, Jenness C, Kimura H, Funabiki H (2014) Nucleosomal regulation of chromatin composition and nuclear assembly revealed by histone depletion. *Nature structural & molecular biology* **21**:617-625 https://doi.org/10.1038/NSMB.2845 | PubMed

Zilberman D, Coleman-Derr D, Ballinger T, Henikoff S (2008) Histone H2A.Z and DNA methylation are mutually antagonistic chromatin marks. *Nature* **456**:125-129 https://doi.org/10.1038/nature07324 | PubMed

Zlatanova J, Thakar A (2008) H2A.Z: View from the Top. *Structure* https://doi.org/10.1016/j.str.2007.12.008 | PubMed

Shih RM, Arimura Y, Konishi HA, Funabiki H (2025) Impacts of DNA methylation on H2A.Z deposition and nucleosome stability. NCBI Gene Expression Omnibus. ID GSE295057 https://www.ncbi.nlm.nih.gov/geo/query/acc.cgi?acc=GSE295057

Shih R (2025) Raw Data and Code for "IMPACTS OF DNA METHYLATION ON H2A.Z DEPOSITION AND NUCLEOSOME STABILITY". Zenodo. https://doi.org/10.5281/zenodo.15360677

Shih RM, Arimura Y, Konishi HA, Funabiki H (2025) Cryo-EM analysis of human H2A.Z on 601L DNA. Worldwide Protein Data Bank. https://doi.org/10.2210/pdb9OH1/pdb

Shih RM, Arimura Y, Konishi HA, Funabiki H (2025) Cryo-EM analysis of human H2A.Z on methylated 601L DNA. Worldwide Protein Data Bank. https://doi.org/10.2210/pdb9OH2/pdb

Shih RM, Arimura Y, Konishi HA, Funabiki H (2025) Cryo-EM analysis of human H2A.Z on Sat2R-P DNA (v1). Worldwide Protein Data Bank. https://doi.org/10.2210/pdb9OGS/pdb

Shih RM, Arimura Y, Konishi HA, Funabiki H (2025) Cryo-EM analysis of human H2A.Z on Sat2R-P DNA (v2). Worldwide Protein Data Bank. https://doi.org/10.2210/pdb9OGZ/pdb

Shih RM, Arimura Y, Konishi HA, Funabiki H (2025) Cryo-EM analysis of human H2A.Z on methylated Sat2R-P DNA. Worldwide Protein Data Bank. https://doi.org/10.2210/pdb9OGR/pdb

Shih RM, Arimura Y, Konishi HA, Funabiki H (2025) Cryo-EM analysis of human H2A.Z on methylated Sat2R-P DNA (v2). Worldwide Protein Data Bank. https://doi.org/10.2210/pdb9OH0/pdb

Peer reviews

Reviewer #1 (Public review):

Summary:

The authors considered the mechanism underlying previous observations that H2A.Z is preferentially excluded from methylated DNA regions. They considered two non-mutually exclusive mechanisms. First, they tested the hypothesis that nucleosomes containing both methylated DNA and H2A.Z might be intrinsically unstable due to their structural features. Second, they explored the possibility that DNA methylation might impede SRCAP-C from efficiently depositing H2A.Z onto these DNA methylated regions.

Their structural analyses revealed subtle differences between H2A.Z-containing nucleosomes assembled on methylated versus unmethylated DNA. To test the second hypothesis, the authors allowed H2A.Z assembly on sperm chromatin in Xenopus egg extracts and mapped both H2A.Z localization and DNA methylation in this transcriptionally inactive system. They compared these data with corresponding maps from a transcriptionally active Xenopus fibroblast cell line. This comparison confirmed the preferential deposition or enrichment of H2A.Z on unmethylated DNA regions, an effect that was much more pronounced in the fibroblast genome than in sperm chromatin. Furthermore, nucleosome assembly on methylated versus unmethylated DNA, along with SRCAP-C depletion from Xenopus egg extracts, provided a means to test whether SRCAP-C contributes to the preferential loading of H2A.Z onto unmethylated DNA.

Strengths:

The strength and originality of this work lie in its focused attempt to dissect the unexplained observation that H2A.Z is excluded from methylated genomic regions.

Weaknesses:

The study has two weaknesses. First, although the authors identify specific structural effects of DNA methylation on H2A.Z-containing nucleosomes, they do not provide evidence demonstrating that these structural differences lead to altered histone dynamics or nucleosome instability. Second, building on the elegant work of Berta and colleagues (cited in the manuscript), the authors implicate SRCAP-C in the selective deposition of H2A.Z at unmethylated regions. Yet the role of SRCAP-C appears only partial, and the study does not address how the structural or molecular consequences of DNA methylation prevent efficient H2A.Z deposition. Finally, additional plausible mechanisms beyond the two scenarios the authors considered are not investigated or discussed in the manuscript.

Comments on revisions:

The authors have addressed all previously raised concerns and propose a revised version of the manuscript. Notably, the abstract and discussion sections have been improved, and new experimental data have been incorporated. Collectively, these revisions enhance the rigor and clarity of the data interpretation and discussion.

Given these improvements, this reviewer believes that the manuscript could be published, particularly if this publication is accompanied by the critical points discussed in the rebuttal letter.

https://doi.org/10.7554/eLife.109762.2.sa3

Reviewer #2 (Public review):

This manuscript aims to elucidate the mechanistic basis for the long-standing observation that DNA methylation and the histone variant H2A.Z occupy mutually exclusive genomic regions. The authors test two hypotheses: (i) that DNA methylation intrinsically destabilizes H2A.Z nucleosomes, thereby preventing H2A.Z retention, and (ii) that DNA methylation suppresses H2A.Z deposition by ATP-dependent chromatin-remodelling complexes. The revised manuscript addresses a number of previous concerns, and the manuscript has therefore improved accordingly. However, several limitations remain.

Comments on revisions:

The authors have addressed a number of my previous concerns, and the manuscript has improved accordingly. However, several limitations remain that, in my view, constrain the strength of the conclusions. In particular, the absence of a direct comparison with a canonical nucleosome assembled on the same DNA template. This control is essential to determine whether the observed effects are specific to H2A.Z or reflect more general properties of methylated DNA-nucleosome interactions. Notably, even within the authors' own data, there is a trend suggesting that methylated canonical H2A nucleosomes may also exhibit increased accessibility. Although this does not reach statistical significance, the authors themselves argue that subtle differences can be biologically meaningful; it is therefore plausible that extended digestion conditions (e.g., longer HinfI exposure) could reveal a significant effect. Unless a direct structural comparison with a canonical nucleosome is performed, the possibility that the reported phenomenon is not specific to H2A.Z remains. This is compounded by the reliance on a single restriction enzyme-based assay, which represents a limited experimental approach. Such an approach is insufficient to unequivocally support the central claim that DNA methylation increases accessibility of H2A.Z-containing nucleosomes. Additional orthogonal assays would be required to substantiate this conclusion. With respect to the cryo-EM analysis of methylated and unmethylated 601L H2A.Z nucleosomes, and in general, the authors still do not adequately consider the positional context of CpG methylation. Extensive literature demonstrates that the effects of DNA methylation on canonical nucleosome structure and stability are highly position-dependent. Without accounting for the location of methylated CpGs relative to key DNA-histone contact sites, the structural data remain difficult to interpret mechanistically. Overall, while the manuscript has improved, it remains a relatively limited study that draws broad mechanistic conclusions from a minimal experimental data.

https://doi.org/10.7554/eLife.109762.2.sa2

Reviewer #3 (Public review):

Summary:

Histone variant H2A.Z is evolutionarily conserved among various species. The selective incorporation and removal of histone variants on the genome play crucial roles in regulating nuclear events, including transcription. Shih et al. aimed to address antagonistic mechanisms between histone variant H2A.Z deposition and DNA methylation. To this end, the authors reconstituted H2A.Z nucleosomes in vitro using methylated or unmethylated human satellite II DNA sequence and examined how DNA methylation affects H2A.Z nucleosome structure and dynamics. The cryo-EM analysis revealed that DNA methylation induces a more open conformation in H2A.Z nucleosomes. Consistent with this, their biochemical assays showed that DNA methylation subtly increases restriction enzyme accessibility in H2A.Z nucleosomes compared with canonical H2A nucleosomes. The authors identified genome-wide profiles of H2A.Z and DNA methylation using genomic assays and found their unique distribution between Xenopus sperm pronuclei and fibroblast cells. Using Xenopus egg extract systems,

the authors showed SRCAP complex, the chromatin remodelers for H2A.Z deposition, preferentially bind to unmethylated DNA to deposit H2A.Z.

Strengths:

The experiments are rigorously performed, and interpretations are clear. The study presents a high-resolution cryo-EM structure of human H2A.Z nucleosome with methylated DNA. Although the effect of DNA methylation on the physical stability of the H2A.Z nucleosome is subtle, this would be important finding that warrants further functional investigation. The discovery that the SRCAP complex senses DNA methylation is novel and provides important mechanistic insight into the antagonism between H2A.Z and DNA methylation.

Weaknesses:

The authors have satisfactorily addressed my concerns.

https://doi.org/10.7554/eLife.109762.2.sa1

Author response:

The following is the authors' response to the current reviews.

Reviewer #1.

We appreciate the constructive comments, which greatly improved this manuscript.

Reviewer #2.

We appreciate Reviewer #2's thorough analysis of our manuscript. However, we are concerned that the reviewer criticized a conclusion different from the one we claim in the manuscript. Although Reviewer #2's public comment stated, "Such an approach is insufficient to unequivocally support the central claim that DNA methylation increases accessibility of H2A.Z-containing nucleosomes", we did not draw such a bold conclusion. In the Abstract, we cautiously described that the impact of DNA methylation we observed was subtle and based on satellite II-derived DNA sequences. We made a nuanced proposal regarding this observation, stating, "Altogether, we propose that SRCAP drives the biased association of H2A.Z to unmethylated DNA, while additional mechanisms, potentially taking advantage of the subtle DNA methylation-induced physical effects, further assist the exclusion of H2A.Z from methylated DNA". We believe our analysis will contribute valuable insights into the mechanistic basis behind the antagonism between DNA methylation and H2A.Z.

Reviewer #3.

We appreciate the constructive comments, which greatly improved this manuscript.

The following is the authors' response to the original reviews.

> ***eLife Assessment***
>
> *This study provides valuable mechanistic insight into the mutually exclusive distributions of the histone variant H2A.Z and DNA methylation by testing two hypotheses: (i) that DNA methylation destabilizes H2A.Z nucleosomes, thereby preventing H2A.Z retention, and (ii) that DNA methylation suppresses H2A.Z deposition by ATP-dependent chromatin remodeling complexes. Through a series of well-designed and carefully executed experiments, findings are presented in support of both hypotheses. However, the evidence in support of either hypothesis is incomplete, so that the proposed mechanisms underlying the enrichment of H2A.Z on unmethylated DNA remain somewhat speculative.*

We would like to thank the editor and reviewers for their critical assessments of our manuscript. While we do acknowledge the limitations of our work, we believe that our results provide important mechanistic insights into the long-standing question of how H2A.Z is preferentially enriched in hypomethylated genomic DNA regions. First, our structural and biochemical data suggest that DNA methylation increases the openness and physical accessibility of H2A.Z, albeit the effect is relatively subtle and is sequence-dependent. Second, using *Xenopus* egg extracts and synthetic DNA templates, we provide the first clear and direct evidence that DNA methylation-sensitive H2A.Z deposition is due to the H2A.Z chaperone SRCAP-C, corroborated by our discovery that SRCAP-C binding to DNA is suppressed by DNA methylation. Although the molecular details by which DNA methylation inhibits binding of SRCAP-C is an important area of future study, in our current manuscript, we do provide evidence that directly links the presence of SRCAP-C to the establishment of the DNA methylation/H2A.Z antagonism in a physiological system. Thanks to criticisms by the reviewers, we realized that we did not clearly state in our Abstract that the impact of DNA methylation on intrinsic H2A.Z nucleosome stability is relatively subtle, although we did explain these observations and limitations in the main text. In our revised manuscript, we are willing to edit the text to better clarify the criticisms raised by the reviewers.

> ***Public Reviews:***
>
> ***Reviewer #1 (Public review):***
>
> *Summary:*
>
> *The authors considered the mechanism underlying previous observations that H2A.Z is preferentially excluded from methylated DNA regions. They considered two non-mutually exclusive mechanisms. First, they tested the hypothesis that nucleosomes containing both methylated DNA and H2A.Z might be intrinsically unstable due to their structural features. Second, they explored the possibility that DNA methylation might impede SRCAP-C from efficiently depositing H2A.Z onto these DNA methylated regions.*
>
> *Their structural analyses revealed subtle differences between H2A.Z-containing nucleosomes assembled on methylated versus unmethylated DNA. To test the second hypothesis, the authors allowed H2A.Z assembly on sperm chromatin in Xenopus egg extracts and mapped both H2A.Z localization and DNA methylation in this transcriptionally inactive system. They compared these data with corresponding maps from a transcriptionally active Xenopus fibroblast cell line. This comparison confirmed the preferential deposition or enrichment of H2A.Z on unmethylated DNA regions, an effect that was much more pronounced in the fibroblast genome than in sperm chromatin. Furthermore, nucleosome assembly on methylated versus unmethylated DNA, along with SRCAP-C depletion from Xenopus egg extracts, provided a means to test whether SRCAP-C contributes to the preferential loading of H2A.Z onto unmethylated DNA.*
>
> *Strengths:*
>
> *The strength and originality of this work lie in its focused attempt to dissect the unexplained observation that H2A.Z is excluded from methylated genomic regions.*
>
> *Weaknesses:*
>
> *The study has two weaknesses. First, although the authors identify specific structural effects of DNA methylation on H2A.Z-containing nucleosomes, they do not provide evidence demonstrating that these structural differences lead to altered histone dynamics or nucleosome instability. Second, building on the elegant work of Berta and colleagues (cited in the manuscript), the authors implicate SRCAP-C in the selective*

> *deposition of H2A.Z at unmethylated regions. Yet the role of SRCAP-C appears only partial, and the study does not address how the structural or molecular consequences of DNA methylation prevent efficient H2A.Z deposition. Finally, additional plausible mechanisms beyond the two scenarios the authors considered are not investigated or discussed in the manuscript.*

Although we acknowledge the limitations of our study and are willing to expand our discussion to more thoroughly discuss these points, we believe our manuscript provides several important mechanistic insights which this reviewer may not have fully appreciated.

Our first conclusion that H2A.Z nucleosomes on methylated DNA are more open and accessible compared to their unmethylated counterparts is supported by both our cryo-EM study and the restriction enzyme accessibility assay. Although the physical effect of DNA methylation is relatively subtle and is likely sequence dependent, as we clearly noted within the manuscript, the difference does exist and is valuable information for the chromatin field at large to consider.

The second major conclusion of our manuscript is that SRCAP-C exhibits preferential binding to unmethylated DNA over methylated DNA, and that SRCAP-C represents the major mechanism that can explain the biased deposition of H2A.Z to unmethylated DNA in *Xenopus* egg extracts. Furthermore, our experiments using *Xenopus* egg extract clearly demonstrated that H2A.Z is deposited by both DNAmethylation sensitive and insensitive mechanisms. Depletion of SRCAP-C almost completely eliminated the levels of DNA-methylation-sensitive H2A.Z deposition and reduced the total level of H2A.Z on chromatin to less than half of that seen in non-depleted extract. This result demonstrated that DNA methylation-sensitive H2A.Z loading is primarily regulated by SRCAP-C, at least in our experimental context where transcription, replication, and other epigenetic modifications are not involved. It is likely that additional mechanisms do further contribute, implicated by our sequencing experiments, particularly at regions with active transcription, and we have noted these possibilities and the rationale for their existence in the Discussion.

Our study also suggests that a SRCAP-independent, DNA methylation-insensitive mechanism of H2A.Z loading exists, which we suspect to be mediated by Tip60-C. In line with this possibility, our data suggest that Tip60-C binds DNA in a DNA methylation-insensitive manner in *Xenopus* egg extract. Since antibodies to deplete Tip60-C from *Xenopus* egg extract are currently unavailable, we were unable to directly test that hypothesis and decided not to include Tip60-C into our final model as we lacked experimental evidence for its role. However, whether or not Tip60-C is the complex responsible for the DNA methylation-insensitive pathway does not influence our final conclusion that SRCAP-C plays a major role in DNA methylation-sensitive H2A.Z loading. We are planning to edit our manuscript to more comprehensively discuss these points.

Please note that while Berta et al reported that DNA methylation increases at H2A.Z loci in tumors defective in SRCAP-C, they selected those regions based off where H2A.Z is typically enriched within normal tissues (Berta et al., 2021). They did not show data indicating whether H2A.Z is still retained specifically at those analyzed loci upon mutation of SRCAP-C subunits. Thus, although we greatly admire their work and are pleased that many of our findings align with theirs, their paper did not directly address whether SRCAP-C itself differentiates between DNA methylation status nor the impact that has on H2A.Z and DNA methylation colocalization. In contrast, our *Xenopus* egg extract system, where de novo methylation is undetectable (Nishiyama et al., 2013; Wassing et al., 2024) offers a unique opportunity to examine the direct impact of DNA methylation on H2A.Z deposition using controlled synthetic DNA substrates. Corroborated with our demonstration that DNA binding of SRCAP-C is suppressed by DNA methylation, we believe that our manuscript provides a specific mechanism that can explain the preferential deposition of H2A.Z at hypomethylated genomic regions.

> ***Reviewer #2 (Public review):***
>
> *This manuscript aims to elucidate the mechanistic basis for the long-standing observation that DNA methylation and the histone variant H2A.Z occupy mutually exclusive genomic regions. The authors test two hypotheses: (i) that DNA methylation intrinsically destabilizes H2A.Z nucleosomes, thereby preventing H2A.Z retention, and (ii) that DNA methylation suppresses H2A.Z deposition by ATPdependent chromatin-remodelling complexes. However, neither hypothesis is rigorously addressed. There are experimental caveats, issues with data interpretation, and conclusions that are not supported by the data. Substantial revision and additional experiments, including controls, would be required before mechanistic conclusions can be drawn. Major concerns are as follows:*

We appreciate the critical assessment of our manuscript by this reviewer. Although we acknowledge the limitations of our study and will revise the manuscript to better describe them, we would like to respectfully argue against the statement that our "conclusions [...] are not supported by the data".

> *(1) The cryo-EM structure of methylated H2A.Z nucleosomes is insufficiently resolved to address the central mechanistic question: where the methylated CpGs are located relative to DNA-histone contact points and how these modifications influence H2A.Z nucleosome structure. The structure provides no mechanistic insights into methylation-induced destabilization.*

The fact that the DNA resolution in the methylated structure was not high enough to resolve the positions of methylated CpGs despite a high overall resolution of 2.78 Å implies that 1) the Sat2R-P DNA was not as stably registered as the 601L sequence, requiring us to create two alternative Sat2R-P atomic models to account for the variable positioning in our samples, and 2) that the presence of DNA methylation increases that positional variability. We understand that one may prefer to see highly resolved density around each methylation mark, but we do believe that our inability to accomplish that is actually a feature rather than a weakness and has important biological implications. The decrease in local DNA resolution on the methylated Sat2R-P structure compared to its unmethylated counterpart is meaningful and suggests to us that DNA methylation weakens overall DNA wrapping and positioning on the nucleosome, supported by the increased flexibility seen at the linker DNA ends as well as an increase in the population of highly shifted nucleosomes amongst the methylated particles. Additionally, one major view in the DNA methylation/nucleosome stability field is that the presence of DNA methylation can make DNA stiffer and harder to bend, causing opening and destabilization of nucleosomes (Ngo et al., 2016). The increased opening of linker DNA ends and accessibility of methylated H2A.Z nucleosomes in our hands also aligns with such an

idea, again suggesting decreased histone-DNA contact stability on methylated DNA substrates. We plan to revise the writing in our manuscript to better reflect these ideas.

> *The experimental system also lacks physiological relevance. The template DNA sequence is artificial, despite the existence of well-characterised native genomic sequences for which DNA methylation is known to inhibit H2A.Z incorporation. Alternatively, there are a number of studies examining the effect of DNA methylation on nucleosome structure, stability, DNA unwrapping, and positioning. Choosing one of these DNA sequences would have at least allowed a direct comparison with a canonical nucleosome. Indeed, a major omission is the absence of a cryo-EM structure of a canonical nucleosome assembled on the same DNA template - this is essential to assess whether the observed effects are H2A.Z-specific.*

The reviewer raises a fair question about whether canonical H2A would experience the same DNA methylation-dependent structural effects. We had considered solving the H2A structures, however, ultimately decided against it for a few reasons. First, there already exists crystal structures of canonical H2A nucleosomes using a DNA sequence highly similar to our Sat2R-P with and without the presence of DNA methylation (PDB: 5CPI and 5CPJ). The authors of this study did not see any physical differences present in their structures (Osakabe et al., 2015). Additionally, we had included canonical H2A conditions within our restriction enzyme accessibility assay and did not see a significant impact of DNA methylation on those samples (Fig 3). Because of the previous report and our own negative data, we expected that only limited additional insights would be obtained from the canonical H2A structures and decided not to pursue that analysis.

One of the primary reasons we chose the Sat2R-P sequence was, as noted above, that there already was a published study examining how DNA methylation affects nucleosome structure using a variant of this sequence which we could compare to our results, as the reviewer has suggested. We did have to modify the sequence, namely by making it palindromic, in order to increase the final achievable resolution. We viewed the Sat2R-P sequence as an attractive candidate because it is physiologically relevant; the initial sequence was taken directly from human satellite II. Several modifications were made for technical reasons, including making the sequence palindromic as described above and also ensuring that each CpG is recognizable by a methylation-sensitive restriction enzyme so that we could be certain about the degree of methylation on our substrates. These practical concerns outweighed the necessity of maintaining a strict physiological sequence to us. However, we still believe the final Sat2R-P more closely mimics physiological sequences than Widom 601. Additionally, human satellite II is a highly abundant sequence in the human genome that is known to undergo large methylation changes on the onset of many disorders, like cancer, as well as during aging. Thus, there are interesting biological questions surrounding how the methylation state of this particular sequence affects chromatin structure.

Furthermore, it has been reported that satellite II is devoid of H2A.Z (Capurso et al., 2012). Beyond those reasons, the satellite II sequence is generally interesting to our lab because we have been studying genes involved in ICF syndrome, where hypomethylation of satellite II sequences forms one of the hallmarks of this disorder (Funabiki et al., 2023; Jenness et al., 2018; Wassing et al., 2024). We understand that sequence context plays a large role in nucleosome wrapping and stability. This is why we strived to test multiple sequences in each of our assays. We do agree that it would be interesting to use DNA sequences where H2A.Z binding has already been described to be affected in a DNA methylation-dependent manner, forming an exciting future study to pursue.

> *Furthermore, the DNA template is methylated at numerous random CpG sites. The authors' argument that only the global methylation level is relevant is inconsistent with the literature, which clearly demonstrates that methylation effects on canonical*

> *nucleosomes are position-dependent. Not all CpG sites contribute equally to nucleosome stability or unwrapping, and this critical factor is not considered.*

We did not argue that only the global methylation level is relevant. We also would appreciate it if the reviewer could provide specific references that "clearly demonstrates that methylation effects on canonical nucleosomes are position-dependent". We are aware of a series of studies conducted by Chongli Yuan's group, including one testing the effect of placing methylated CpGs at different positions along the Widom 601 sequence. In that study (Jimenez-Useche et al., 2013), they did find that positioning of mCpGs has differential impacts on the salt resistance of the nucleosomes, with 5 tandem mCpG copies at the dyad causing the most dramatic nucleosome opening whereas having mCpGs only at the DNA major grooves, but not elsewhere, increased nucleosome stability. However, they did also find that methylation of the original Widom 601 sequence also caused destabilization, albeit to a lesser degree, and another study by the same group (Jimenez-Useche et al., 2014) also found that CpG methylation decreased nucleosome-forming ability for all tested variants of the Widom 601 sequence, regardless of CpG density or positioning.

Other studies monitored how distribution of methylated CpGs correlates with nucleosome positioning (Collings et al., 2013; Davey et al., 1997; Davey et al., 2004). However, these studies assessed the sequence-dependent effects specifically on nucleosome assembly during *in vitro* salt dialysis, which is a different physical process than the one our manuscript focuses on, especially when considering the fact that H2A.Z is deposited onto preassembled H2A-nucleosome. Our cryo-EM analysis examines the structural changes induced by DNA methylation on already formed nucleosomes rather than the process of formation. Thus, probing accessibility changes using a restriction enzyme was the more appropriate biochemical assay to verify our structures.

We do very much agree that DNA context can influence nucleosome stability under different conditions. A study of molecular dynamics simulations concluded that the "combination of overall DNA geometrical and shape properties upon methylation" makes nucleosomes resistant to unwrapping (Li et al., 2022), while another modeling study suggests that DNA methylation impacts nucleosome stability in a manner dependent on DNA sequence, where "[s]trong binding is weakened and weak binding is strengthened" (Minary and Levitt, 2014). While G/C-dinucleotides are preferentially placed at major groove-inward positions in the nucleosomes *in vivo* (Chodavarapu et al., 2010; Segal et al., 2006) and G/C-rich segments are excluded from major groove-outward positions in Widom 601-like nucleosomes (Chua et al., 2012), methylated CpG dinucleotides are preferably, if not exclusively, located at major groove-outward positions *in vivo*. Mechanisms behind this biased mCpG positioning on the nucleosome remain speculative, likely caused by a combination of multiple factors, but the fact that we did not observe clear structural impacts using the Widom 601L sequence, where mCpGs are located at the major groove-outward and -inward positions ((Chua et al., 2012) and our structure), deserves a space for discussion. On the other hand, positioning of mCpG on satellite II-derived sequences that we used in this study was based on a physiological sequence, and thus it may not be appropriate to say that those CpGs are placed at multiple "random" positions. Although we decided not to discuss the position of 5mC on our Sat2R nucleosome structure due to ambiguous base assignments, neither of our two atomic models is consistent with an idea that DNA methylation repositions the CpG to the outward major grooves. As the potential contribution of how DNA methylation affects the nucleosome structure via modulating DNA stiffness has been extensively studied (Choy et al., 2010; Li et al., 2022; Ngo et al., 2016; Perez et al., 2012), we believe that it is appropriate to consider overall DNA properties along the whole DNA sequence, though we are willing to discuss potential positional effects in the revised manuscript.

Perhaps one of the most important points that we did not emphasize enough in our original manuscript was that in contrast to the subtle intrinsic effect of DNA methylation that was

DNA sequence dependent, we observed SRCAP-dependent preferential H2A.Z deposition to unmethylated DNA over methylated DNA in both 601 and satellite II DNAs. In the revised manuscript, we will make the value of comparative studies on 601 and satellite II in two distinct mechanisms.

> *Finally, and most importantly, the reported increase in accessibility of the methylated H2A.Z nucleosome is negligible compared with the much larger intrinsic DNA accessibility of the unmethylated H2A.Z nucleosome. These data do not support the authors' hypothesis and contradict the manuscript's conclusions. Claims that methylated H2A.Z nucleosomes are "more open and accessible" must therefore be removed, and the title is misleading, given that no meaningful impact of DNA methylation on H2A.Z nucleosome stability is demonstrated.*

We respectfully disagree with this reviewer's criticism. We investigated the potential impact of DNA methylation on nucleosome stability to the best of our abilities through complementary assays and reported our observations. The effect of DNA methylation is smaller than the difference between H2A.Z and H2A, but we were able to see an effect. It is also not uncommon for small differences to have functional impacts in biological systems. We agree that further testing is required to determine whether this subtle effect is functionally important, and it remains the subject of future research due to the many technical challenges associated with addressing said question. We would like to note that 18 years have passed since Daniel Zilberman first reported the antagonistic relationship between H2AZ and DNA methylation (Zilberman et al., 2008) but very few studies have since directly tested specific mechanistic hypotheses. We believe that our study lays the groundwork for exciting future investigation that better elucidates the pathways that contribute to this antagonism and will have meaningful impacts on the field in general. However, thanks to the reviewer's criticism, we realized that we did not clearly state in the Abstract the relatively subtle effect of DNA methylation on the intrinsic H2A.Z nucleosome stability. Therefore, we will accordingly revise the Abstract to make this point clearer.

> *(2) The cryo-EM structures of methylated and unmethylated 601L H2A.Z nucleosomes show no detectable differences. As presented, this negative result adds little value. If anything, it reinforces the point that the positional context of CpG methylation is critical, which the manuscript does not consider.*

We believe the inclusion and factual reporting of negative data is important for the scientific community as one of the major issues currently in biology research is biased omission of negative data. We considered eLife as a venue to publish this work for this reason. We understand that the reviewer believes our 601L structures may detract from the overall message of our manuscript. We believe this data rather emphasizes the importance of DNA sequence context, something that the reviewer also rightfully notes. It is standard practice in the nucleosome field to use the Widom 601 sequence, along with its variants. Our experience has shown that use of an artificially strong positioning sequence may mask weaker physical effects that could play a physiological role. Thus, we were careful to validate all further assays with multiple DNA sequences and believed it important to report these sequence-dependent effects on nucleosome structure.

> *(3) Very little H3 signal coincides with H2A.Z at TSSs in sperm pronuclei, yet this is neither explained nor discussed (Supplementary Figure 10D). The authors need to clarify this.*

Our H3 signal, which represents the global nucleosome population, is more broadly distributed across the genome than H2A.Z, which is known to localize at specific genomic sites. Since both histone types were sequenced to similar read depths, H3 peaks are generally shallower than H2A.Z and peak heights cannot be directly compared (i.e. they should be represented in separate appropriate data ranges).

> *(4) In my view, the most conceptually important finding is that H2A.Z-associated reads in sperm pronuclei show ~43% CpG methylation. This directly contradicts the model of strict mutual exclusivity and suggests that the antagonism is context-dependent. Similarly, the finding that the depletion of SRCAP reduces H2A.Z deposition only on unmethylated templates is also very intriguing. Collectively, these result warrants further investigation (see below).*
>
> *(5) Given that H2A.Z is located at diverse genomic elements (e.g., enhancers, repressed gene bodies, promoters), the manuscript requires a more rigorous genomic annotation comparing H2A.Z occupancy in sperm pronuclei versus XTC-2 cells. The authors should stratify H2A.Z-DNA methylation relationships across promoters, 5'UTRs, exons, gene bodies, enhancers, etc., as described in Supplementary Figure 10A.*

We agree that the substantial presence of co-localized H2A.Z and DNA methylation specifically in the sperm pronuclei samples and the changes in pattern between nuclear types are highly interesting and require further investigation. However, we faced technical challenges in our sequencing experiments that made us refrain from conducting a more detailed analysis for fear of over-interpreting potential artifacts. These challenges mainly stemmed from the difficulties in collecting enough material from *Xenopus* egg extracts and Tn5's innate bias towards accessible regions of the genome. Because of this, open regions of the genome tend to be overrepresented in our data (as noted in our Discussion), making it challenging to rigorously compare methylation profiles and H2A.Z/H3 associated genomic elements.

While the degree of separation seems to be dependent on nuclei type, we still believe the antagonism exists in both the sperm pronuclei and XTC-2 samples when comparing H2A.Z methylation profiles to the corresponding H3 condition. Our study also demonstrates that H2A.Z is preferentially deposited to hypomethylated DNA in a manner dependent of SRCAP-C (the loss of SRCAP only reduces H2A.Z on unmethylated substrates) but an additional methylation-insensitive H2A.Z deposition mechanism also exists. We realized that this interesting point was not clearly highlighted in Abstract, so we will revise it accordingly.

> *(6) Although H2A.Z accumulates less efficiently on exogenous methylated substrates in egg extract, substantial deposition still occurs (~50%). This observation directly challenges the strong antagonistic model described in the manuscript, yet the authors do not acknowledge or discuss it. Moreover, differences between unmethylated and methylated 601 DNA raise further questions about the biological relevance of the cryo-EM 601 structures.*

As depicted in Figure 6 and described in the Discussion, we clearly indicated that both methylation-sensitive and methylation-insensitive pathways exist to deposit H2A.Z within the genome. We also directly stated in our Discussion that a substantial proportion of H2A.Z colocalizes with DNA methylation both in our study as well as in previous reports, which is of major interest for future study. Additionally, we further discussed how the absence of transcription in *Xenopus* eggs is a likely reason for the more limited effect of DNA methylation restricting H2A.Z deposition in our egg extract system.

As noted in our response to (2), the lack of a clear impact on our 601L structures implies that this is due to the extraordinarily strong artificial nucleosome positioning capacity of the 601 sequence and its variants. Since 601 is heavily used in chromatin biology, including within DNA methylation research, such negative data are still useful to include and publish.

> *(7) The SRCAP depletion is insufficiently validated i.e., the antibody-mediated depletion of SRCAP lacks quantitative verification. A minimum of three biological replicates with quantification is required to substantiate the claims.*

We are willing to address this concern. However, please note that our data showed that methylation-dependent H2A.Z deposition is almost completely erased upon SRCAP depletion, indicating functionally effective depletion. The specificity of the custom antibody against Xenopus SRCAP was verified by mass spectrometry. Additionally, we have obtained the same effect using another commercially available SRCAP antibody, though we did not include this preliminary result in our original manuscript. Due to its relatively low abundance and high molecular weight, SRCAP western blot signals are weak, making it challenging to quantify the degree of depletion. We also believe that the value of quantification in this context, with the points noted above, is rather limited. In the past, our lab has published papers on depleting the H3T3 kinase Haspin from *Xenopus* egg extracts (Ghenoiu et al., 2013; Kelly et al., 2010) but were never able to detect Haspin via western blot. This protein was only detected by mass spectrometry specifically on nucleosome array beads with H3K9me3 (Jenness et al., 2018). However, depletion of Haspin was readily monitored by erasure of H3T3ph, the enzymatic product of Haspin. In these experiments, it was impossible, and not critical, to quantitatively monitor the depletion of Haspin protein in order to investigate its molecular functions. Similarly, in this current study, the important fact is that depletion of SRCAP suppressed methylation-sensitive H2A.Z deposition and quantifying the degree of SRCAP depletion would not have a major impact on this conclusion.

> *(8) It appears that the role of p400-Tip60 has been completely overlooked. This complex is the second major H2A.Z deposition complex. Because p400 exhibits DNA methylation-insensitive binding (Supplementary Figure 14), it may account for the deposition of H2A.Z onto methylated DNA. This possibility is highly significant and must be addressed by repeating the key experiments in Figure 5 following p400-Tip60 depletion.*

We are aware that the Tip60 complex is a very likely candidate for mediating DNA methylation insensitive H2A.Z deposition, which is why we tested whether DNA binding of p400 is methylation sensitive. Therefore, the reviewer's statement that we "completely overlooked" Tip60-C's role does not fairly report on our efforts. We wished to test the potential contribution of Tip60-C, but, unfortunately, the antibodies we currently have available to us were not successful in depleting the complex from egg extract. Since we had no direct experimental evidence indicating the role Tip60-C plays, we decided to take a conservative approach to our model and leave the methylation-insensitive pathway as mediated by something still unidentified. While further investigating Tip60-C's contribution to this pathway is of definite value, we do not believe that it impacts our major conclusion that SRCAP-C is the main mediator responsible for H2A.Z deposition on unmethylated DNA and thus remains a subject for future study.

> *(9) The manuscript repeatedly states that H2A.Z nucleosomes are intrinsically unstable; however, this is an oversimplification. Although some DNA unwrapping is observed, multiple studies show that H3/H4 tetramer-H2A.Z/H2B interactions are more stable (important recent studies include the following: DOI: 10.1038/s41594-021-00589-3; 10.1038/s41467-021-22688-x; and reviewed in 10.1038/s41576-02400759-1).*

We understand that the H2A.Z stability field is highly controversial. We have introduced the many conflicting reports that have been published in the field but can further expand on the controversies if desired. We also understand that the term "nucleosome stability" is broad and encompasses many physical aspects. As noted in a prior response, we will better specify our use of the term within the manuscript. In our assays, we are most focused on the DNA wrapping stability of the nucleosome and have consistently seen in our hands that H2A.Z nucleosomes are much more open and accessible compared to canonical H2A on satellite II-derived sequences, regardless of methylation status. However, we do understand that many groups have observed the opposite findings while others have obtained results similar to us. We reported on our findings of the general H2A.Z stability with the hopes to help clarify some of the field's controversies.

> *In summary, the current manuscript does not present a convincing mechanistic explanation for the antagonism between DNA methylation and H2A.Z. The observation that H2A.Z can substantially coexist with DNA methylation in sperm pronuclei, perhaps, should be the conceptual focus.*

We appreciate this reviewer's advice. However, please note that the first author who led this project has already successfully defended their PhD thesis primarily based on this project, making it impractical and unrealistic to completely change the focus of this manuscript to include an entirely new avenue of research. We believe that our data provide important insights into the mechanisms by which H2A.Z is excluded from methylated DNA, particularly via the DNA methylation-sensitive binding of SRCAP-C, which has never been described before. We agree that many questions are still left unanswered, including the exact molecular mechanism behind how DNA methylation prevents SRCAP-C binding. We have preliminary data that suggest none of the known DNA-binding modules of SRCAP-C, including ZNHIT1, by themselves can explain this sensitivity. This implies that domain dissection in the context of the holo-SRCAP complex is required to fully address this question. We believe this represents a very exciting future avenue of study; however, it does not negate our finding that SRCAP-C itself is important for maintaining the DNA methylation/H2A.Z antagonism. Therefore, we respectfully disagree with this reviewer's summary statement, which misleadingly undermines the impact of our work.

> ***Reviewer #3 (Public review):***
>
> *Summary:*
>
> *Histone variant H2A.Z is evolutionarily conserved among various species. The selective incorporation and removal of histone variants on the genome play crucial roles in regulating nuclear events, including transcription. Shih et al. aimed to address antagonistic mechanisms between histone variant H2A.Z deposition and DNA methylation. To this end, the authors reconstituted H2A.Z nucleosomes in vitro using methylated or unmethylated human satellite II DNA sequence and examined how DNA methylation affects H2A.Z nucleosome structure and dynamics. The cryo-EM analysis revealed that DNA methylation induces a more open conformation in H2A.Z nucleosomes. Consistent with this, their biochemical assays showed that DNA methylation subtly increases restriction enzyme accessibility in H2A.Z nucleosomes compared with canonical H2A nucleosomes. The authors identified genome-wide profiles of H2A.Z and DNA methylation using genomic assays and found their unique distribution between Xenopus sperm pronuclei and fibroblast cells. Using Xenopus egg extract systems, the authors showed SRCAP complex, the chromatin remodelers for H2A.Z deposition, preferentially deposit H2A.Z on unmethylated DNA.*
>
> *Strengths:*
>
> *The study is solid, and most conclusions are well-supported. The experiments are rigorously performed, and interpretations are clear. The study presents a high-resolution cryo-EM structure of human H2A.Z nucleosome with methylated DNA. The discovery that the SRCAP complex senses DNA methylation is novel and provides important mechanistic insight into the antagonism between H2A.Z and DNA methylation.*

We are grateful that this reviewer recognizes the importance of our study.

> *Weaknesses:*
>
> *The study is already strong, and most conclusions are well supported. However, it can be further strengthened in several ways.*

> *(1) It is difficult to interpret how DNA methylation alters the orientation of the H4 tail and leads to the additional density on the acidic patch. The data do not convincingly support whether DNA methylation enhances interactions with H2A.Z mono-nucleosomes, nor whether this effect is specific to methylated H2A.Z nucleosomes.*

The altered H4 tail orientation and extra density seen on the acidic patch were incidental findings that we thought could be interesting for the field to be aware of but decided not to follow up on as there were other structural differences that were more directly related to our central question. We do believe that the above two differences are linked to each other because we used a highly purified and homogenous sample for cryo-EM analysis and the H4 tail/acidic patch interaction is a well characterized contact that mediates inter-nucleosome interactions. Additionally, other groups have reported that the presence of DNA methylation causes condensation of both chromatin and bare DNA (cited within our manuscript), though the mechanics behind this phenomenon remain to be elucidated. We believed that our structure data may also align with those findings. However, the reviewer is fair in pointing out that we do not provide further experimental evidence in verifying the existence of these increased interactions. We can revise our writing to clarify that these points are currently hypotheses rather than validated results.

> *(2) It remains unclear whether DNA methylation alters global H2A.Z nucleosome stability or primarily affects local DNA end flexibility. Moreover, while the authors showed locus-specific accessibility by HinfI digestion, an unbiased assay such as MNase digestion would strengthen the conclusions.*

We would like to thank the reviewer for bringing up these issues. Although our current data cannot explicitly clarify these possibilities, we favor an idea that DNA methylation specifically alters histone to DNA contacts and that this effect is felt globally across the entire nucleosome rather than only at specific locations. The intrinsic flexibility of linker DNA ends means that that region tends to exhibit the greatest differences under different physical influences, hence the focus on characterizing that area; flexibility of a thread on a spool is most pronounced at the ends. However, we also found that the DNA backbone of H2A.Z on methylated DNA had a lower local resolution compared to its unmethylated counterpart, despite that structure having a higher global resolution, which suggested to us that DNA positioning along the nucleosome is overall weaker under the presence of DNA methylation. This is corroborated by the increased population of open/shifted structures in our classification analysis. The reviewer raises a fair point about the use of a specific restriction enzyme versus MNase. We agree that our accessibility assay is highly influenced by the position of the restriction site and have previously seen that moving the cut site too close to the linker DNA end will abolish any DNA methylation-dependent differences. We did initially attempt an MNase digestion-based assay, but the data were not as reproducible as with the use of a specific restriction enzyme. We do not know the reason behind this irreproducibility though we believe that the processivity of MNase could make it difficult to capture subtle effects like those induced by DNA methylation on already highly accessible H2A.Z nucleosomes. Overall, while we believe that DNA methylation does exert a physical effect, its subtlety may explain the many contradictory studies present within the DNA methylation and nucleosome stability field.

References

Berta, D.G., H. Kuisma, N. Valimaki, M. Raisanen, M. Jantti, A. Pasanen, A. Karhu, J. Kaukomaa, A. Taira, T. Cajuso, S. Nieminen, R.M. Penttinen, S. Ahonen, R. Lehtonen, M. Mehine, P. Vahteristo, J. Jalkanen, B. Sahu, J. Ravantti, N. Makinen, K. Rajamaki, K. Palin, J. Taipale, O. Heikinheimo, R. Butzow, E. Kaasinen, and L.A. Aaltonen. 2021. Deficient H2A.Z deposition is associated with genesis of uterine leiomyoma. Nature. 596:398–403.

Capurso, D., H. Xiong, and M.R. Segal. 2012. A histone arginine methylation localizes to nucleosomes in satellite II and III DNA sequences in the human genome. BMC Genomics. 13:630.

Chodavarapu, R.K., S. Feng, Y.V. Bernatavichute, P.Y. Chen, H. Stroud, Y. Yu, J.A. Hetzel, F. Kuo, J. Kim, S.J. Cokus, D. Casero, M. Bernal, P. Huijser, A.T. Clark, U.

Kramer, S.S. Merchant, X. Zhang, S.E. Jacobsen, and M. Pellegrini. 2010. Relationship between nucleosome positioning and DNA methylation. Nature. 466:388–392.

Choy, J.S., S. Wei, J.Y. Lee, S. Tan, S. Chu, and T.H. Lee. 2010. DNA methylation increases nucleosome compaction and rigidity. J Am Chem Soc. 132:1782–1783.

Chua, E.Y., D. Vasudevan, G.E. Davey, B. Wu, and C.A. Davey. 2012. The mechanics behind DNA sequence-dependent properties of the nucleosome. Nucleic Acids Res. 40:6338–6352.

Collings, C.K., P.J. Waddell, and J.N. Anderson. 2013. Effects of DNA methylation on nucleosome stability. Nucleic Acids Res. 41:2918–2931.

Davey, C., S. Pennings, and J. Allan. 1997. CpG methylation remodels chromatin structure in vitro. J Mol Biol. 267:276–288.

Davey, C.S., S. Pennings, C. Reilly, R.R. Meehan, and J. Allan. 2004. A determining influence for CpG dinucleotides on nucleosome positioning in vitro. Nucleic Acids Res. 32:4322–4331.

Funabiki, H., I.E. Wassing, Q. Jia, J.D. Luo, and T. Carroll. 2023. Coevolution of the CDCA7-HELLS ICF-related nucleosome remodeling complex and DNA methyltransferases. Elife. 12.

Ghenoiu, C., M.S. Wheelock, and H. Funabiki. 2013. Autoinhibition and polo-dependent multisite phosphorylation restrict activity of the histone h3 kinase haspin to mitosis. Mol Cell. 52:734–745.

Jenness, C., S. Giunta, M.M. Muller, H. Kimura, T.W. Muir, and H. Funabiki. 2018. HELLS and CDCA7 comprise a bipartite nucleosome remodeling complex defective in ICF syndrome. Proc Natl Acad Sci U S A. 115:E876–E885.

Jimenez-Useche, I., J. Ke, Y. Tian, D. Shim, S.C. Howell, X. Qiu, and C. Yuan. 2013. DNA methylation regulated nucleosome dynamics. Sci Rep. 3:2121.

Jimenez-Useche, I., D. Shim, J. Yu, and C. Yuan. 2014. Unmethylated and methylated CpG dinucleotides distinctively regulate the physical properties of DNA. Biopolymers. 101:517–524.

Kelly, A.E., C. Ghenoiu, J.Z. Xue, C. Zierhut, H. Kimura, and H. Funabiki. 2010. Survivin reads phosphorylated histone H3 threonine 3 to activate the mitotic kinase Aurora B. Science. 330:235– 239.

Li, S., Y. Peng, D. Landsman, and A.R. Panchenko. 2022. DNA methylation cues in nucleosome geometry, stability and unwrapping. Nucleic Acids Res. 50:1864–1874.

Minary, P., and M. Levitt. 2014. Training-free atomistic prediction of nucleosome occupancy. Proc Natl Acad Sci U S A. 111:6293–6298.

Ngo, T.T., J. Yoo, Q. Dai, Q. Zhang, C. He, A. Aksimentiev, and T. Ha. 2016. Effects of cytosine modifications on DNA flexibility and nucleosome mechanical stability. Nat Commun. 7:10813.

Nishiyama, A., L. Yamaguchi, J. Sharif, Y. Johmura, T. Kawamura, K. Nakanishi, S. Shimamura, K. Arita, T. Kodama, F. Ishikawa, H. Koseki, and M. Nakanishi. 2013. Uhrf1-dependent H3K23 ubiquitylation couples maintenance DNA methylation and replication. Nature. 502:249–253.

Osakabe, A., F. Adachi, Y. Arimura, K. Maehara, Y. Ohkawa, and H. Kurumizaka. 2015. Influence of DNA methylation on positioning and DNA flexibility of nucleosomes with pericentric satellite DNA. Open Biol. 5.

Perez, A., C.L. Castellazzi, F. Battistini, K. Collinet, O. Flores, O. Deniz, M.L. Ruiz, D. Torrents, R. Eritja, M. Soler-Lopez, and M. Orozco. 2012. Impact of methylation on the physical properties of DNA. Biophys J. 102:2140–2148.

Segal, E., Y. Fondufe-Mittendorf, L. Chen, A. Thastrom, Y. Field, I.K. Moore, J.P. Wang, and J. Widom. 2006. A genomic code for nucleosome positioning. Nature. 442:772–778.

Wassing, I.E., A. Nishiyama, R. Shikimachi, Q. Jia, A. Kikuchi, M. Hiruta, K. Sugimura, X. Hong, Y. Chiba, J. Peng, C. Jenness, M. Nakanishi, L. Zhao, K. Arita, and H. Funabiki. 2024. CDCA7 is an evolutionarily conserved hemimethylated DNA sensor in eukaryotes. Sci Adv. 10:eadp5753.

Zilberman, D., D. Coleman-Derr, T. Ballinger, and S. Henikoff. 2008. Histone H2A.Z and DNA methylation are mutually antagonistic chromatin marks. Nature. 456:125–129.

> ***Recommendations for the authors:***
>
> ***Reviewer #1 (Recommendations for the authors):***
>
> *The authors designed two sets of experiments to explore the molecular mechanisms underlying the mutually exclusive distribution of H2A.Z and DNA methylation previously reported by several groups.*
>
> *First, they examined how DNA methylation affects the physical stability of H2A.Z-containing nucleosomes. Although their results point to subtle differences between nucleosomes assembled on methylated versus unmethylated DNA, the authors did not extend their analyses to directly test the stability of these H2A.Z-containing nucleosomes under more challenging conditions. Prior studies have demonstrated that certain nucleosomes, such as those containing H3.3-H2A.Z or H2A.Z-H3K56Q, exhibit specific instability, but such instability is only revealed under challenging conditions, for example, altered salt concentrations or the presence of additional factors like FACT (PMID: 17575053; PMID: 19633671; PMID: 19639024; PMID: 41303375). In light of this literature, the observable structural features noted here for nucleosomes containing H2A.Z and methylated DNA are suggestive of increased instability, yet the authors did not employ comparable approaches to rigorously test whether such instability might explain the absence of H2A.Z from methylated genomic regions.*
>
> *As a result, at this stage of analysis, the idea that nucleosomes containing both H2A.Z and methylated DNA are intrinsically unstable, and that this instability accounts for the depletion of H2A.Z from methylated regions, remains unsubstantiated.*

We thank the reviewer's constructive criticisms. Through our response to these points, we were able to significantly improve our manuscript, including major rewriting of the Abstract and Discussion as well as incorporation of new data.

We agree that combinations with other histone variants, modifications, and mutations could further affect our observed impact of DNA methylation on H2A.Z-nucleosome stability. What we observed based on satellite II-derived DNA was that DNA methylation made H2A.Znucleosomes (with H3.2) more open, although the effect of DNA methylation is relatively small (as compared to the general impact of H2A.Z incorporation). We readily admit that such a subtle physical effect is unlikely to be the main driver of the antagonistic distribution of H2A.Z and DNA methylation, though small physical changes have been known

to influence larger biological functions, and sought to describe additional regulatory factors that could play major roles.

We also agree that H3.3 is of major interest when discussing H2A.Z. In our Xenopus egg extract experiments using DNA beads, the primary H3 variant deposited is H3.3 as no DNA replication occurs on the beads to allow for H3.1/.2 replication-coupled deposition. From those experiments, we demonstrated that preferential loading of H2A.Z can be primarily explained by SRCAP. In other words, in the absence of SRCAP, loading/retention of H2A.Z on H3.3nucleosomes was not noticeably affected by DNA methylation, indicating that DNA methylation's physical effects on H2A.Z nucleosomes plays little, if any, role in the preferential accumulation of H2A.Z on unmethylated DNA at least in the context of synthetic DNA beads incubated in

Xenopus egg extract lacking active transcription. Our sequencing data hints at the interesting possibility that transcription, along with other factors missing in egg extract, may be involved in further pruning H2A.Z from methylated DNA which conceivably could take advantage of subtle physical alterations. However, we agree we lack firm supporting evidence for such a mechanism which led us to forgo including that in our final model figure and we instead only report on our observations with discussions on potential biological implications and limitations. Of note, it has been reported that the H2A.Z nucleosome is more accessible than the H2A nucleosome, while inclusion of H3.3 does not further enhance accessibility of the H2A.Z nucleosome (PMID 38920622). We have now noted these points in the Discussion of our revised manuscript.

We appreciate and agree with this reviewer's point that nucleosome instability sometimes requires challenging conditions to be fully revealed. However, in our system, use of H2A.Z was the challenge provided as we find in our hands that H2A.Z by itself substantially destabilizes histone-DNA contacts compared to canonical H2A. And it is only with this already destabilized nucleosome that we see further enhancement of accessibility/openness in the presence of DNA methylation. This is similar to findings by [PMID: 23260052] that reported that only an intrinsically destabilized sub-population of canonical H2A nucleosomes on 601 DNA experienced detectable physical changes in the presence of DNA methylation.

In response to this reviewer's comment, we edited the Abstract and Discussion to clearly note the subtly of the impact of DNA methylation on H2A.Z nucleosome structure, and that the potential functional significance remains an open question.

> *Second, the authors investigated whether SRCAP-C contributes to preferential H2A.Z incorporation into unmethylated DNA. The absence of H2A.Z from methylated regions does not necessarily imply that it cannot be incorporated there; it may instead reflect the chromatin environment associated with DNA methylation, which could disfavor SRCAP-C activity, whereas open chromatin environments strongly promote SRCAP-dependent H2A.Z deposition.*

This reviewer suggested an alternative model where SRCAP prefers to act on open chromatin and that the apparent preferential H2A.Z deposition to unmethylated DNA is due solely to the increased accessibility associated with unmethylated DNA. Following such a model, one would predict that SRCAP-C's preference to unmethylated DNA would be eliminated on nucleosome-free DNA in Xenopus egg extracts. To test this alternative model, we repeated the SRCAP-C binding experiment in egg extracts depleted of the HIRA complex, the H3.3-H4 chaperone responsible for de novo nucleosome assembly on exogenously added DNA in egg extracts. Contrary to this prediction, both SRCAP and ZNHIT1 still display preferential binding to unmethylated DNA substrates in HIRA-depleted extracts in which nucleosome assembly is suppressed (newly added Suppl Fig 16). The results argue that discrimination of SRCAP-C from methylated DNA is not due to a potential effect of chromatin compaction by DNA methylation. Furthermore, our new result is in line with an idea that SRCAP employs 1D

diffusion on the linker DNA before engaging the H2A nucleosome (PMID 39131301), implying that discrimination of SRCAP-C from methylated linker DNA contributes to this process. This is now illustrated in the new model Figure 6.

Please note we also indicate in both our model and in text that there exists an additional methylation-insensitive mechanism that drives H2A.Z deposition on methylated DNA, leading to a substantial amount of colocalized H2A.Z and DNA methylation. Why two different deposition pathways for H2A.Z differing in their methylation sensitivities must exist is an interesting topic for future work and has not been described prior to our report.

> *This interpretation is consistent with the authors' own comparative mapping of H2A.Z and DNA methylation in sperm pronuclei incubated in egg extract versus a transcriptionally active Xenopus fibroblast line. They observed that about 40% of H2A.Z-associated genomic DNA is methylated in sperm pronuclei, but only 3% in fibroblasts. As they note, the major difference between these systems is the presence of transcription in fibroblasts, a process known to drive H2A.Z eviction/recycling, and which is absent in the egg-extract system. Thus, no specific inhibition of SRCAP-C by methylated DNA needs to be invoked: H2A.Z deposition on both methylated and unmethylated accessible regions, followed by preferential eviction from methylated sites in active nuclei, could fully account for the observed patterns.*

As the reviewer correctly notes here, we proposed that transcription is likely to play an important role in pruning H2A.Z from methylated DNA. Our observations and proposed mechanism do not argue against the possible existence of a DNA methylation-insensitive, transcription-dependent mechanism that promotes dissociation of H2A.Z from methylated DNA, which we believe likely would be correlated to gene body methylation. In fact, we did propose in our Discussion that such a transcription-mediated mechanism may conceivably take advantage of the subtly destabilized DNA wrapping of H2A.Z nucleosomes on methylated DNA to further selectively prune H2A.Z at colocalized regions. However, such a mechanism would be an additional component to what we have already described and does not explain the observed preferential recruitment of SRCAP-C to unmethylated DNA in Xenopus egg extracts in the absence of active transcription.

> *In this respect, studies from the Felsenfeld laboratory showing that double-variant nucleosomes are highly unstable under physiological ionic conditions are particularly relevant (PMID: 19633671; PMID: 19639024). They demonstrated that such unstable nucleosomes are only evident under low ionic strength extraction conditions, emphasizing that the apparent absence of H2A.Z may reflect facilitated removal rather than failure of assembly.*
>
> *The authors may also have been influenced by the study of Berta et al. (cited in the manuscript), which examined uterine leiomyomas harboring somatic or germline mutations in SRCAP-C subunits. In those tumors, the normal association of H2A.Z with accessible, active chromatin, and its exclusion from methylated regions, was lost. However, this observation does not demonstrate that SRCAP-C actively prevents H2A.Z incorporation into methylated DNA. Instead, it may simply reflect that in the absence of SRCAP-C, a default, less efficient deposition pathway operates regardless of whether the chromatin environment is normally permissive or restrictive for SRCAP-dependent activity.*
>
> *Even if one accepts the more straightforward interpretation proposed by the present authors, that SRCAP-C is actively inhibited by methylated DNA, as suggested by their pull-down experiments from Xenopus egg extracts using unmethylated and methylated DNA, the hypothesis lacks mechanistic support.*

Considering this reviewers' criticism, we have expanded our discussion to indicate a possibility that SRCAP-C may have an alternative mechanism to find open chromatin independent of DNA methylation status. However, our data show that SRCAP-C preferentially binds to unmethylated DNA in a manner independent of transcription or other epigenetic status in Xenopus egg extracts, and that SRCAP-C carries the major mechanism that explains preferential deposition of H2A.Z to unmethylated DNA. Therefore, we believe that our study for the first time offers a mechanistic explanation of how H2A.Z discrimination from methylated DNA is accomplished through SRCAP-dependent H2A.Z deposition.

> *The following points summarize the issues discussed above:*
>
> *(1) The authors did not sufficiently test the hypothesis that H2A.Z-methylated DNA nucleosomes are inherently unstable and could explain the exclusion of H2A.Z from methylated genomic regions.*

We stand by our conclusion that DNA methylation has an intrinsic capacity to make the H2A.Z nucleosome more open and accessible, even though the effect is subtle. We did not argue that this subtle effect can fully explain the exclusion of H2A.Z from methylated genomic regions. Rather, our Xenopus egg extract experiment suggested that in the transcriptionally inactive egg extract setting, such a mechanism plays little or no role and it is SRCAP-C instead that is the major driver. Whether this physical mechanism also contributes to their exclusion in cells with active transcription remains a future subject of study.

> *(2) The proposed active role of SRCAP-C in preventing H2A.Z assembly on methylated DNA is supported only by limited experimental data and lacks a mechanistic explanation. In particular, this hypothesis does not account for the significant H2A.Z assembly observed on methylated DNA regions in sperm nuclei after incubation in egg extract.*

We respectfully disagree with this summary assessment. Our conclusions are well aligned with the substantial H2A.Z association with methylated DNA in sperm pronuclei assembled in Xenopus egg extracts seen. We demonstrated that:

(1) In transcriptionally-silent Xenopus egg extracts using synthetic DNA beads, DNAbinding of SRCAP-C is inhibited by DNA methylation.

(2) In this set up, H2A.Z is preferentially, if not exclusively, loaded to unmethylated DNA over methylated DNA.

(3) Depletion of SRCAP-C almost completely eliminated preferential association of H2A.Z to unmethylated DNA, while leaving some DNA methylation-insensitive H2A.Z loading.

(4) These data indicate the presence of a SRCAP-C-dependent, DNA methylationsensitive mechanism as well as a SRCAP-C-independent, DNA-methylation-insensitive mechanism to load H2A.Z to chromatin. This conclusion matches well with our genomic analysis showing that H2A.Z is preferentially but not exclusively loaded to hypomethylated genomic segments to sperm pronuclei in Xenopus egg extracts.

(5) As we clearly discussed, this SRCAP-C-dependent mechanism by itself is insufficient to explain the much clearer exclusion of H2A.Z in somatic cells. We discussed the possibility that transcription contributes to further pruning of H2A.Z from methylated DNA.

To deliver this overall message with nuances that we noted above, we have heavily revised the Abstract, the model Figure 6, and Discussion. Thanks to the criticisms raised by this reviewer, we believe that our revised manuscript has been significantly improved.

> ***Reviewer #2 (Recommendations for the authors):***

> *(1) A major omission is the absence of a cryo-EM structure of a canonical nucleosome assembled on the same DNA template - this is essential to assess whether the observed effects are H2A.Z-specific.*

We had considered solving the H2A structures, however, ultimately decided against it for a few reasons. First, there already exists crystal structures of canonical H2A nucleosomes using a DNA sequence highly similar to our Sat2R-P with and without the presence of DNA methylation (PDB: 5CPI and 5CPJ). The authors of this study did not see any physical differences present in their structures (Osakabe et al., 2015). Additionally, we had included canonical H2A conditions within our restriction enzyme accessibility assay and did not see a significant impact of DNA methylation on those samples (Fig 3). Because of the previous report and our own negative data, we expected that only limited additional insights would be obtained from the canonical H2A structures and decided not to pursue that analysis, considering the cost and effort for this additional cryo-EM analysis.

> *(2) The reported increase in accessibility of the methylated H2A.Z nucleosome is negligible compared with the much larger intrinsic DNA accessibility of the unmethylated H2A.Z nucleosome. Claims that methylated H2A.Z nucleosomes are "more open and accessible" must therefore be removed, and the title is misleading, given that no meaningful impact of DNA methylation on H2A.Z nucleosome stability is demonstrated.*

We respectfully disagree with this reviewer's criticism. We investigated the potential impact of DNA methylation on nucleosome stability to the best of our abilities through complementary assays and reported our observations. The effect of DNA methylation is smaller than the difference between H2A.Z and H2A, but we were able to see an effect. It is also not uncommon for small differences to have functional impacts in biological systems. We agree that further testing is required to determine whether this subtle effect is functionally important, and it remains the subject of future research due to the many technical challenges associated with addressing said question. We would like to note that 18 years have passed since Daniel Zilberman first reported the antagonistic relationship between H2AZ and DNA methylation (Zilberman et al., 2008) but very few studies have since directly tested specific mechanistic hypotheses. We believe that our study lays the groundwork for exciting future investigation that better elucidates the pathways that contribute to this antagonism and will have meaningful impacts on the field in general. However, thanks to the reviewer's criticism, we realized that we did not clearly state in the Abstract that the effect of DNA methylation on intrinsic H2A.Z nucleosome stability is relatively subtle. We will accordingly revise the Abstract, the model Figure 6, and Discussion to make this point clearer.

> *(3) The cryo-EM structures of methylated and unmethylated 601L H2A.Z nucleosomes show no detectable differences. As presented, this negative result adds little value and should be removed.*

We believe the inclusion and factual reporting of negative data is important for the scientific community as one of the major issues currently in biology research is biased omission of negative data. We considered eLife as a venue to publish this work for this reason. We understand that the reviewer believes our 601L structures may detract from the overall message of our manuscript, however, we believe that this data rather emphasizes the importance of DNA sequence context, something that the reviewer also rightfully notes. It is standard practice in the nucleosome field to use the Widom 601 sequence, along with its variants. Our experience has shown that use of an artificially strong positioning sequence may mask weaker physical effects that could play a physiological role. Thus, we were careful to validate all further assays with multiple DNA sequences and believed it important to report these sequence-dependent effects on nucleosome structure.

> *(4) Very little H3 signal coincides with H2A.Z at TSSs in sperm pronuclei, yet this is neither explained nor discussed (Supplementary Figure 10D). The authors need to clarify this.*

Our H3 signal, which represents the global nucleosome population, is more broadly distributed across the genome than H2A.Z, which is known to localize at specific genomic sites. Since both histone types were sequenced to similar read depths, H3 peaks are generally shallower than H2A.Z and peak heights cannot be directly compared (i.e. they should be represented in separate appropriate data ranges).

> *(5) In my view, the most conceptually important finding is that H2A.Z-associated reads in sperm pronuclei show ~43% CpG methylation. This directly contradicts the model of strict mutual exclusivity and suggests that the antagonism is context-dependent. Similarly, the finding that the depletion of SRCAP reduces H2A.Z deposition only on unmethylated templates is also very intriguing. Collectively, these result warrants further investigation (see below).*
>
> *(6) Given that H2A.Z is located at diverse genomic elements (e.g., enhancers, repressed gene bodies, promoters), the manuscript requires a more rigorous genomic annotation comparing H2A.Z occupancy in sperm pronuclei versus XTC-2 cells. The authors should stratify H2A.ZDNA methylation relationships across promoters, 5'UTRs, exons, gene bodies, enhancers, etc., as described in Supplementary Figure 10A.*

We appreciate recognition of the importance of our finding by this reviewer. We agree that the substantial presence of co-localized H2A.Z and DNA methylation specifically in the sperm pronuclei samples and the changes in pattern between nuclear types are highly interesting and require further investigation. However, we faced technical challenges in our sequencing experiments that made us refrain from conducting a more detailed analysis for fear of over-interpreting potential artifacts. These challenges mainly stemmed from the difficulties in collecting enough material from Xenopus egg extracts and Tn5's innate bias towards accessible regions of the genome. Because of this, open regions of the genome tend to be overrepresented in our data (as noted in our Discussion), making it challenging to rigorously compare methylation profiles and H2A.Z/H3 associated genomic elements.

While the degree of separation seems to be dependent on nuclei type, we still believe the antagonism exists in both the sperm pronuclei and XTC-2 samples when comparing H2A.Z methylation profiles to the corresponding H3 condition. Our study also demonstrates that H2A.Z is preferentially deposited to hypomethylated DNA in a manner dependent of SRCAP-C (the loss of SRCAP only reduces H2A.Z on unmethylated substrates) but an additional methylationinsensitive H2A.Z deposition mechanism also exists. We realized that this interesting point was not clearly highlighted in Abstract, so we will revise it accordingly.

> *(7) Although H2A.Z accumulates less efficiently on exogenous methylated substrates in egg extract, substantial deposition still occurs (~50%). This observation directly challenges the strong antagonistic model described in the manuscript. The authors need to discuss this in more detail.*

As depicted in Figure 6 and described in the Discussion, we indicated that both methylation-sensitive and methylation-insensitive pathways exist to deposit H2A.Z within the genome. We also directly stated in our Discussion that a substantial proportion of H2A.Z colocalizes with DNA methylation both in our study as well as in previous reports, which is of major interest for future study. Additionally, we further discussed how the absence of transcription in Xenopus eggs is a likely reason for the more limited effect of DNA methylation restricting H2A.Z deposition in our egg extract system. In the revised manuscript, we heavily edited the Discussion to better clarify these points.

> *(8) The SRCAP depletion is insufficiently validated, i.e., the antibody-mediated depletion of SRCAP lacks quantitative verification. A minimum of three biological replicates with quantification is required to substantiate the claims.*

In response to this, quantification of the SRCAP depletion is now included as Supplementary Figure 13A and B. Since our anti-ZNHIT1 antibodies reproducibly detected ZNHIT1 on DNA beads isolated from egg extracts, we have conducted additional verification of the SRCAP depletion by probing for SRCAP and ZNHIT1 on DNA beads, confirming that these proteins were depleted on DNA beads upon immunodepletion with anti-SRCAP antibodies (Author response image 1). To further validate this conclusion, we added data showing that the effect of SRCAP depletion on methylation-sensitive H2A.Z deposition was reproduced through use of a different commercially available antibody raised against human SRCAP (newly added Suppl Fig 14).

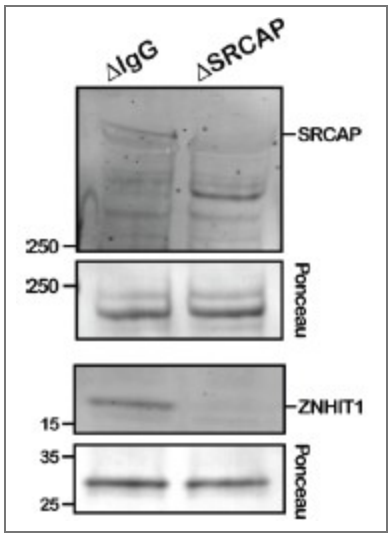

Author response image 1. Verification of SRCAP depletion using DNA beads. DNA beads were incubated in interphase-cycled *Xenopus* egg extract that had been depleted with either our custom SRCAP antibody or an IgG negative control. SRCAP and ZNHIT1 association was then assessed via Western Blot.

> *(9) It appears that the role of p400-Tip60 has been completely overlooked. This complex is the second major H2A.Z deposition complex. Because p400 exhibits DNA methylation-insensitive binding (Supplementary Figure 14), it may account for the deposition of H2A.Z onto methylated DNA. This possibility is highly significant and must be addressed by repeating the key experiments in Figure 5 following p400-Tip60 depletion.*

Thank you very much for raising this interesting point. We were aware that the TIP60 complex is a very likely candidate for mediating DNA methylation-insensitive H2A.Z deposition, which is why we tested whether DNA binding of p400 is methylation sensitive (shown in the revised Supplementary Figure 15). We wished to test the potential contribution of TIP60-C, but, unfortunately, the antibodies we currently have available to us were not successful in depleting the complex from egg extract. Since we had no direct experimental evidence indicating the role TIP60-C plays, we decided to take a conservative approach to our model and leave the methylation-insensitive pathway as mediated by something still unidentified. While further investigating TIP60-C's contribution to this pathway is of definite value, we do not believe that it impacts our major conclusion that SRCAP-C is the main mediator responsible for H2A.Z deposition on unmethylated DNA and thus remains a subject for future study. However, we have now added descriptions to note that TIP60-C is a likely candidate to execute the SRCAPindependent and methylation-insensitive mechanism of

H2A.Z loading in Xenopus egg extracts. In the model figure, we initially did not include Tip60-C, but we now infer TIP60-C is a likely candidate in the revised model (Figure 6) to facilitate the future research in the field.

> *(10) The manuscript repeatedly states that H2A.Z nucleosomes are intrinsically unstable; however, this is an oversimplification. Although some DNA unwrapping is observed, multiple studies show that H3/H4 tetramer-H2A.Z/H2B interactions are more stable (important recent studies include the following: DOI: 10.1038/s41594-021-00589-3; 10.1038/s41467-021-22688-x; and reviewed in 10.1038/s41576-024-00759-1). These references should be considered.*

We appreciate that the reviewer points out this important issue. Although we had described that controversy exists regarding how H2A.Z and DNA methylation contributes to nucleosome stability, it was not clearly explained. We understand that this confusion was in part due to the term "nucleosome stability", which is broad and encompasses many physical aspects. As noted in a prior response, we now better specify our use of the term within the manuscript, emphasizing the nucleosome openness and accessibility, particularly at the nucleosome core particle entry/exit sites. As noted by published studies (PMID 38920622), the impact on nucleosome stability may differ between the internal and external segments of nucleosomal DNA. In our assays, we are most focused on the DNA wrapping stability of the nucleosome and have consistently seen in our hands that H2A.Z nucleosomes are much more open and accessible at DNA ends compared to canonical H2A on satellite II-derived sequences, regardless of methylation status. However, we do understand that many groups have observed the opposite findings while others have obtained results similar to us. This may be caused by usage of different assays (for example, nucleosome assembly during salt dialysis or salt sensitivity vs openness/accessibility of preassembled nucleosome). In the Discussion of the revised manuscript, we now explain these factors, with the hope that our study will help clarify some of the field's controversies.

> ***Reviewer #3 (Recommendations for the authors):***
>
> *(1) Since the cryo-EM structure determined by single-particle analysis represents only one major population, it would be important to determine the dyad axis position by complementary biochemical assays, such as MNase-seq or chemical digestion by the Fenton reaction (PMID: 22929776).*

We would like to thank the reviewer for bringing up this important issue. We agree that the high-resolution structure represents only a subpopulation in which we specifically selected for the most stably wrapped nucleosomes in each sample. This issue is why we then supplemented our high-resolution structure with our *in-silico* classification analysis to survey the overall structure distribution of the full nucleosome particle population. The classification input contains all nucleosome-like particles picked from both unmethylated and methylated sample micrographs mixed together, ensuring that all particles are taken into consideration and that both samples have been analyzed in an identical manner. From our sorting analysis, we find an increased population of open and shifted nucleosome structures present in our methylated DNA sample, indicating destabilization of DNA-histone wrapping with DNA methylation. This is corroborated by the lower local resolution seen on the DNA backbone of our high-resolution H2A.Z on methylated DNA structure, despite it having a higher global resolution compared to its unmethylated counterpart. This suggested to us that DNA positioning along the nucleosome is overall weaker under the presence of DNA methylation.

The reviewer raises a fair point about the use of a specific restriction enzyme versus MNase. We agree that our accessibility assay is highly influenced by the position of the restriction site and have previously seen that moving the cut site too close to the linker DNA end will abolish any DNA methylation-dependent differences. We realized that we did not explain how we

decided to place the HinfI site in the context of our solved cryo-EM structure. In the revised Figure 3B, we now illustrate that the HinfI site is located at a segment where H2A/H2A.Z directly contacts the DNA and explained that this segment belongs to the region that exhibited clear methylation-induced flexibility in our cryo-EM structures. Thus, our structure helped us design this experiment.

We did initially attempt an MNase digestion-based assay, but the data were not as reproducible as with the use of a specific restriction enzyme. We do not know the reason behind this irreproducibility though we believe that the processivity of MNase could make it difficult to capture subtle effects like those induced by DNA methylation on already highly accessible H2A.Z nucleosomes, as subtle technical errors in the MNase concentration can have significant effects. Overall, while we believe that DNA methylation does exert a physical effect, its subtlety may explain the many contradictory studies present within the DNA methylation and nucleosome stability field.

> *(2) I assume that the authors confirmed complete DNA methylation by restricted enzyme digestion. It would be helpful to include this validation in supplementary figures.*

We would like to thank the reviewer for pointing out that this critical verification was missing from our initial manuscript. DNA methylation of Sat2R-P and Sat2R was verified via BstBI digestion (Suppl Fig 1B and 7D, respectively); 601L verified with HpaII digestion (Suppl Fig 6B); and 19x601 DNA verified via BstUI digestion (Suppl Fig 11A). All data has been added to the specified figures. Unfortunately, the 16xHSat2 DNA substrate we used in our assays does not contain appropriate cut-sites for methylation-sensitive restriction enzymes. Due to that, we always prepared the 16xHSat2 DNA in parallel with the 19x601 substrate under identical conditions then use digestion of the 19x601 substrate to verify quality of methylation for each batch. To more directly verify methylation of 16xHSat2 DNA, we used Xenopus laevis ZHX2 and ZHX3, which we recently identified as proteins that selectively associate with methylated DNA in Xenopus egg extracts. Although identification and characterization of Xenopus ZHX2/3 will be described elsewhere, previous published proteomic studies have also identified mammalian ZHXs as proteins that enrich on methylated DNA (PMID 21029866, 23434322). By incubating DNA beads in Xenopus egg extract and probing for endogenous ZHX2/3 (our antibody recognizes both ZHX2 and ZHX3), we verified that ZHXs selectively binds to methylated 16xHSat2 but not unmethylated DNA (Author response image 2). Although this does not necessarily verify that all CpGs in 16xHSat2 were methylated, we observed comparable methylation-induced inhibition of SRCAP binding between 16x601 and 16HSat2, supporting our conclusion.

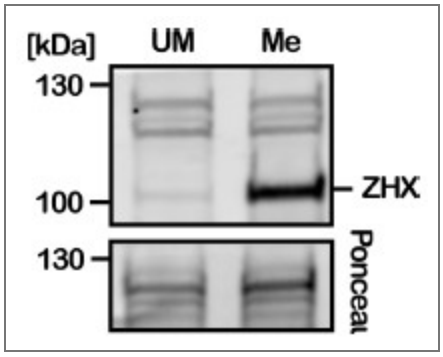

Author response image 2. Verification of 16xHSat2 methylation status via ZHX2/3 protein binding. 16xHSat2 DNA beads were incubated in *Xenopus* egg extract and endogenous ZHX2/3 protein binding assessed via Western Blot with a custom generated antibody that recognizes both ZHX2 and ZHX3.

> *(3) Figure 1A: The dyad position is difficult to identify. Please indicate it clearly using a distinct color (not green).*

We now directly indicate each sequence midpoint with a black triangle and also changed the font of DNA sequences to further clarify that the dyad resides at the palindromic center.

https://doi.org/10.7554/eLife.109762.2.sa0